MATHEMATICAL ASSOCIATION OF NIGERIA
(M.A.N)

abacus

THE JOURNAL OF THE
MATHEMATICAL ASSOCIATION OF NIGERIA

VOLUME 49, NUMBER 3
MATHEMATICS SCIENCE SERIES
SEPTEMBER, 2022

NR-ISSN 0001 3099

Editor-in-Chief:
Professor Muhammad Lawan Kaurangini, FICA
Kano University of Science and Technology, Wudil, Nigeria

National Executive Officers
(2021-2023)

1. Prof. K. O. Usman	President
2. Prof. M. A. Yusha'u	Vice President
3. Alhaji Jimoh Taylor	National Secretary
4. Prof. B. Y. Isah	Asst. Nat. Secretary
5. Mrs. Okodugha Brigitta Eno	Treasurer
6. T. A. Muhammad	Financial Secretary
7. Dr. Sadiq Abubakar	Publicity Secretary
8. Dr. Aliyu Taiwo	Business Manager
9. Prof. Muhammad L. Kaurangini	Editor-in-Chief
10. Dr. Olayemi O. Oshin	Deputy Editor-in-Chief
11. Prof. Mamman Musa	Immediate Past President
12. Dr. A. J. Alkali	Immediate Past National Secretary
13. Mr. Bankole J	Ex-Officio I
14. Dr. Chika C. Ugwuanyi	Ex-Officio II
15. Dr. Abimbola N. G. A	S. A. to President

Abacus:

Submission of the paper

Authors are requested to visit www.man-nigeria.org.ng to submit manuscripts in Microsoft word and make payment accordingly.

Preparation of the manuscript

General: The manuscripts should be in English and typed with single column and single line spacing on single side of A4 paper. The first page of an article should contain;
(1) a title of paper which well reflects the contents of the paper (Arial, 12pt),
(2) all the name(s) and affiliations(s) of authors(s) (Arial, 12pt),
(3) an abstract of 100-250 words (Times New Roman, 11 pt),
(4) 3-5 keywords following the abstract, and
(5) footnote (personal title and email address of the corresponding author). The paper should be concluded by proper conclusions which reflect the findings in the paper. The normal length of the paper should be between 10 to15 journal pages.

Tables and figures: Tables and figures should be consecutively numbered and have short titles. They should be referred to in the text as following examples (e.g., Fig. 1(a), Figs. 1 and 2, Figs. 1(a)-(d) / Table 1, Tables 1-2, etc). Tables should have borders (1/2pt plane line) with the captions right before the table. Figures should be properly located in the text as an editable image file (.jpg) with captions on the lower cell.

Units and Mathematical Expressions: It is desirable that units of measurements and abbreviations should follow the System International (SI) except where the other unit system is more suitable. The numbers identifying the displayed mathematical expression should be placed in the parentheses and referred in the text as following examples (e.g., Eq. (1), Eqs. (1)-(2)). Mathematical expressions must be inserted as an object (set as Microsoft Equations 3.0) for Microsoft Word 2007 and later versions. Image-copied text or equations are not acceptable unless they are editable. The raised and lowered fonts cannot be used for superscription and subscription.

References : A list of references which reflect the current edition of APA format, to locate after conclusion of the paper.

Review

All the submitted papers will undergo a peer-review process, and those papers positively recommended by at least two expert reviewers will be finally accepted for publication in the Abacus Journals or after any required modifications are made and a payment of **₦15,000.00** as publication fee. The normal length of the paper should be between 8 to 12 pages. Any extra page will attract additional charges at the rate of **₦500.00** per page.

Copyright

Submission of an article to Abacus Journal implies that it presents the original and unpublished work, and not under consideration for publication elsewhere. On acceptance of the submitted manuscript, it is implied that the copyright thereof is transferred to the Abacus. The Transfer of Copyright Agreement may also be submitted.

Abacus (Mathematics Science Series)
Vol. 49, No 3, September. 2022

Editorial Board

Associate Editors (2021-2023)

TABLE OF CONTENTS

Abacus (Mathematics Science Series)
Vol. 49, No 3, September. 2022

STUDY OF A PURSUIT DIFFERENTIAL GAME PROBLEM WITH A PURSUER AND MANY EVADERS

[1]Abbas Ja'afaru Badakaya and [2]Aliyu Ibrahim Kiri

[1,2]Department of Mathematical Sciences, Bayero University, Kano, Nigeria
E-mail addresses: ajbadakaya.mth@buk.edu.ng and badakaya@yahoo.com

Abstract

Abstract: This paper is concern with the study of a pursuit differential game with one pursuer and many evaders in the space R^n . In the game, players move according to certain first-order differential equations with integral constraints on control functions of the players. Pursuit is said to be completed if the geometric position of the pursuer coincides with that of each of the evader for some finite times. A theorem that provides sufficient conditions for completion of pursuit is formulated and proved. Moreover, pursuer's admissible strategy that ensures completion of pursuit is constructed.

Keywords: Differential games; Pursuer; Evader; Integral constraints.

Introduction

There is a sizable literature on pursuit differential games with multiple players. A sample of literature on this type of study is the collection of works [1]-[18] and some references therein. Most of these cited works are dedicated to problems with simple motions differential game. For example, in the works [1]-[6]; [8]-[10] and [13]-[15] considered simple motion pursuit differential games with a finite number of pursuers and one evader. Problem with a finite number of pursuers and many evaders are investigated in [7]; [16] and [18]. The former group of examples seem to be dominant in the literature.

Ivanov and Ledyaev in [12] investigated a simple motion differential game of several players with geometric constraints in the space R^n

Ibragimov and Satimov [7] studied a simple motion differential game of many pursuer and many evaders on a nonempty convex subset of R^n The result obtained was a sufficient condition for completion of pursuit. Specifically, they consider a pursuit problem in which motion of the players is described by the equations

$$\begin{cases} \dot{x}_i(t) = \varphi(t)u_i(t), & x_i(0) = x_i^0, \ i = 1,2,\dots,h, \\ \dot{y}_i(t) = \varphi(t)v_i(t), & y_i(0) = y_i^0, \ i = 1,2,\dots,m, \end{cases}$$

where it is required that

$$\left(\int_0^\tau \varphi^2(s)ds\right)^{1/2} < \infty, \qquad \tau > 0, \qquad \lim_{\tau\to\infty} \int_0^\tau \varphi^2(s)ds = \infty. \tag{2}$$

This generalized many works such as [1]-[10], [13], [15], [16] and [18]. However, this work leaves a gap for the problems in which the function $\varphi(t)$ is not satisfying the conditions in (2). For example, if $\varphi(t) = e^{-\lambda t}, \lambda > 0,$ then the second condition in (2) is not satisfied.

This paper attempts to solve the pursuit differential game considered in [7] with $h = 1$ and a finite number of evaders in the space R^n. The function $\varphi(t)$ is considered to be bounded instead. This study set forth further reduces the gap left in [7].

2. Formulation of the problem and result

Let the motion of a pursuer P and finite number of evaders $E_i,\ i \in I = \{1,2,\dots,m\},$ be described by the equations

$$\begin{cases} P: & \dot{x}(t) = \varphi(t)u(t), \quad x(t_0) = x^0, \\ E_i: & \dot{y}_i(t) = \varphi(t)v_i(t), \quad y_i(t_0) = y_i^0, \ i \in I, \end{cases} \tag{3}$$

where $x(t)$, x^0, $u(t)$, $y_i(t)$, y_i^0, $v_i(t) \in R^n$; $u(t) = (u_1(t), u_2(t), \dots, u_n(t))$ and $v_i(t) = (v_{i1}(t), v_{i2}(t), \dots, v_{in}(t))$ are control parameters of the pursuer P and evader E_i respectively and $\varphi(\cdot)$ is scalar measurable function satisfying some conditions. Let t_0 be initial time of the game and T to denote the time instant at the pursuer captures the last evader and is not fixed. This instant T is equal to $+\infty$ if some evaders are never captured.

Definition 2.1 *A measurable function* $u(t) = (u_1(t), u_2(t), \dots, u_n(t)), t_0 \le t \le \theta$, *satisfying the inequality*

$$\int_{t_0}^{\theta} \| u(s) \|^2 \, ds \le \rho^2, \tag{4}$$

where ρ is a positive real number, is called an admissible control of the pursuer.

Definition 2.2 *A measurable function* $v_i(t) = (v_{i1}(t), v_{i2}(t), \dots, v_{in}(t)), t_0 \le t \le \theta$, *satisfying the inequality*

$$\int_{t_0}^{\theta} \| v_i(t) \|^2 \, dt \le \sigma_i^2, \tag{5}$$

where σ_i is a positive number, is called an admissible control of the i^{th} evader.

Whenever the players' admissible controls $u(\cdot)$ and $v_i(\cdot)$ are chosen, the corresponding motions of a pursuer and the i^{th} evader (solution of equations (3)) are given by

$$\begin{aligned} &x(t) = (x_1(t), x_2(t), \dots, x_n(t)), \; x_k(t) = x_k^0(t) + \int_{t_0}^{t} \varphi(s) u_k(s) ds \\ &y_i(t) = (y_{i1}(t), y_{i2}(t), \dots, y_{in}(t)), \; y_{ik}(t) = y_{ik}^0(t) + \int_{t_0}^{t} \varphi(s) v_{ik}(s) ds. \end{aligned} \tag{6}$$

Definition 2.3 *A function* $U(x(\cdot), v_1(\cdot), \dots v_m(\cdot), x(\cdot), y_1(\cdot), y_2(\cdot), \dots, y_m(\cdot)), U: R^n \times (R^n)^{2m} \to R^n$, *for which the system*

$$\begin{cases} \dot{x}(t) = \varphi(t) U(x(\cdot), v_1(\cdot), \dots v_m(\cdot), x(\cdot), y_1(\cdot), y_2(\cdot), \dots, y_m(\cdot)), & \mathrm{x}(\mathrm{t}_0) = \mathrm{x}^0, \\ \dot{y}_i(t) = \varphi(t) v_i(t), & \mathrm{y_i}(\mathrm{t}_0) = \mathrm{y_i^0}, i \in I, \end{cases}$$

has a unique absolutely continuous solution $(x(t), y_1(t), \dots, y_m(t))$, for any admissible controls $v_i(t), i \in I, t_0 \le t \le \theta$, of the evader is called a strategy of the pursuer. A strategy $U(\cdot)$ of the pursuer is said to be admissible if every control it generates is admissible.

Definition 2.4 *Pursuit is said to be completed in the game (3)-(5) from initial positions* $\{x^0, y_1^0, y_2^0, \dots, y_m^0\}$, $x^0, y_i^0 \in R^n$, *if there exists a strategy* $U(\cdot)$ *of the pursuer such that for all admissible controls of the evaders* $v_i(\cdot)$, $i \in I$, *the relations* $x(t_i) = y_i(t_i)$ *hold for all* $i \in I$, *where* $t_i \in [t_0, T]$.

To elaborate on this definition, completion of pursuit means that the lone pursuer is to pursue the i^{th} evader and catch it for the time t_i and any other evader whose state coincides with that of the i^{th} evader at the time t_i. When the pursuer catches at least the i^{th} evader at time t_i then that evader(s) is/are considered to be inactive or vanished. This allow the pursuer to move against the j^{th} evader until catches it for some time t_j. This is continued until all the evaders are exhausted.

In what will follow in the paper, the game described by (3)-(5) in which the function $\varphi(\cdot)$ satisfies the inequality $0 < a \le |\varphi(t)| \le \alpha$ for all $t \ge t_0$, will be referred to as game G_1.

Research Question: Find a condition for the completion of pursuit in the game G_1.

3. Results

In this section, main result of the research work is presented. To begin with, we introduce the following notations:

$$\breve{\rho} = \frac{\rho}{\sum_{i=1}^{m} \sigma_i} \text{ and } \beta = \min\{1, a\}.$$

Let $t_i \in [t_0, T]$ for all $i \in I$, such that $t_0 \leq t_1 \leq t_2 \leq \cdots \leq t_m = T$. We define the instant at which the i^{th} evader is to be captured as $t_i = t_{i-1} + \frac{\|y_i(t_{i-1}) - x(t_{i-1})\|^2}{(\gamma_i - \sigma_i)^2}$, where γ_i is a positive number and is such that $\gamma_i = \breve{\rho}\sigma_i = \rho \frac{\sigma_i}{\sum_{i=1}^{m} \sigma_i}$. Observe that $t_i = t_{i-1}$ whenever $y_i(t_{i-1}) = x(t_{i-1})$. In accordance with these definitions, we have the following Lemma:

Lemma 3.1 *If $\rho > \sum_{i=1}^{m} \sigma_i$ then for any $x(t_{i-1})$ and $y_i(t_{i-1})$ there exists a pursuer's control $U(\cdot)$ to ensure the equality $x(t_i) = y_i(t_i)$ for $i \in I$ in the game G_1 with that*

$$\left(\int_{t_{i-1}}^{t_i} |U(s)|^2 ds\right)^{\frac{1}{2}} \leq \gamma_i.$$

Proof. For $t \in [t_{i-1}, t_i)$, let the pursuer use the control

$$U(x(t_{i-1})y_i(t_{i-1}), v_i(t)) = \begin{cases} 0, & \text{if } y_i(t_{i-1}) = x(t_{i-1}) \\ \frac{y_i(t_{i-1}) - x(t_{i-1})}{\varphi(t)(t_i - t_{i-1})} + v_i(t), & \text{if } y_i(t_{i-1}) \neq x(t_{i-1}). \end{cases} \quad (7)$$

For the case $y_i(t_{i-1}) = x(t_{i-1})$, the pursuer has its desired goal, then according (7) the pursuer remains static . In the other hand, if $y_i(t_{i-1}) \neq x(t_{i-1})$, then the pursuer chases the evader E_i according to (7) until it achieves the equality $x(t_i) = y_i(t_i)$. That is,

$$\begin{aligned} x(t_i) &= x(t_{i-1}) + \int_{t_{i-1}}^{t_i} \varphi(s)u(s)ds \\ &= x(t_{i-1}) + \int_{t_{i-1}}^{t_i} \left(\frac{y_i(t_{i-1}) - x(t_{i-1})}{t_i - t_{i-1}} + \varphi(s)v_i(s)\right) ds \\ &= x(t_{i-1}) + \frac{y_i(t_{i-1}) - x(t_{i-1})}{t_i - t_{i-1}} \int_{t_{i-1}}^{t_i} ds + \int_{t_{i-1}}^{t_i} \varphi(s)v_i(s)ds \\ &= x(t_{i-1}) + y_i(t_{i-1}) - x(t_{i-1}) + \int_{t_{i-1}}^{t_i} \varphi(s)v_i(s)ds = y_i(t_i). \end{aligned}$$

The control of the pursuer satisfies the inequality

$$\left(\int_{t_{i-1}}^{t_i} ||U(s)||^2 ds\right)^{\frac{1}{2}} \leq \gamma_i. \quad (8)$$

Indeed, using the Minkowski inequality, definition of t_i and the fact that $\gamma_i = \breve{\rho}\sigma_i > \sigma_i$ (since $\breve{\rho} > 1$) one gets

$$\left(\int_{t_{i-1}}^{t_i} ||U(s)||^2 ds\right)^{\frac{1}{2}} = \left(\int_{t_{i-1}}^{t_i} \left|\left|\frac{y_i(t_{i-1})-x(t_{i-1})}{\varphi(s)(t_i-t_{i-1})} + v_i(s)\right|\right|^2 ds\right)^{\frac{1}{2}}$$
$$\leq \left(\int_{t_{i-1}}^{t_i} \left(\frac{||y_i(t_{i-1})-x(t_{i-1})||^2}{\varphi^2(s)(t_i-t_{i-1})^2}\right) ds\right)^{\frac{1}{2}} + \left(\int_{t_{i-1}}^{t_i} ||v_i(s)||^2 ds\right)^{\frac{1}{2}}$$
$$\leq \left(\int_{t_{i-1}}^{t_i} \left(\frac{||y_i(t_{i-1})-x(t_{i-1})||^2}{\beta^2(t_i-t_{i-1})^2}\right) ds\right)^{\frac{1}{2}} + \left(\int_{t_{i-1}}^{t_i} ||v_i(s)||^2 ds\right)^{\frac{1}{2}}$$
$$\leq \frac{||y_i(t_{i-1})-x(t_{i-1})||}{\beta(t_i-t_{i-1})}\left(\int_{t_{i-1}}^{t_i} ds\right)^{\frac{1}{2}} + \left(\int_{t_0}^{T} ||v_i(t)||^2 ds\right)^{\frac{1}{2}}$$
$$\leq \frac{||y_i(t_{i-1})-x(t_{i-1})||}{\beta\sqrt{t_i-t_{i-1}}} + \frac{\sigma_i}{\beta}$$
$$= \frac{\gamma_i-\sigma_i}{\beta} + \frac{\sigma_i}{\beta} = \gamma_i.$$

The proof of the case $y_i(t_{i-1}) = x(t_{i-1})$ is trivial. This completes the proof of the lemma.

Now the main result of the research work is presented below.

Theorem 3.1 *If* $\rho > \sum_{i=1}^{m} \sigma_i$, *then the pursuit can be completed in the game* G_1.

Proof. Define the strategy of the pursuer as follows:

$$U(x(\cdot), y_1(\cdot), y_2(\cdot), \dots, y_m(\cdot), v_1(\cdot), \dots, v_m(\cdot)) = \begin{cases} U^*_{[t_0,t_1)}(t), & t_0 \leq t < t_1, \\ U^*_{[t_1,t_2)}(t), & t_1 \leq t < t_2, \\ \vdots & \\ U^*_{[t_{m-1},t_m)}(t), & t_{m-1} \leq t < t_m, \end{cases} \quad (9)$$

where

$$U^*_{[t_{i-1},t_i)}(t) = \begin{cases} 0, & if\ y_i(t_{i-1}) = x(t_{i-1}), \\ \frac{y_i(t_{i-1})-x(t_{i-1})}{\varphi(t)(t_i-t_{i-1})} + v_i(t), & if\ y_i(t_{i-1}) \neq x(t_{i-1}), \end{cases}$$

for all $i \in I$ and $v_i(\cdot)$ is the admissible control of i^{th} evader. Using the result of the Lemma 3.1 and the inequality $\sum_{i=1}^{m} \sigma_i^2 \leq (\sum_{i=1}^{m} \sigma_i)^2$, we show the admissibility of this strategy as follows:

$$\int_{t_0}^{T} ||U(s)||^2 ds = \sum_{i=1}^{m} \int_{t_{i-1}}^{t_i} ||U(s)||^2 ds = \sum_{i=1}^{m} \left[\left(\int_{t_{i-1}}^{t_i} ||U(s)||^2\right)^{\frac{1}{2}}\right]^2$$
$$\leq \sum_{i=1}^{m} [\gamma_i]^2 = \sum_{i=1}^{m} [\breve{\rho}\sigma_i]^2 = \breve{\rho}^2(\sum_{i=1}^{m} [\sigma_i]^2)^2$$
$$= \frac{\rho^2}{(\sum_{i=1}^{m} [\sigma_i])^2}(\sum_{i=1}^{m} [\sigma_i]^2)^2 \leq \rho^2.$$

If the pursuer uses the strategy (9) then according to Lemma 3.1, the following equations $x(t_1) = y_1(t_1)$, $x(t_2) = y_2(t_2), \dots, x(t_m) = y_m(t_m)$, hold. By this strategy , the pursuer is expected to complete pursuit for the time t_m. This proves the theorem.

A pursuit differential games with one pursuer and R^n where integral constraint on each control function of the player is considered. Sufficient condition for the single pursuer to complete pursuit in finite time, is obtained. This condition requires that the energy of the pursuer to be bigger than the sum of the energies of the evaders. The real life situational example of this, is a problem of single predator that runs after multiple preys with mission to kill all the preys one after the other. This study affirmed that the predator can accomplish its mission provided that the condition stated in the theorem is satisfied.

Finding optimal pursuit time for the problem studied in this paper can be a potential further research. Moreover, the problem can be studied in the Hilbert space l_2.

References

[1] I. A. Alias, G. Ibragimov, A. Kuchkarov, *Differential game with many pursuers when controls are subject to coordinate-wise integral constraints. Malaysian Journal of Mathematical Sciences.* **10**(2), 195-207(2016)

[2] I. A. Alias, R. N. R. Ramli, G. Ibragimov and A. Narullaev, *Simple motion pursuit differential game of many pursuers and one evader on convex compact set. International Journal of Pure and Applied Mathematics.* **102**(4) , 733-745 (2015)

[3] G. I. Ibragimov and A. Sh. Kuchkarov, *Fixed duration pursuit-evasion differential game with integral constraints.* em J. Phys.: Conf Ser. **435**, 012017(2013)

[4] G. I. Ibragimov and B. B. Rikhsiev, *On some Sufficient conditions for optimalty of the pursuit time in the differential game with multiple pusuers. Automation and Remote Control.* **67**(4) , 529-537(2006)

[5] I. I. Gafurjan , *Collective pursuit with integral constraints on the controls of the players. Siberian Adv. Math.* **14**(2), 627-635(2004)

[6] G. I. Ibragimov, *Optimal pursuit with countably many pursuers and one evader. Differential Equations.* **41**(5), 627-635(2005)

[7] G. Ibragimov and N. Satimov, *A Multiplayer pursuit differential game on a convext set with integral constraints. Abstract and Applied Analysis.* doi: 10.1155/2012/460171, (2012)

[8] G. I. Ibragimov, *A Game of optimal pursuit of one object by several. Journal of Applied Mathematics and Mechanics.* **62**(2), 187-192(1998)

[9] G. Ibragimov, *On a multiperson pursuit problem with integral constraints on the controls of the players. Mathematical Notes.* **70**(2), 201-212(2001)

[10] G. Ibragimov, N. Abd Rashia, A. Kuchkarov and F. Ismail, *Multi pursuer differential game of optimal approach with integral constraints on controls of the players. Taiwanese Journal of Mathematics.* **19**(3) , 963-976(2015)

[11] G. I. Ibragimov, *An n-person differential game with integral constraints on the controls of the players. Izvestiya Vysshikh Uchebnykh Zavedenii. Matematik.* **70**(2), 48-52(2004)(Russian).

[12] R. P. Ivanov and Yu. S. Ledyaev, *Optimality of pursuit time in a simple motion differential game of many objects. Trudy Matematicheskogo Instituta imeni V. A. Steklova.* **158**, 87-97(1981)

[13] A. Kuchkarov, G. Ibragimov and M. Ferrara, *Simple motion pursuit and evasion differential*

games with many pursuers on manifolds with euclidean metric. Discrete Dynamics in Nature and Soceity. http://dx.doi.org/10.1155/2016/1386242, (2016)

[14] A. Yu., Levchenkov, and A. G. Pashkov, *Differential game of optimal Approach of two inertial pursuers to a noninertial evader. Journal of Optimization Theory and Applications.* **65**(3), 501-518(1990)

[15] B. T. Samatov, *Problems of group pursuit with integral constraints on controls of the players. . Cybernetics and System Analysis.* **49**(5), 756–767 (2013)

[16] B. T. Samatov, *Problems of group pursuit with integral constraints on controls of the players, II. Cybernetics and System Analysis.* **49**(6),907-921(2013) .

[17] N. Y. Satimov, B. B. Rikhsiev and A. A. Khamdamov *On pursuit problems for multiperson linear differential and discrete games. Dokl. Akad. Nauk UzSSR* . **3**, 3-5(1983)

[18] D. A. Vagin and N. N. Petrov, *A problem of group pursuit with phase constraints. Journal of Applied Mathematics and Mechanics.* **66**(2) , 225-232(2002)

Abacus (Mathematics Science Series)
Vol. 49, No 3, September. 2022

ON THE FLOW OF RADIATIVE POROUS MEDIA OF AN ELECTRICALLY CONDUCTING FLUID (MHD) IN THE PRESENCE OF SLIP AND CONVECTIVE BOUNDARY CONDITIONS

Bashiru Abdullahi[1], Isah Bala Yabo [2], Ibrahim Sa'idu[3]

[1] Department of Mathematics and Statistics Abdu Gusau Polytechnic, Talata Mafara.
[2] Department of Mathematics Usmanu Danfodiyo University, Sokoto.
[3] Department of Information and Technology Usmanu Danfodiyo University, Sokoto.

Abstract

The influence of slip and convective boundary conditions in the presence of thermal radiation through parallel porous plates was deliberated analytically and numerical. A non-linear Roseland approximation was used to describe the radiative heat flux in the energy equation where the magnetic field is combined in the momentum equation. The solution of the governing differential equation that described the flow was solved using the Perturbation method in order to obtain the analytical solution which was used to confirm the validity of the numerical solution. The finite difference method was employed to find the numerical solution to the governing equations. Equations that represent the velocity, temperature, skin friction, and Nusselt number are obtained and their behaviors are discussed with help of line graphs. The results obtained show that suction/injection, slip velocity and convective boundary conditions play important role in changing the behavior of velocity, temperature, skin friction and Nusselt number.

Keywords: Convective boundary condition, Porous media, Magnetohydrodynamic (MHD), Slip parameter, Thermal radiation.

Introduction

The study of fluid flow through porous walls is a very significant branch of fluid mechanics. The impact of suction and or injection is one of the renowned present-day topics of research. However, in the plan of updraft oil retrieval and radial diffusers, suction is used. Suction is also functional to chemical procedures to confiscate reactants and injection is useful in adding reactants, cool the surface, stop corrosion or scaling and decrease the drag. Considering the application MHD flow through pours medium, in the areas of engineering technology, in recent time many authors researched the related topic. Uwanta and Hamza (2014) conducted research on the influence of porous medium on Unsteady Hydromagnetic convective flow of Reactive viscous fluid between vertical porous plates with thermal diffusion. In the findings it was revealed that the establishment of the least flow takes place close the wall where suction happens, while the extreme flow forms near the wall where the injection occurs. Feng *et al*. (2015) analyzed the consequence of drag Force and fluid flow within porous channels on a chemically reactive MHD flow and found that the channel hotness declined for fluid suction and increasing Prandtl number but both enlarged the rate of heat transfer. Other researchers that talked about the effect of suction and injection include: (Jha *et al.* 2016, Goyal and Rathore 2017, Jha *et al*.(2018), Sasikumar and Govindorajan 2018, Hamza 2019, Ighoroje *et al.* 2019, Jitender *et al.* 2019, Rehman *et al.* 2019, Upreti *et al.* 2020)

Fluid slip boundary condition arises in several practices such as in Nano-channels and it is used where a thin film of light oil is attached to the moving channels or when the surface is covered with special coatings such as a thick monolayer of hydrophobic octadecyl trichlorosilane. Slip boundary conditions are also applied in the polishing of artificial heart valves and internal cavities, fluid motion within the human body, etc. Many researchers, considering the application of slip velocity in science and technology researched its effect on MHD (Venkateswarlu *et al.* 2016, Gnaneswa 2017, Mohamed and Ahmed 2018, Ellahi *et al.* 2018, Manjula and Jayalakshmi 2018, Nandal and Kumari 2019, Mohammad *et al.* 2020)

Thermal radiation continues have a great upshot on MHD flow and heat transfer problems. For instance, at high functioning

temperatures, the radiation effect can be quite significant. Dulal and Babulal (2013) stated that many processes in manufacturing areas such as Atomic power plants, and the various impulsion devices for aircraft, missiles, and space vehicles, thermal radiation consequence becomes very imperative. Considering the sway of thermal radiation on MHD several authors researched on the subject matter (Misra and Sinha 2013, Kalidas 2014, Mohammad *et al.* 2014, Kho *et al.2018, Isah et al. 2018*)

Boundary conditions with convective behavior are useful in many manufacturing and industrial processes (transpiration, cooling process, and material drying). Therefore, numerous scholars have revealed their concern in finding solutions of problems on MHD fluids flow due to convective boundary conditions (Wubshet 2016, Siti *et al.* 2017, Yahaya *et al.* 2018)

Motivated by the significance of slip and convective boundary conditions on the flow of MHD in science and engineering, the present work is aimed at extending the work of Isah *et al.* (2018) to incorporate slip and convective boundary conditions and to investigate their influences.

Mathematical Analysis

The current study investigate free convective heat transfer flow of steady and unsteady laminar and fully developed on MHD fluids. A uniform transverse magnetizing field of strength B_0 is applied in the existence of heat change of strength q_y, which is gripped by the wall and moved to the fluid as presented in Figure 1. At constant temperature T_0 before the start-up, both the fluid and walls are assumed to be at rest ($t' \leq 0$). At start-up the temperature of the wall positioned at $y' = 0$ is $-k^* \frac{\partial T'}{\partial y'}\Big|_{y'=0} = h_1[T_1 - T'(0,t)]$ and the other wall at a distance H from it is constant ($t' > 0$). The stream wise coordinate is denoted by x' taken upright upward direction and that normal to it is denoted by y'. The axial (*x-direction*) velocity depends only on the transverse coordinate, y'. The governing equations for the present physical situation (using the Bossiness's approximation), in the dimensional form are:

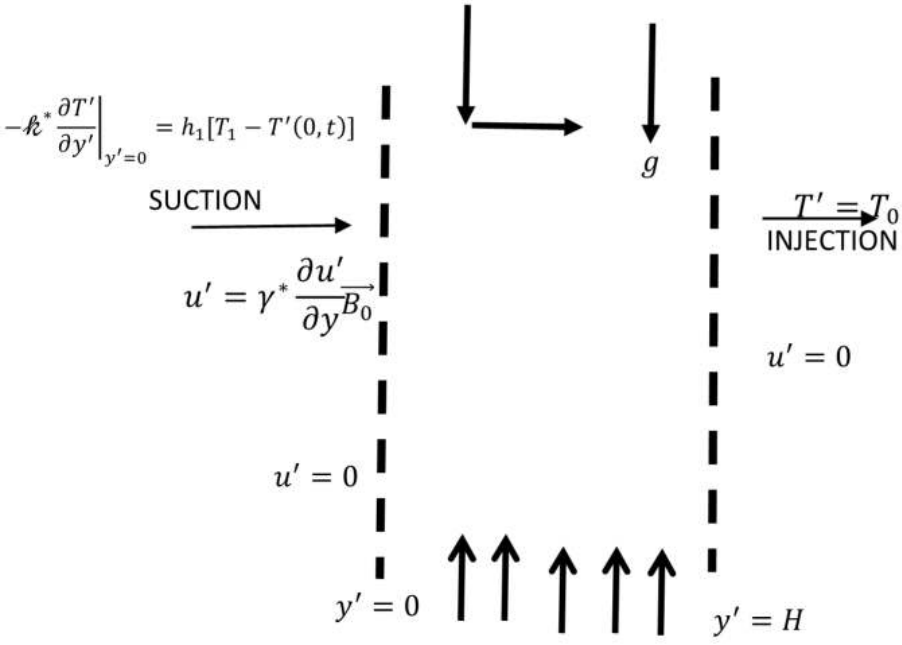

Figure 1: Geometry of the problem for the porous channel

$$\frac{\partial u'}{\partial t'} + V_0 \frac{\partial u'}{\partial y'} = \nu \frac{\partial^2 u'}{\partial y'^2} + g\beta(T_1 - T_0) - \sigma \frac{{B_0}^2 u'}{\rho}$$
(1)

$$\frac{\partial T'}{\partial t'} + V_0 \frac{\partial T'}{\partial y'} = \alpha \left[\frac{\partial^2 T'}{\partial y'^2} - \frac{1}{K}\frac{\partial q_y}{\partial y'}\right]$$
(2)

The required initial and boundary conditions to be satisfied are:

$$\left.\begin{array}{l} t' \le 0: \ for \ 0 \le y' \le H, \quad u' = 0; \quad T' = T_0 \\ t' > 0: u' = \gamma^* \frac{\partial u'}{\partial y}, -\cancel{k}^* \frac{\partial T'}{\partial y'}\Big|_{y'=0} = h_1[T_1 - T'(0,t)], at \ y' = 0 \\ u' = 0, \ T' = T_0, at \ y' = H \end{array}\right\}$$
(3)

To find the non-dimensional form of the above dimensional equations, the following dimensionless variables are introduced:

$$t = \frac{t'\gamma}{H^2}, \quad y = \frac{y'}{H}, \quad P_r = \frac{\gamma}{\alpha} \quad , \quad \theta = \frac{T' - T_0}{T_1 - T_0}, B_{i1} = \frac{h_1 H}{\cancel{k}}, G_r = \frac{[g\beta H^2(T_1 - T_0)]}{\nu U},$$

$$M^2 = \frac{\sigma \beta_0^2 H^2}{\rho \nu}, u = \frac{u'}{U}, S = \frac{V_0 H}{\nu}, \gamma = \frac{\gamma^*}{H}, u' = \gamma^* \frac{\partial u'}{\partial y} \qquad (4)$$

The radiation heat flux (q_y)term in the problem is simplified by using the Roseland approximation

$$q_y = \frac{-4\sigma \partial T'^4}{3\cancel{k}^* \partial y'} \qquad (5)$$

Using Equations (4) and (5) in equations (1) and (2) subject to the new boundary conditions, we acquire the following non-dimensional equations for velocity and temperature equations respectively.

$$\frac{\partial u}{\partial t} + S\frac{\partial u}{\partial y} = \frac{\partial^2 u}{\partial y^2} + Gr\theta - M^2 u \qquad (6)$$

$$P_r\left(\frac{\partial \theta}{\partial t} + \frac{\partial \theta}{\partial y}\right) = \left[1 + \frac{4R}{3}(C_T + \theta)^3\right]\frac{\partial^2 \theta}{\partial y^2} + 4R[C_T + \theta]^2\left(\frac{\partial \theta}{\partial y}\right)^2$$
(7)

With fresh initial and boundary conditions:

$$\left.\begin{array}{l} at \ t \le 0, \quad 0 \le y \le 1: \quad u = 0; \quad \theta = 0 \\ at \ t > 0 \begin{cases} y = 0: \ u = \gamma \frac{\partial u}{\partial y}, -\frac{\partial \theta}{\partial y}\Big|_{y=0} = B_{i1}[1 - \theta], \\ y = 1: u = 0, \ \theta = 0 \end{cases} \end{array}\right\}$$
(8)

Analytical Solution

Analytical results are very vital in authenticating the solution of time-dependent equations. Equations (6) and (7) are highly non-linear such that analytical solution can't be obtained. Hence one can obtain its steady-state solution using the perturbation method by putting

$\frac{\partial u}{\partial t} = \frac{\partial \theta}{\partial t} = 0$, and these equations become:

$$S\frac{du}{dy} = \frac{d^2u}{dy^2} + Gr\theta - M^2u \tag{9}$$

$$P_rS\frac{d\theta}{dy} = \left[1 + \frac{4R}{3}(C_T + \theta)^3\right]\frac{d^2\theta}{dy^2} + 4R[C_T + \theta]^2\left(\frac{d\theta}{dy}\right)^2 \tag{10}$$

With fresh initial and boundary conditions:

$$\left.\begin{array}{l} t \le 0, \quad 0 \le y \le 1: \quad u = 0; \quad \theta = 0 \\ t > 0, \ y = 0: \ u = \gamma\frac{du}{dy}, -\frac{d\theta}{dy}\Big|_{y=0} = B_{i1}[1-\theta], \\ \qquad y = 1: u = 0, \ \theta = 0 \end{array}\right\} \tag{11}$$

The solution to the dimensionless set of ordinary differential equations in (9) and (10) can be obtained by representing velocity and temperature as follows:

$$u(y) = u_0(y) + Ru_1(y) + \cdots + \sum R^n u_n \tag{12}$$

$$\theta(y) = \theta_0(y) + R\theta_1(y) + \cdots + \sum R^n \theta_n \tag{13}$$

Putting equations (12) and (13) into equations (9) and (10) respectively and equating like powers of R, one obtains the momentum and energy equations as

$$u(y) = a_3e^{x_1y} + a_4e^{x_2y} + a_5 + a_6e^{P_rSy} + R(G_1e^{x_3y} + G_2e^{x_4y} + G_3 + G_4e^{P_rSy} + G_5ye^{P_rSy} + G_6e^{2P_rSy} + G_7e^{3P_rSy} + G_8e^{4P_rSy}) \tag{14}$$

$$\theta(y) = a_1 + a_2e^{P_rSy} + R(d_1 + d_2e^{P_rSy} + d_3ye^{P_rSy} + d_4e^{2P_rSy} + d_5e^{3P_rSy} + d_6e^{4P_rSy}) \tag{15}$$

At a steady-state the skin frictions and Nusselt number are as follows:

Skin friction $\tau_{0,1}$

$$\tau_0 = \frac{du}{dy}\Big|_{y=0} = a_3x_1 + a_4x_2 + a_6P_rS + Re_1x_3 + Re_2x_4 + Rk_2P_rS + Rk_3 + 2Rk_4P_rS + 3Rk_5P_rS + 4Rk_6P_rS \tag{16}$$

$$\tau_1 = \frac{du}{dy}\Big|_{y=1} = a_3x_1e^{x_1} + a_4x_2e^{x_2} + a_6P_rSe^{P_rS} + Re_1x_3e^{x_3} + Re_2x_4e^{x_4} + Rk_2P_rSe^{P_rS} + Rk_3P_rSe^{P_rS} + Rk_3e^{P_rS} + 2Rk_4P_rSe^{2P_rS} + 3Rk_5P_rSe^{3P_rS} + 4Rk_6P_rSe^{4P_rS} \tag{17}$$

Nusselt number $Nu_{0,1}$

$$Nu_0 = \left.\frac{d\theta}{dy}\right|_{y=0} = a_2P_rS + Rd_2P_rS + Rd_3 + 2Rd_4P_rS + 3Rd_5P_rS + 4Rd_6P_rS \quad (18)$$

$$Nu_1 = \left.\frac{d\theta}{dy}\right|_{y=1} = a_2P_rSe^{P_rS} + Rd_2P_rSe^{P_rS} + Rd_3P_rSe^{P_rS} + Rd_3e^{P_rS} + 2Rd_4P_rSe^{2P_rS} + 3Rd_5P_rSe^{3P_rS} + 4Rd_6P_rS\,e^{4P_rS} \quad (19)$$

Numerical solution

The time dependent solution of (6) and (7) are found using the implicit finite difference method as:

$$\frac{u_i^{j+1}-u_i^j}{\Delta t} + S\frac{u_{i+1}^j-u_{i-1}^j}{2\Delta y} = \left[\frac{u_{i-1}^{j+1}-2u_i^{j+1}+u_{i+1}^{j+1}}{(\Delta y)^2}\right] - M^2u_i^j + Gr\theta_i^j \quad (20)$$

$$P_r\left[\frac{\theta_i^{j+1}-\theta_i^j}{\Delta t} + S\frac{\theta_{i-1}^j-\theta_{i+1}^j}{2\Delta y}\right] = z_1\left[\frac{\theta_{i-1}^{j+1}-2\theta_i^{j+1}+\theta_{i+1}^{j+1}}{(\Delta y)^2}\right] + z_2\left(\frac{\theta_{i-1}^j-\theta_{i+1}^j}{2\Delta y}\right)^2 \quad (21)$$

Subject to the new boundary conditions:

$$\left.\begin{aligned} u_{i-1}^{j+1} &= \gamma\left[\frac{-3u_{i-1}^{j+1}+4u_i^{j+1}-u_{i+1}^{j+1}}{2\Delta y}\right] \\ &-\left[\frac{-3\theta_{i-1}^{j+1}+4\theta_i^{j+1}-\theta_{i+1}^{j+1}}{2\Delta y}\right] = B_{i1}\left[1-\theta_i^j\right] \qquad for\ all\ i=0 \\ u_M^j &= 0, \theta_M^j = 0, \text{for all i} = \text{M} \end{aligned}\right\} \quad (22)$$

Further simplification (20) and (21) respectively give:

The velocity equation:

$$B_lu_0^{j+1} + B_cu_1^{j+1} + B_r\,u_2^{j+1} = r_1u_0^j - r_1u_2^j + (1-\Delta tM^2)u_1^j + \Delta tGr\theta_1^j \quad (23)$$

Temperature equation:

$$A_l\theta_{i-1}^{j+1} + A_c\theta_i^{j+1} + A_r\theta_{i+1}^{j+1} = Pr\theta_i^j + \Pr r_1\,\theta_{i+1}^j - \Pr r_1\,\theta_{i-1}^j + z_2r_3\left(\theta_{i-1}^j - \theta_{i+1}^j\right)^2 \quad (24)$$

Due to convectivity of the boundary of the momentum and energy equations at $y = 0$, from equation (22) we have

$$u_{i-1}^{j+1} = \gamma\left[\frac{-3u_{i-1}^{j+1}+4u_i^{j+1}-u_{i+1}^{j+1}}{2\Delta y}\right] \quad (25)$$

$$\theta_{i-1}^{j+1} = \frac{(4-2\Delta yB_{i1})}{3}\theta_i^{j+1} - \frac{1}{3}\theta_{i+1}^{j+1} + \frac{2}{3}\Delta yB_{i1} \quad (26)$$

$$\theta_{i-1}^{j} = \frac{(4-2\Delta y B_{i1})}{3}\theta_i^j - \frac{1}{3}\theta_{i+1}^j + \frac{2}{3}\Delta y B_{i1} \quad (27)$$

Putting $i = 1$ into (25), (26) and (27) substituting into (23) and (24) and simplify, then the velocity and temperature equation respectively become:

$$\left(\frac{4}{3}B_l - \frac{2\Delta y}{3\gamma}B_l + B_c\right)u_1^{j+1} + \left(B_r - \frac{Bl}{3}\right)u_2^{j+1} = \left(r_1\frac{4}{3} - \frac{2\Delta y}{3\gamma}r_1 + 1 - \Delta t M^2\right)u_1^j - \left(\frac{1}{3}r_1 + r_1\right)u_2^j + \Delta t Gr\theta_1^j \quad (28)$$

$$\left(\frac{(4-2\Delta y B_{i1})}{3}A_l + A_c\right)\theta_1^{j+1} + \left(A_r - \frac{A_l}{3}\right)\theta_2^{j+1} + \frac{2}{3}A_l\Delta y B_{i1} = \left(Pr - \frac{(4-2\Delta y B_{i1})}{3}\Pr r_1\right)\theta_1^j + \frac{4}{3}\Pr r_1\,\theta_2^j - \frac{2}{3}\Pr r_1\,\Delta y B_{i1} + z_2 r_3\left(\frac{(4-2\Delta y B_{i1})}{3}\theta_1^j - \frac{4}{3}\theta_2^j + \frac{2}{3}\Delta y B_{i1}\right)^2 \quad (29)$$

Result validation

Numerical solution efficiency is authenticated by comparing with the steady-state solution obtained by the regular perturbation method. The perfect agreement was found between the steady-state and unsteady-state solution at large values of time t, It was also found that steady-state for both velocity and temperature of water and air were reached at the same magnitude but at a different time see the figure 2 below:

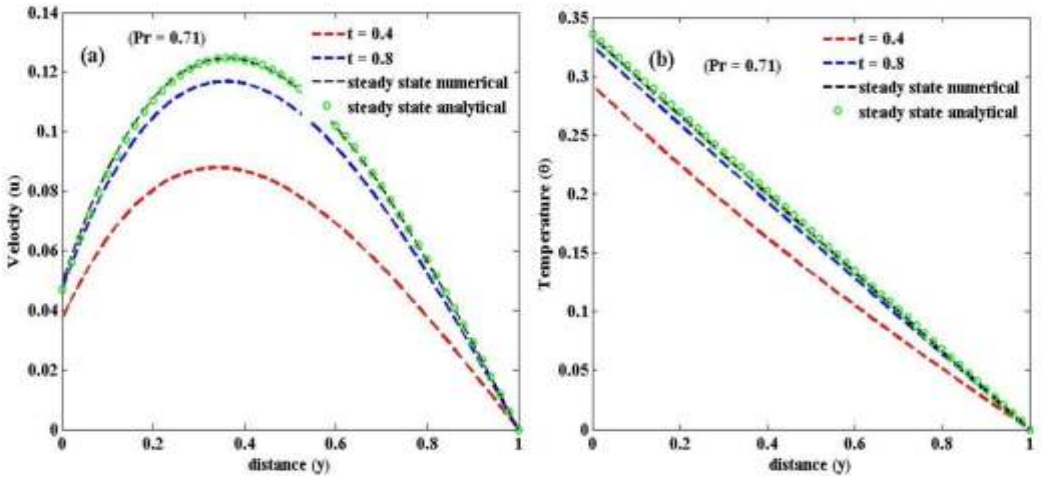

Figure 2: Upshot of time on the steady-state velocity and temperature profiles ($\lambda = 0.3, S = 0.03$)

Results and discussion

The present work, studies the steady/unsteady state natural convection heat transfer flow through vertical porous plates in the presence of thermal radiation, under the influence of a uniform magnetic field subject to slip and convective boundary conditions. The system of governing equations (6) and (7) with the boundary conditions (8) is solved using the perturbation series method to obtain the analytical solution, the whereas implicit finite difference method was used to obtain the numerical solution. The impact of the flow governing parameters i.e. magnetic parameter (M) , radiation parameter (R) , temperature difference parameter (C_T), Prandtl number (Pr), Biot numbers (B_{i1}), suction/injection parameter (S), slip parameter (λ) and Grashof number (Gr) on the pertinent parameters on velocity $u(y,t)$, temperature $\theta(y,t)$, skin friction $\tau_{0,1}$ and Nusselt number $Nu_{0,1}$, have been analyzed and deliberated using line graph as shown from figure 2 to figure 28. Pr = 0.71 and 7.0, which physically represent air and water respectively were used, while all other parameters $M=1$, $R= 0.0001$, $C_T = 0.01$, $B_{i1} = 0.5, S = 0.1$ *and* $Gr = 5.0$ are used for the analysis unless otherwise stated.

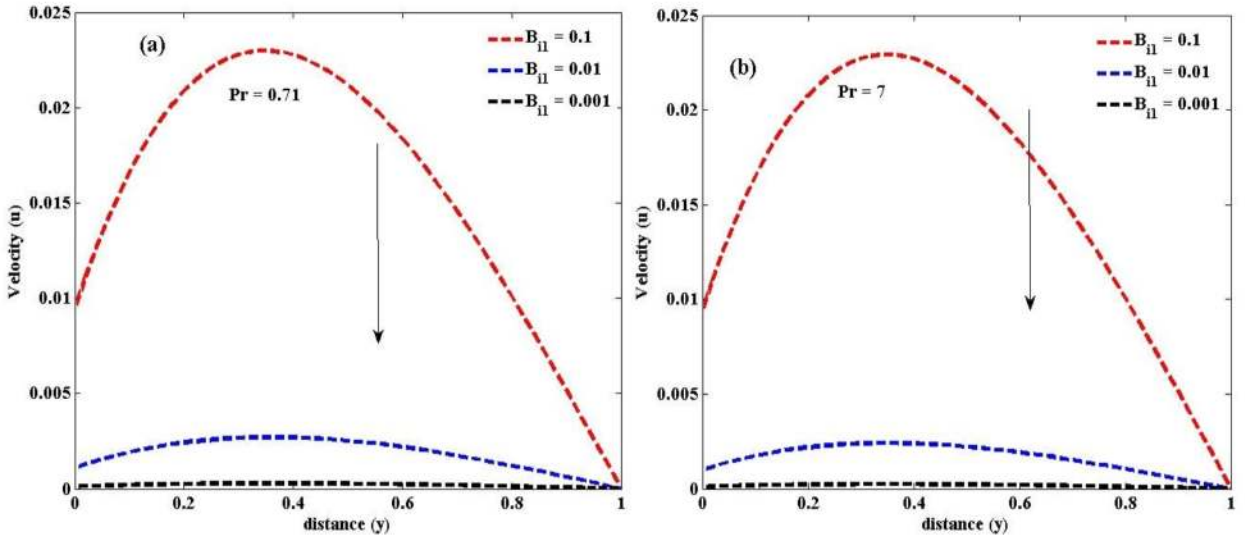

Figure 3: Upshot of B_{i1} on $u(y,t)$

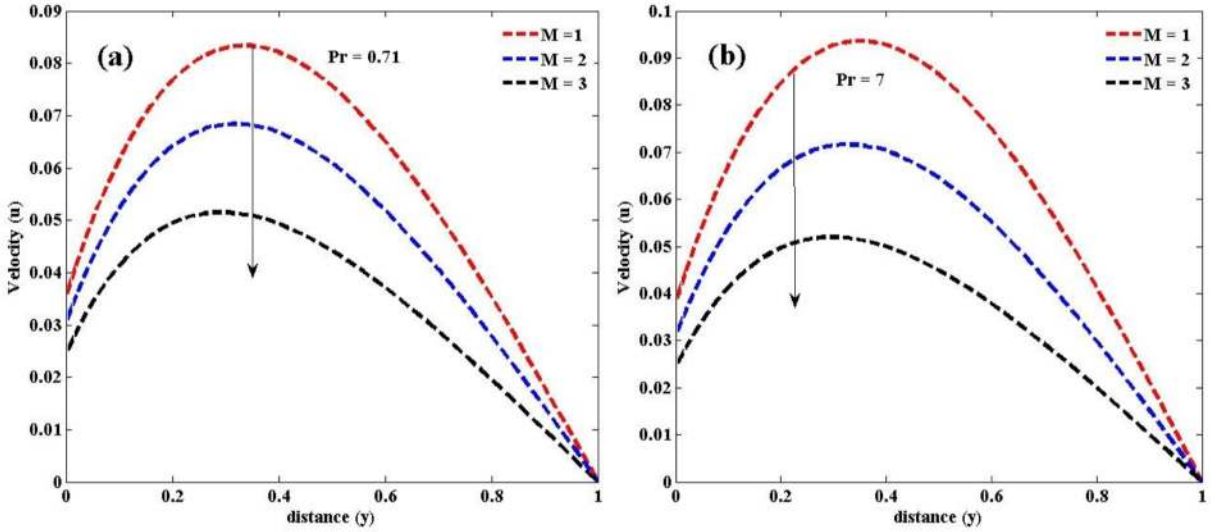

Figure 4: Upshot of M on $u(y,t)$

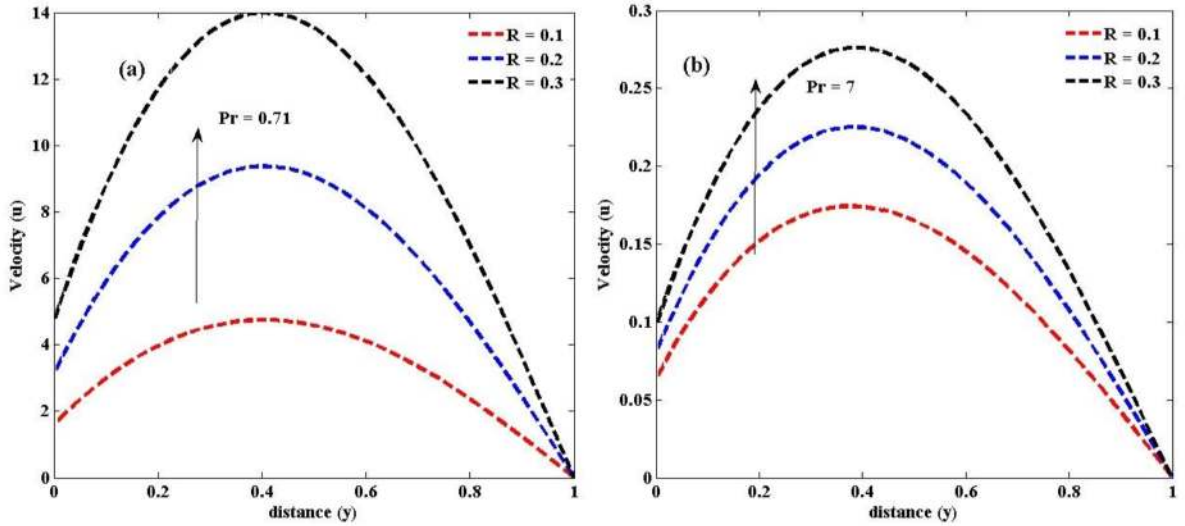

Figure 5: Upshot of R on $u(y,t)$

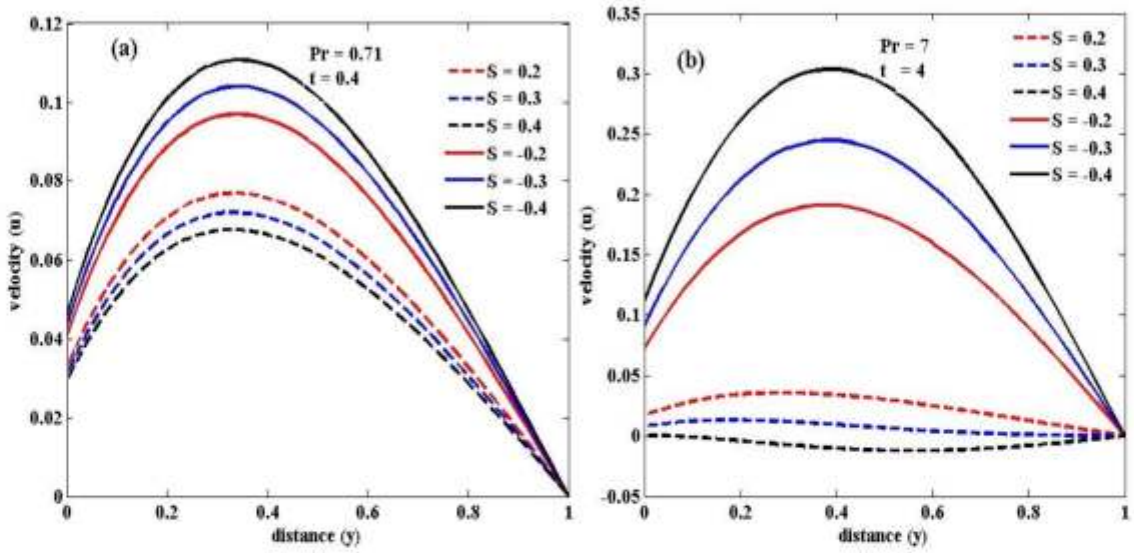

Figure 6: Upshot of S on $u(y,t)$

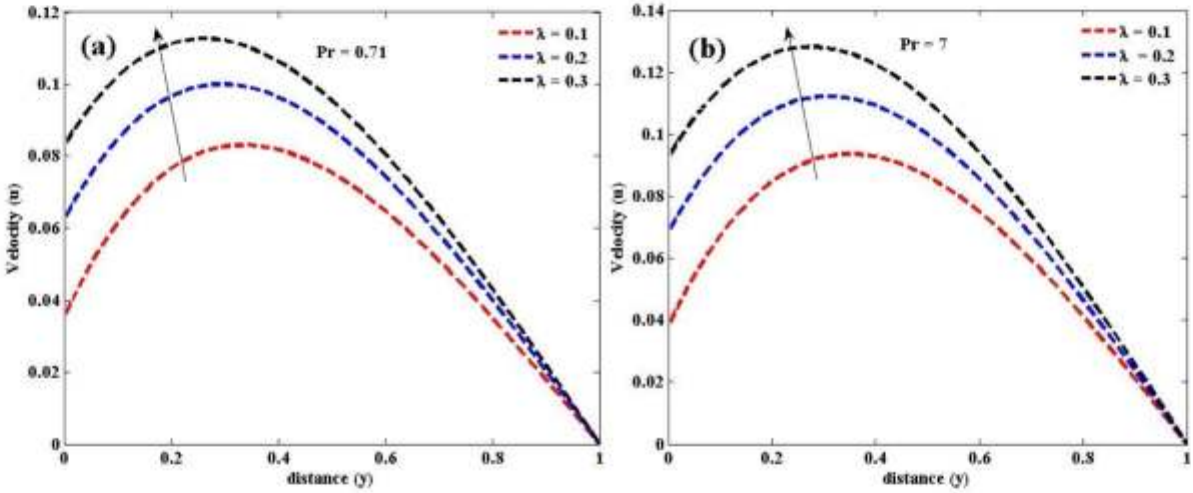

Figure 7: Upshot of$\boldsymbol{\lambda}$ on $u(y,t)$

Figures 3 to 7 show the consequence of dimensionless control flow parameters on $u(y,t)$. The impact of B_{i1} on $u(y,t)$ for air and water is discussed in Figure 3a and b. velocity decreases with decreasing B_{i1}. It also shows that, as B_{i1} approaches zero the velocity also diminishes. Figure 4a and b illustrate the upshot of M on $u(y,t)$. It indicates that, for both air and water the velocity decrease with increasing M. This conclusion agrees with the fact that, the magnetizing field exerts retarding force on the free convective fluids. Figures 5a and b illustrate the outcome of R on $u(y,t)$. It displays that velocity enhances with increasing R. Figures 6a and b demonstrate the influence of S on $u(y,t)$. The velocity of the fluid slows up due to suction while it improved due to injection. The physical cause for such a manner is that while stronger blowing is distributed, the heated fluid is pushed further from the wall where the buoyancy forces can turn to accelerate the flow with less impact on the viscosity. This effect acts to increase the shear by growing the maximum velocity within the boundary layer. Equal attitude operates but in opposite direction in the case of suction. It is also noticed that, in the case of suction, velocity of the fluid travels away from the channel center line towards the plate and, in case of injection, the maximum velocities are lifted towards the right porous plate. Figure 7 shows the influence of $\boldsymbol{\lambda}$ on $u(y,t)$. It is observed that velocity enhances with increasing $\boldsymbol{\lambda}$ while other controlling parameters assume arbitrary values.

Temperature profile

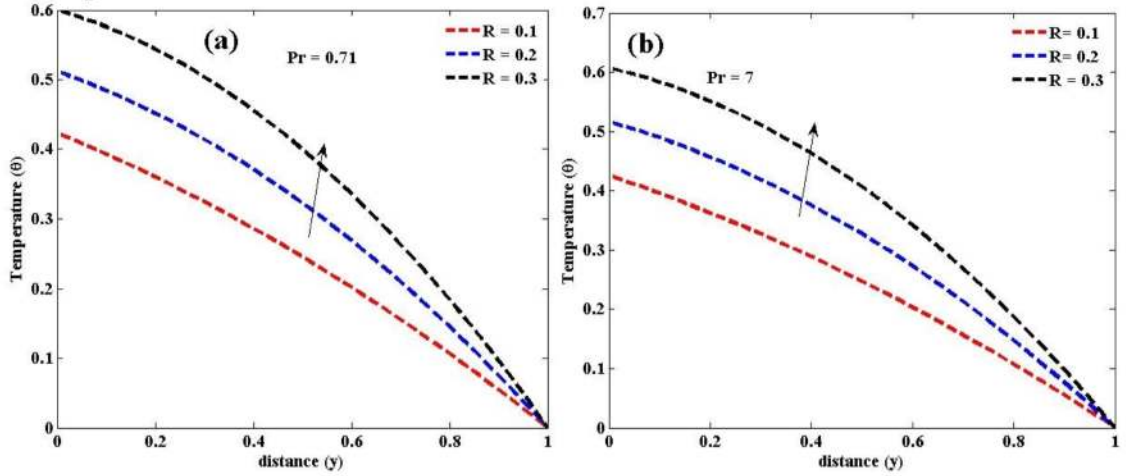

Figure 8: influence of R on $\theta(y,t)$

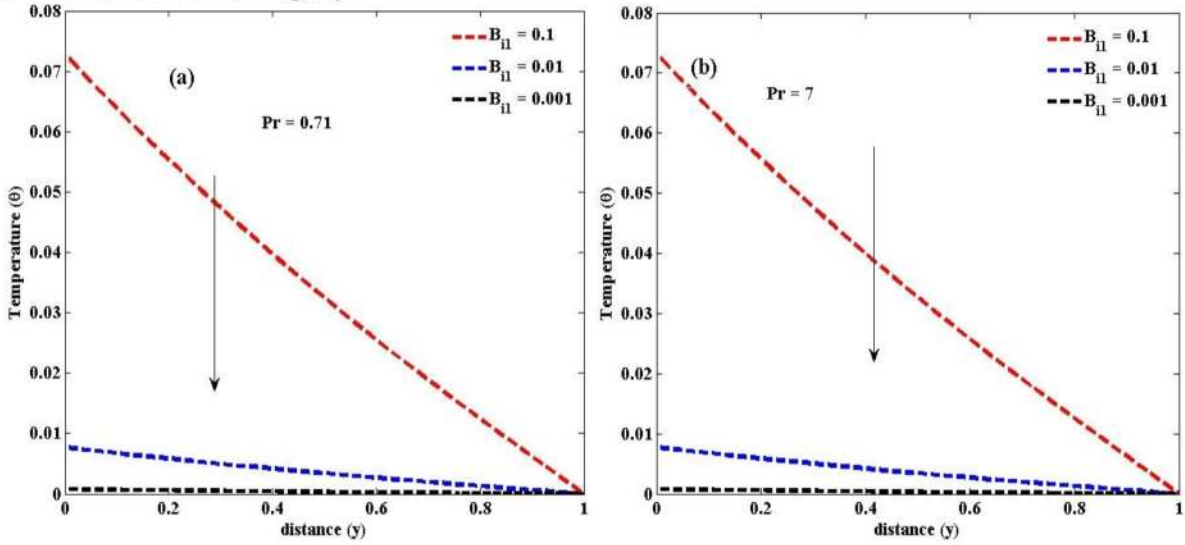

Figure 9: influence of B_{i1} on $\theta(y,t)$

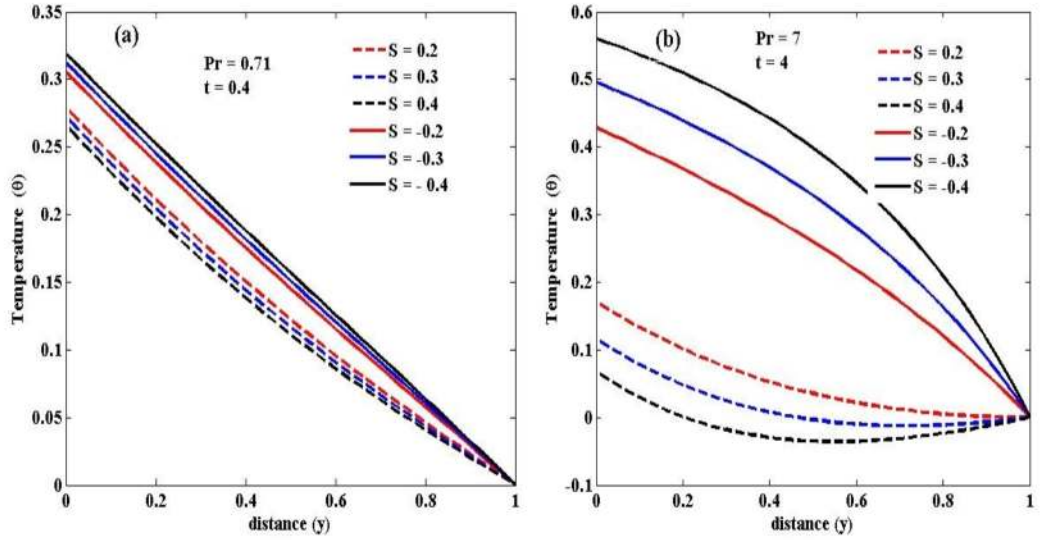

Figure 10: influence of Son $\theta(y,t)$

Figures 8 to 10 depict the sway of pertinent parameters on $\theta(y,t)$. Figures 8a and b demonstrate the consequence of R on $\theta(y,t)$. It shows that temperature enhances with the rise in R while other controlling parameters assumed arbitrary values. Figure 9a and b demonstrates the effect of B_{i1} on $\theta(y,t)$. It is observed from the figure that temperature decreases with decreasing B_{i1} and as B_{i1} approaches zero, the left wall is insulated. Figure 10a and b illustrate the influence of S on $\theta(y,t)$. It is observed that temperature declines due to suction but upsurges due to injection. In case of suction, the fluid at ambient situation is taken closer to the surface and condenses the thermal boundary layer thickness. The same attitude works but in opposite direction in case of injection.

Skin friction

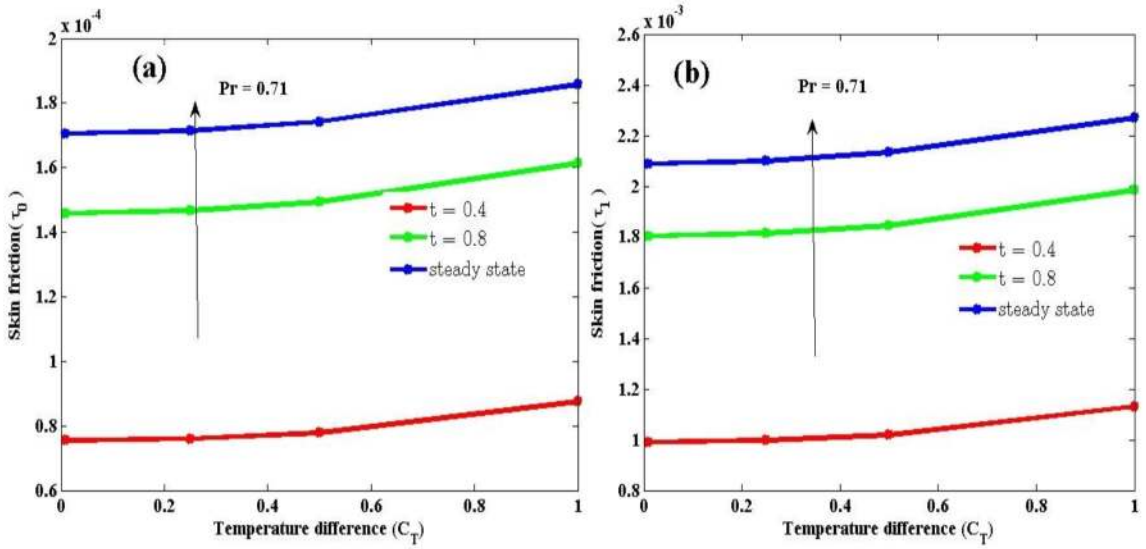

Figure 11: effect of t and C_T on $\tau_{0,1}$ (Pr = 0.71)

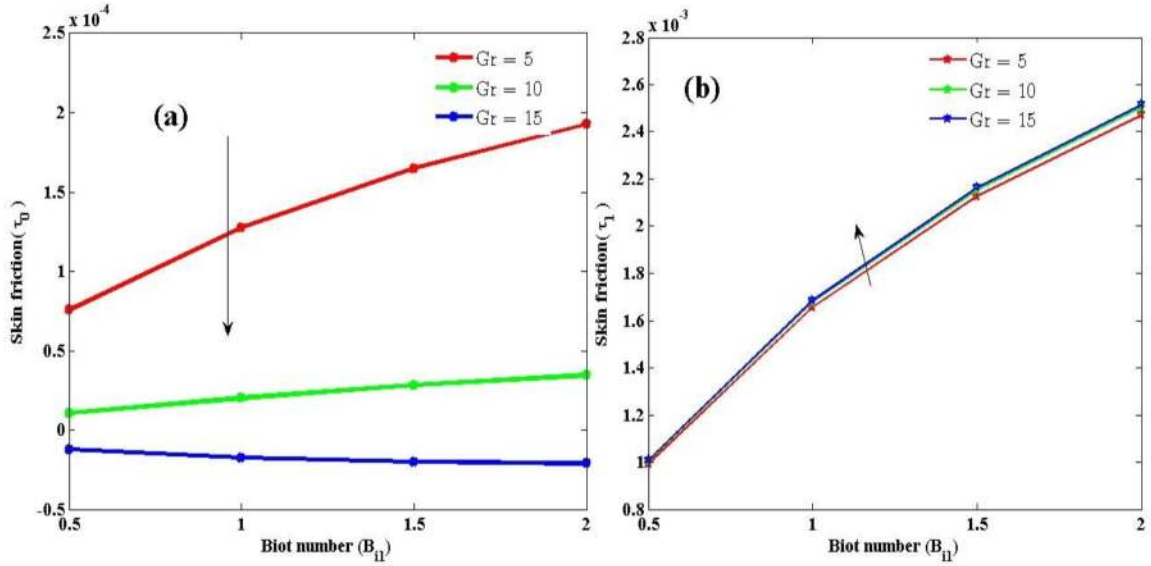

Figure 12: effect of Gr and B_{ii} on $\tau_{0,1}$ (Pr = 0.71)

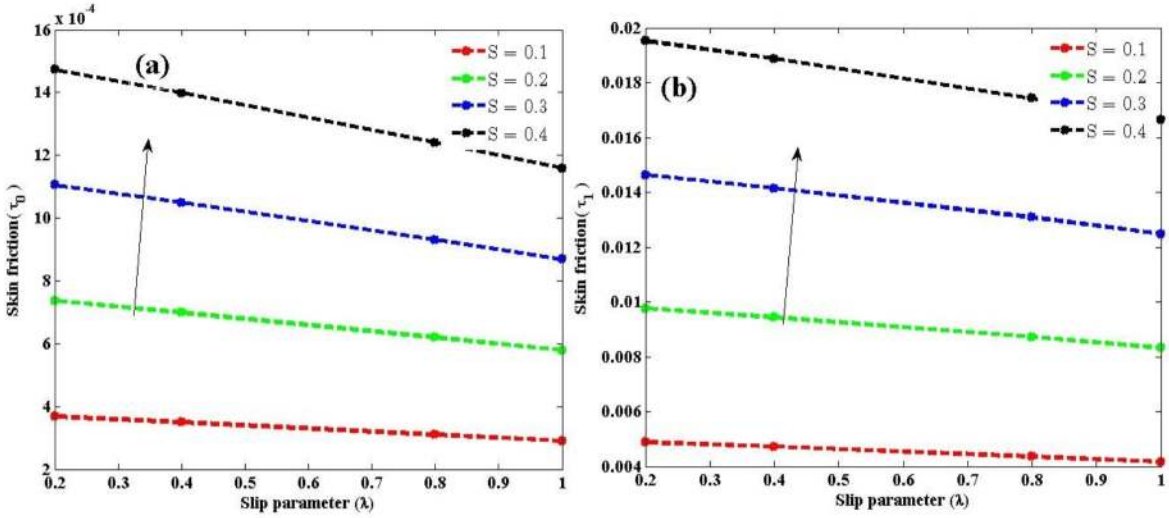

Figure 13: effect of S and λ on $\tau_{0,1}$ (Pr = 0.71, t = 0.4)

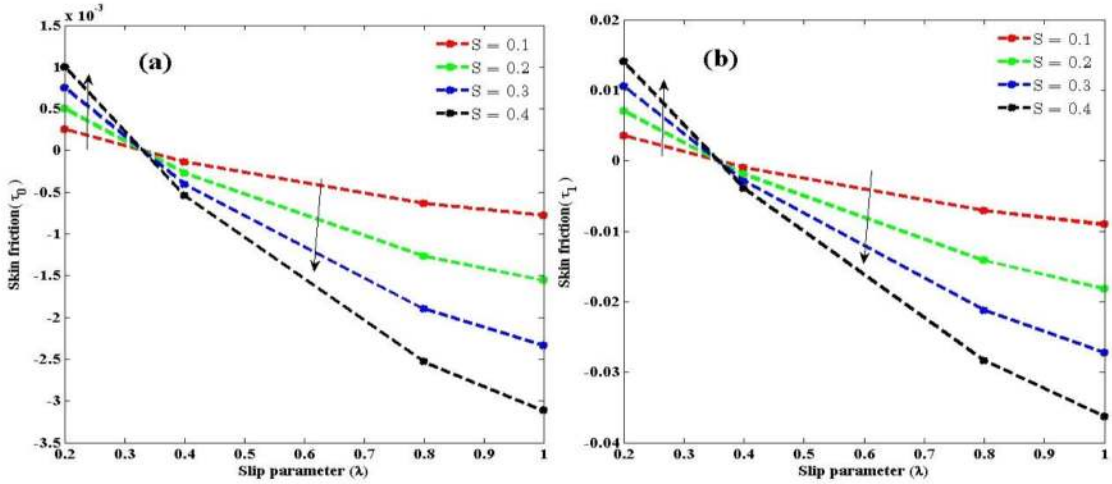

Figure 14: effect of S and λ on $\tau_{0,1}$ (Pr = 7.0, t = 4.0)

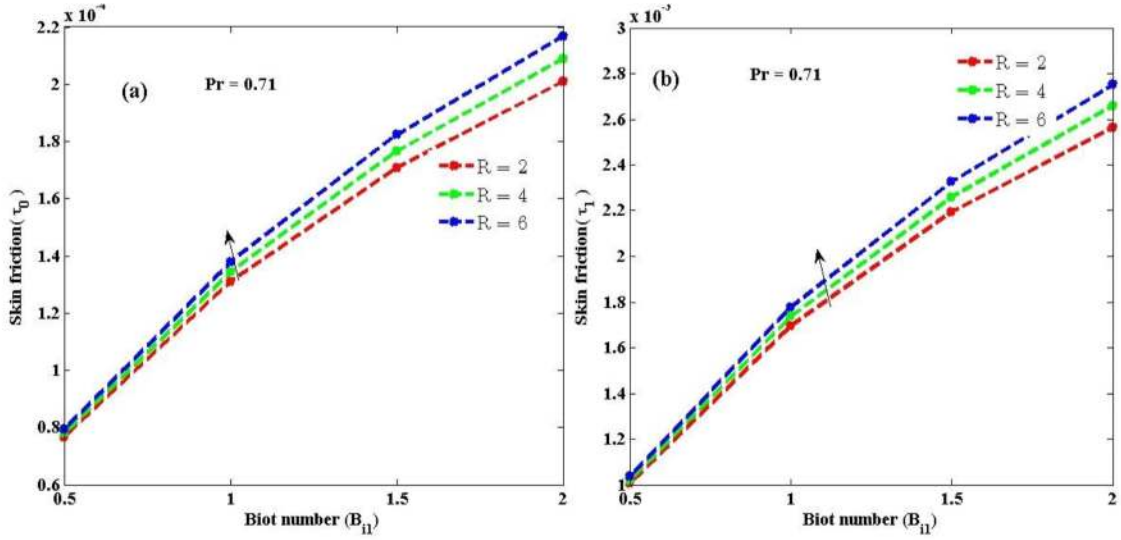

Figure 15: effect of R and B_{i1} on $\tau_{0,1}$ (Pr = 0.71, t = 0.4, S = 0.02)

Figures 11 to 15 demonstrates the influence of pertinent parameters on $\tau_{0,1}$. Figures 11a and b illustrate the upshot of time and C_T on $\tau_{0,1}$. Skin friction increases with increasing time and C_T and

attains steady state after large value of time at both walls. Figures 12a and b show the influence of Gr and B_{i1} on $\tau_{0,1}$. It is obseved that τ_0 decline with growing Gr τ_1 enhances with increasing Gr. It is also obseverved that increase in B_{i1} at letf wall leads to decline in τ_0; while increase in B_{i1} at right wall leads to upsurge in τ_0. Figures 13 and 14 depict the effect of S and λ on $\tau_{0,1}$ for air and water respectively. It is observed from the figures that $\tau_{0,1}$ upsurges with growing S. It is also witnessed that, at $\lambda > 0.3$ the skin friction of (Pr = 7.0) changes its state and starts declining along the flow. Whereas $\tau_{0,1}$ drops with growing λ at both walls. Figures 15a and b describe the consequence of R on $\tau_{0,1}$. It is observed that, $\tau_{0,1}$ improve with growing R at both left and right walls.

Nusselt number

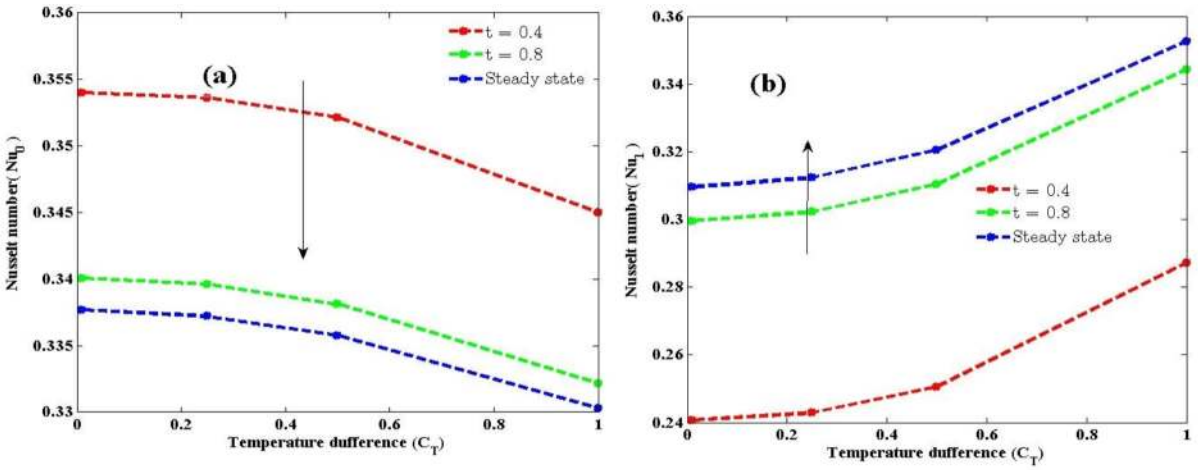

Figure 16: Sway of t and C_T on $Nu_{0,1}$ (Pr = 0.71)

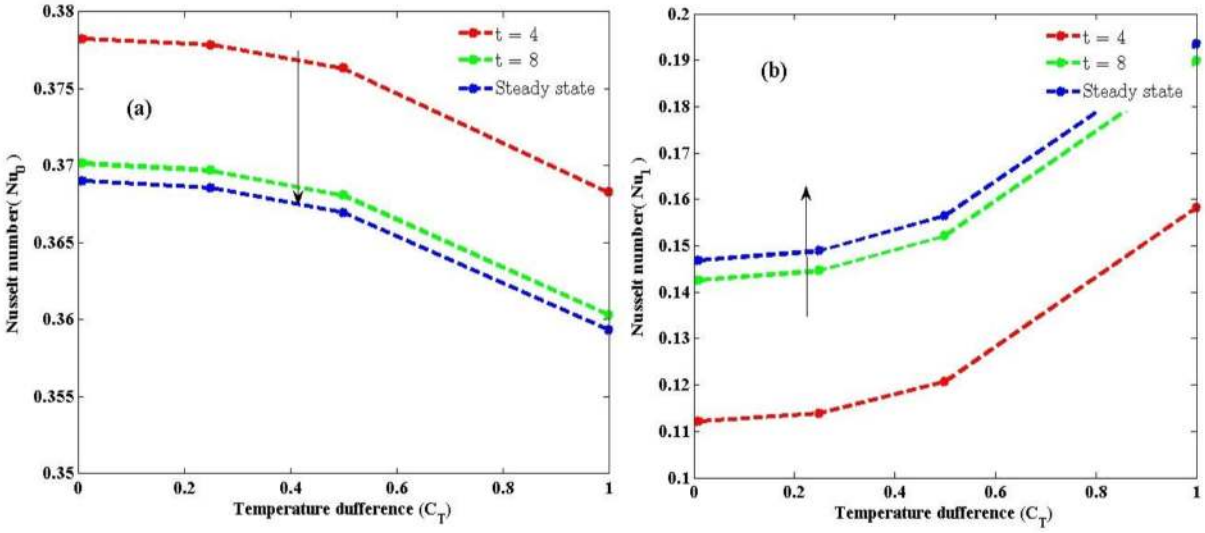

Figure 17: Sway of t and C_T on $Nu_{0,1}$ (Pr = 7.0)

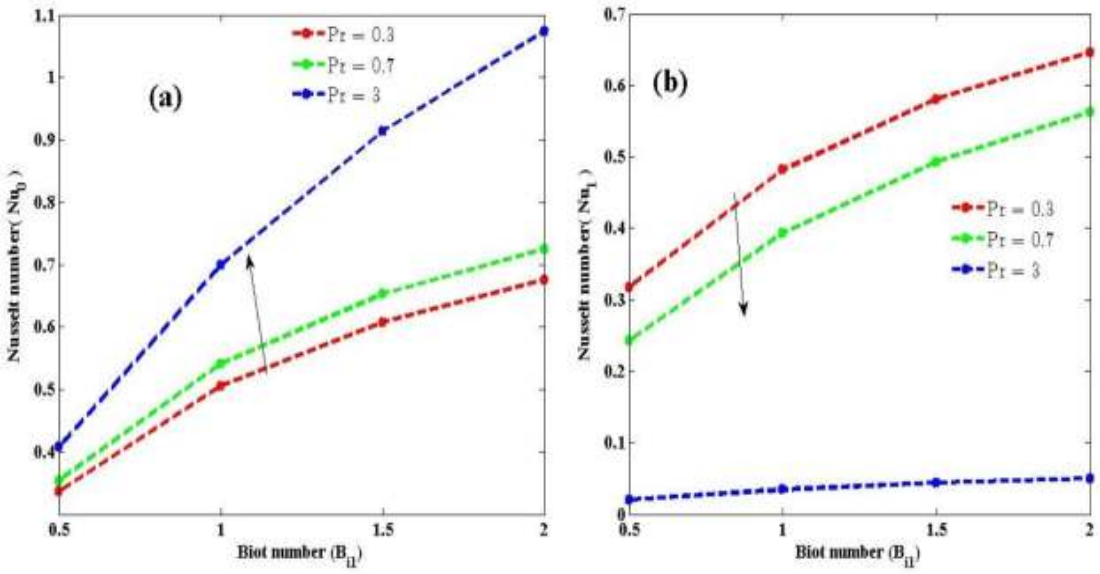

Figure 18: Sway of Pr and B_{i1} on $Nu_{0,1}$ (t= 0.4)

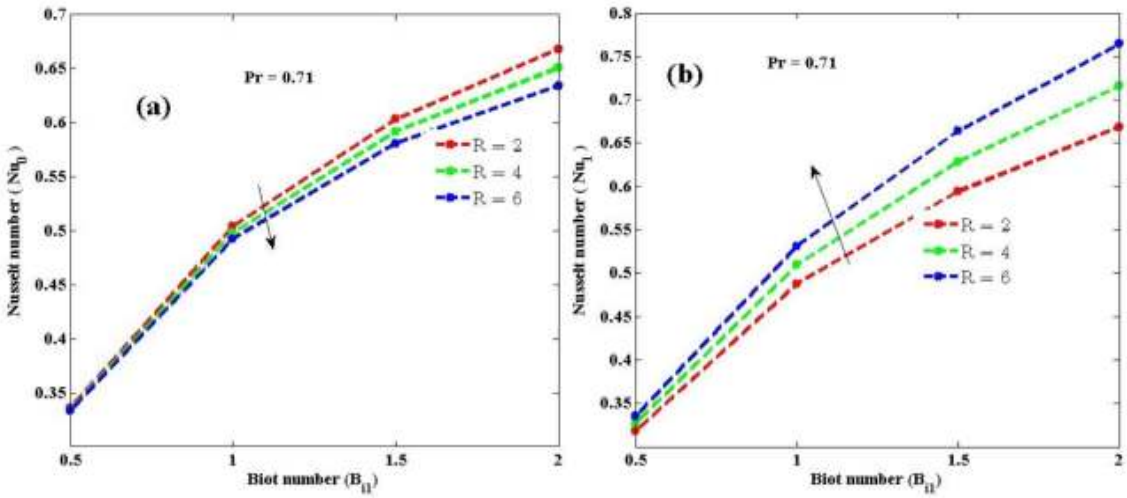

Figure 19: Sway of R and B_{i1} on $Nu_{0,1}$ (t= 1.2)

Figures 16 to 19 describe the influence of controlling parameters on $Nu_{0,1}$. Figures 16 and 17 illustrate the sway of t and C_T on $Nu_{0,1}$. It is observed that, at y = 0 Nu_0 drops with growing t and C_T and attains steady state for large value of time while other controlling parameters assume fixed values; whereas Nu_1 enhances with increasing t and C_T at the right wall $(y = 1)$ and also attains steady state. Figure 18a and b shows the impact of Pr and B_{i1} on $Nu_{0,1}$ for both air and water. It is observed that, at left wall $(y = 0)$, increase in Pr leads to increase in Nu_0 but Nu_1 decline when Pr upsurges; whereas increase in B_{i1} leads to increase in $Nu_{0,1}$. Figures 19a and b demonstrate the influence of R on $Nu_{0,1}$. It is noticed that Nu_0 decline with increasing R at left wall, but Nu_1 .improves with growing R at right wall.

Conclusion

The Steady/unsteady heat transfers flow of viscous, non-compressible, and electrically conduction fluid (MHD) flow through vertical parallel porous walls due to convective boundary conditions in the presence of slip velocity has been studied. The upshot of non-dimensional controlling parameters on velocity $u(y,t)$, temperature $\theta(y,t)$, skin friction $\tau_{0,1}$ and, Nusselt number $Nu_{0,1}$ were discovered and reported using a line graph. The finding discovered that:

i. velocity and temperature improve with growing time and attain a steady state for large value of t
ii. upturn in $B_{i1}, \lambda,$ $and\ R$ boosts the velocity
iii. Rise in R, $C_T\ and\ B_{i1}$ enriches temperature
iv. velocity and temperature decrease with increasing S and M
v. Increase in $R, Gr\ and\ C_T$ enhances skin friction
vi. Skin friction decreases with increasing $Gr,\ and\ B_{i1}$ at convected wall (y=0) but increases at non-convected wall (y=1).
vii. Skin friction increases with $R, C_T\ and\ S$ but declines with increasing M and λ at both walls.
viii. Nusselt number upsurge with growing time and Pr at left wall $(y = 0)$ while drops with increasing time and Pr at right wall $(y = 1)$
ix. Increase in $R, and\ C_T$ lead to decrease in heat transfer at left wall while increase at right wall
x. Increase in Biot number leads to increase in heat transfer at both walls

Reference

Dulal P. and Babulal T. (2013) "Influence of hall current and thermal radiation on MHD convective heat and mass transfer in a rotating porous channel with chemical reaction, International Journal of Engineering Mathematics, Article ID 367064, 13 pp

Ellahi R., Sultan Z. A., Abdul B. and Majeed A. (2018) "Effects of MHD and slip on heat transfer boundary layer flow over a moving plate based on specific entropy generation", Journal of Taibah University for Science, 12:4, 476-482,

Fenug O.J., Adigun J. A., Hassan A.R., and Olanrewaju P.O. (2015) "Comment on the effects of Buoyancy Force and Fluid Injection/Suction on a Chemically Reactive MHD Flow with Heat and Mass Transfer over a Permeable Surface in the Presence of Heat Source/Sink", International Journal of Scientific & Engineering Research, Volume 6,

Goyal M. and Rathore K. S. (2017) "Effect of Suction/Injection, radiation and heat source/sink On MHD flow and heat transfer over an exponentially stretching sheet", Journal of Rajasthan Academy of Physical Sciences, ISSN: 0972-6306; Vol.16, No.1&2, pp 83-92

Gnaneswara R M. (2017) Velocity and thermal slip effects on MHD third-order blood flow in an irregular channel through porous medium with homogeneous/heterogeneous reactions, Nonlinear Engineering 6(3): 167–177

Hamza S. E.E. (2019) The Effect of Suction and Injection on MHD Flow between Two Porous Concentric Cylinders Filled with Porous Medium, Journal of Advances in Physics, Vol 16 ISSN: 2347-3487

Ighoroje W., Okuyade A. and Tega O. (2019) "Unsteady MHD Free Convective Chemically Reacting Flow over a Heated Vertical Plate with Heat Source, Thermal Radiation and Oscillating Wall Temperature, Concentration and Suction Effects", American Journal of Fluid Dynamics, (2019) 9(2): 35-43

Isah B. Y, Jha B. K, Lin J. E. (2018) "On a Couette Flow of Conducting Fluid, International Journal of Theoretical and Applied Mathematics", Vol. 4, No. 1, pp. 8-21.

Jha B. K., Isah B.Y. and Uwanta I. J. (2016) "Combined effect of suction/injection on MHD free-convection flow in a vertical channel with thermal radiation, Ain Shams Engineering Journal

Jha, B. K. Luqman A. A. and Michael O. O. (2018) "Unsteady hydro magnetics-free convection flow with suction/injection", Journal of Taibah University for Science, (2018) 13:1, pp: 136-145

Jitender S., Mahabaleshwar U. S and Bognár G.(2019) "Mass Transpiration in Nonlinear MHD Flow Due to Porous Stretching Sheet", Journal of scientific reports, *9:18484*

Kalidas D. (2014) "Radiation and melting effects on MHD boundary layer flow over a moving surface", Ain Shams Engineering Journal, vol. 5, pp 1207- 1214

Kho Y B, Hussanan A, Mohamed M. K A, Sarif N. M, Ismail Z. and Salleh M. Z, (2018) "Thermal radiation effect on MHD Flow and heat transfer analysis of Williamson Nano-fluid past over a stretching sheet with constant wall temperature" Journal of physics conference series vol. 890 pp. 8 – 10

Manjula D and Jayalakshmi K. (2018) "Slip Effects on Unsteady MHD and Heat Transfer Flow over A Stretching Sheet Embedded with Suction in A Porous Medium Filled With A Jeffrey Fluid". International Journal of Research ISSN NO: 2236-6124

Misra J.C and Sinha A. (2013) "Effect of thermal radiation on MHD flow of blood and heat transfer in a permeable capillary in stretching motion", Heat and mass transfer, vol. 49, pp. 617 – 628

Mohammad A. H, Anwar H. A. and Mohammad A. A. (2020) "The Effect of Slip Velocity and Temperature Jump on the Hydrodynamic and Thermal Behaviors of MHD Forced Convection Flows in horizontal Micro-channels", Iranian Journal of Science and Technology:

Mohamed A. and Ahmed A. A.(2018) "Influences of Slip Velocity and Induced Magnetic Field on MHD Stagnation-Point Flow and Heat Transfer of Caisson Fluid over a Stretching Sheet", Mathematical Problems in Engineering, Volume 2018, Article ID 9402836, 11 pages

Mohammad M. R, Behnam R., Navid F. and Saied A. (2014) "Free convective heat and mass transfer for MHD ?uid ?ow over a permeable vertical stretching sheet in the presence of the radiation and buoyancy e? ects" Ain Shams Engineering Journal 5(3):901–912

Nandal J. and Kumari S. (2019) "The effect of slip velocity on unsteady peristalsis MHD blood flow through a constricted artery experiencing body acceleration", *Int. J. of Applied Mechanics and Engineering, vol.24, No.3, pp.645-659.*

Rehman S., Idrees M., Shah R. A. and Khan Z (2019) "Suction/injection effects on an unsteady MHD Casson thin film flow with slip and uniform thickness over a stretching sheet along variable

flow properties", *Boundary Value Problems*: 26

Sasikumar J. and Govindarajan A. (2018) "Effects of Suction and Injection on MHD oscillatory convective Flow in an inclined channel with oscillating wall temperatures and thermal radiation", International Journal of Pure and Applied Mathematics, Volume 119 No. 13, pp: 289-297 ISSN: 1314-3395

Siti S. P. M. I., Norihan M. A, Roslinda N, Norfifah B, and Fadzilah M. A. (2017) "The effect of convective boundary condition on MHD mixed convection boundary layer flow over an exponentially stretching vertical sheet", Journal of Physics: Conf. Series 949 012016.

Upreti H, Pandey A. K, and Kumar M (2020) "Thermophoresis and suction/injection roles on free convective MHD flow of Ag–kerosene oil Nano fluid", *Journal of Computational Design and Engineering*, 7(3), 386–396

Uwanta I. J. and Hamza M. M. (2014), "Effect of Suction/Injection on Unsteady Hydromagnetic convective Flow of Reactive Viscous Fluid between Vertical Porous Plates with Thermal Diffusion", Hindawi Publishing Corporation International Scholarly Research Notices, Volume 2014, Article ID 980270, 14 pages

Venkateswarlu M. and Venkata L. D. (2016) Slip velocity distribution on MHD oscillatory Heat and mass transfer flow of a viscous Fluid in a parallel plate channel, Ganit *J. Bangladesh Math. Soc.* (ISSN 1606-3694) Vol: 36 PP: 91-112

Wubshet I, (2016) "The effect of induced magnetic field and convective boundary condition on MHD stagnation point flow and heat transfer of upper-convected Maxwell fluid in the presence of nanoparticle past a stretching sheet" Propulsion and Power Research p p 164-175

Yahaya S D, Zainal A, Zuhaila I and Faisal S, (2018) "Effects of slip and convective conditions on MHD flow of Nano-fluid over a porous nonlinear stretching/shrinking sheet", vol. 16 pp 213-229

Abacus (Mathematics Science Series)
Vol. 49, No 3, September. 2022

THE EFFECT OF DAMPING ON THE RESPONSE OF BEAM RESTING ON PASTERNAK FOUNDATION SUBJECTED TO MOVING LOAD

[1,]Famuagun K. S., [2]Adedowole A. [3]Akinremi B.V.

[1,3] Department of Mathematics, Adeyemi Federal University of Education Ondo, Ondo, Ondo State, Nigeria.
[2]Department of Mathematics, Adekunle Ajasin University Akungba Akoko, Ondo State, Nigeria.

Abstract

The paper examined the dynamic analysis of a damped beam resting on a uniform foundation subjected to distributed moving Load. The governing equation of motion of the beam was transformed into a coupled ordinary differential equations using separation of variables technique. The analytic solution valid for a simply supported boundary condition was obtained using a special form of convolution integral known as Duhamel's integral. The effect of damping on the displacement of the beam was investigated for when damping ratio $\zeta < 1$, $\zeta = 1$ *and* $\zeta > 1$ *at various values of dimensionaless time* $\bar{t}$. *It is found that the amplitude of the displacement of the beam is maximum for absolute values of deflection when the damping values are zero for damping ratio* $\zeta < 1$. *The deflection curve attains maximum amplitude at dimensionless time* $\bar{t} = 10$, *which implies that the greatest amplitude of the beam displacement occurred at the middle-span of the structure. Finally, it was evidently observed that as the damping values are increased for damping ratio* $\zeta > 1$, *the amplitude displacement of the vibrating beam decreases. This analysis may be used for validation of structural dynamical system in Civil Engineering most especially in Bridge Engineering.*

Key Words: Damping Response, Pasternak Foundation, Moving Load

Introduction

The dynamic response of structures subjected to moving Load is an interesting study area in structural dynamic which has its application in several fields such as Applied Mathematics, Engineering and Applied Physics. A large number of studies have been devoted by many researchers, to this subject matter for example Fryba L. (1972) worked on the vibration of solids and structures under moving Load, Gbadeyan J.A. and Oni S.T, (1995) investigated the dynamic behaviours of beams and rectangular plates under moving Loads and in 2007, Gbadeyan J.A and Dada M.S. studied the effect of linearly varying distributed moving Loads on Beam. None of the aforementioned researcher above incorporated damping mechanism into their mathematical models. Also in all these studies, a number of foundation models having various degree of sophistication have been used to capture the complex behaviour of the soil. The simplest model for the soil is the one-parameter Winkler model. In this model, the foundation reaction is assumed to be proportional to the vertical displacement of the foundation at the same point and consequently. The Winkler model does not accurately represent the characteristics of practical foundation soils and the predictions as observed in Lev Khazanovich (2003) exhibit discrepancies. One of the most important deficiencies of Winkler model is that it assumes no interaction between the adjacent springs and thus neglects the vertical shearing stress that occurs within subgrade materials. In addition, a displacement discontinuity appears between the loaded and the unloaded part of the foundation surface but, in reality, the soil surface does not show any discontinuity. In order to address the deficiencies of Winkler foundation model, a more realistic elastic foundation model, Bi-parametric, known as Pasternak foundation model, which considers the continuity of the surface displacement beyond the region of the load is considered in this study.

Furthermore, it is noted that, in most of the investigations available in literature, the problem

of assessing the dynamic behaviour of structural members carrying moving loads has been restricted to the case in which the moving loads are simplified as moving concentrated forces. However, in practice, it is well known that loads are actually distributed over a small segment or over the entire length of the structural member they traverse. **T**his paper attempts to discuss the vibration analysis of damped structure resting on Pasternak foundation under the influence of a distributed moving load.

Formulation of the Problem

We consider a distributed load advancing uniformly on a beam with constant velocity U. The load is assumed to strike the beam at time t = 0 and travels across it as shown below.

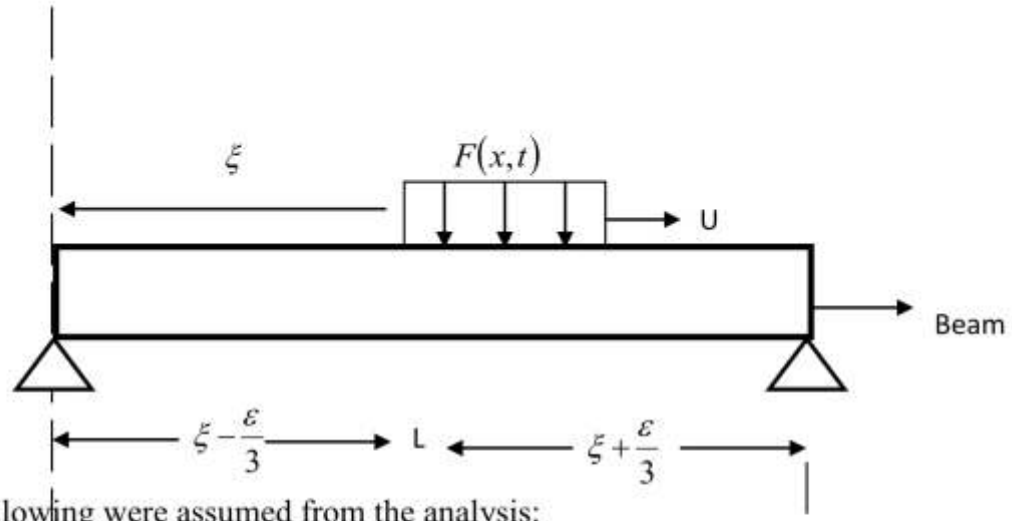

The following were assumed from the analysis;

1. The beam characteristics are described by Euler-Bernoulli equation.
2. The load moves at constant velocity and keeps in contact with the beam at all times.
3. The transverse displacement response $V(x,t)$ is a product of position and time.

Based on the above descriptions and assumptions, the problem of interest is described to be a partial differential equation of the form:

$$\frac{\partial^2}{\partial x^2}\left[N_1(x,t)\right] + N_2(x,t) + N_3(x,t) + K(x)V(x,t) - G(x)N_4(x,t) = F(x,t) \quad (1)$$

where

$N_1(x,t)=EI(x)\left(\frac{\partial^2 V(x,t)}{\partial x^2}+a_1\frac{\partial^3 V(x,t)}{\partial x^2\partial t}\right)$ is the basis of moment-curvature of the system

$N_2(x,t)=m(x)\frac{\partial^2 V(x,t)}{\partial t^2}$ is the force due to acceleration of the beam,

$N_3(x,t)=C(x)\frac{\partial V(x,t)}{\partial t}$ is the force due to damping effect,

the expression $K(x)V(x,t)-G(x)N_4(x,t)$ represents the foundations on which the structure is resting on and $N_4(x,t)=\frac{\partial^2 V(x,t)}{\partial x^2}$ represents the differential form of the displacement

Where $F(x,t)$ is the applied moving Load. The symbols used in the equation (1) are defined as follows.

$EI(x)$ is the flexural rigidity of the beam

E is the modulus of elasticity

I is the cross moment of inertia

C is the damping coefficient

a_1 is the stiffness proportionality factor define for Rayleigh damping

$V(x,t)$ is the displacement of the beam at point x and time t, measure from the equilibrium position when unloaded.

t is the time

x is the axial co-ordinate

m is the constant mass per unit length of the beam

The following are the given boundary and initial conditions respectively

$$V(0,t)=V(L,t)=V''(L,t)=0 \quad \text{and} \quad V(x,t)=\frac{\partial V(x,0)}{\partial t}=0$$

Solution Procedure

The governing equation (1) is reduced to second order differential equation by separation of variable techniques as follows.

We set the distributed parameters such as $EI(x), m(x), C(x), K(x)$ and $G(x)$

to constant EI, m, C, K and G respectively. Then we assumed the solution of the form

$$V(x,t)=\sum_{n} X_n(x)T_n(t) \tag{2}$$

The simplification of equation (1) after substitution of equation (2) yields

$$\ddot{T}_n(t)+2\omega_n\zeta\dot{T}_n(t)+\omega_n^2 T_n(t)=$$
$$\left\{-\frac{Mg}{m_t}\int_O^L X_K(x)dx-\frac{M}{m_t}\sum_n\left[\begin{array}{l}\ddot{T}(t)\int_O^L X_n(x)X_K(x)dx+u^2T_n(t)\int_O^L X_n^{11}(x)X_K(x)dx\\ 2u\,\dot{T}_n(t)\int_O^L X_n^{1}(x)X_K(x)dx\end{array}\right]\right\}$$
$$\left\{H\left(x-(\xi+\frac{\varepsilon}{2})\right)-H\left(x-(\xi-\frac{\varepsilon}{2})\right)\right\}dx \tag{3}$$

The vibrating configuration for simply supported system is introduced into equation (3), hence the normalise deflection curves $X_n(x)$ is given as

$$X_n(x)=\sqrt{\frac{2}{L}}\,Sin\frac{n\Pi x}{L}\Big\}_{n=1,2,3} \tag{4}$$

Substitution of eq. (4) into equation (3) and further simplification gives

$$\ddot{T}_n(t)+2\omega_n\xi\dot{T}_n(t)+\omega_n^2 T_n(t)=-\sqrt{\frac{2}{L}}\frac{Mg\,2L}{M_t K\Pi}Sin\frac{K\Pi\xi}{L}Sin\frac{K\Pi\varepsilon}{2L}-\frac{2M}{LM_t}$$
$$\sum\left\{\ddot{T}_n(t)\left[\begin{array}{l}\frac{L}{n(n-K)}\left(Sin\frac{\Pi\xi}{L}(n-K)Cos\frac{\Pi\varepsilon}{2L}(n-K)\right)\\ -\frac{L}{\Pi(n+K)}\left(Sin\frac{\Pi\xi}{L}(n+K)Cos\frac{\Pi\varepsilon}{2L}(n+K)\right)\end{array}\right]\right\}$$
$$+\frac{2Mu^2}{LM_t}\left(\frac{n\Pi}{L}\right)^2\sum\left\{T_n(t)\left[\begin{array}{l}\frac{L}{\Pi(n-K)}Sin\frac{\Pi\xi}{L}(n-K)Cos\frac{\Pi\varepsilon}{2L}(n-K)\\ -\frac{L}{\Pi(n+K)}Sin\frac{\Pi\xi}{L}(n+K)Cos\frac{\Pi\varepsilon}{2L}(n+K)\end{array}\right]\right\}$$
$$-\frac{4Mu^2}{LM_t}\left(\frac{n\Pi}{L}\right)\sum\dot{T}_n(t)\left\{\begin{array}{l}-\frac{L}{\Pi(n+K)}Sin\frac{\Pi\xi}{L}(n+K)Sin\frac{\Pi\varepsilon}{2L}(n+K)\\ +\frac{L}{\Pi(n-K)}Sin\frac{\Pi}{L}(n-K)Sin\frac{\Pi}{L}(n-K)\left(-\frac{\varepsilon}{2}\right)\end{array}\right\}$$

The solution of the equation above subjected to the initial conditions is given by the Duhamel's integral as:

$$T_n(t)=\frac{1}{w_n}\int_0^t p_n(\tau)\exp\left[-\tfrac{1}{2}M_n^2(t-\tau)\sin W_n(t-\tau)\right]d\tau$$

Where τ is the time at which the effect of the load is being considered on the structure, ω_n is the natural angular frequency of undamped system , ω_d free-vibration of a damped system , and ξ is the damping ratio. Also

$$p_n(\tau)=Q.\frac{R}{n}[\cos J-\cos \$]$$

$$-QRF\sum_{K=1}^{\infty}\frac{1}{8k^2n(n-k)}\Gamma_1[2\sin X_1+2\sin X_2+2\sin X_4-\sin X_3-\sin X_5]$$

$$-QRF\sum_{K=1}^{\infty}\frac{1}{8k^2n(n-k)}\Gamma_2[\sin X_2+\sin X_6-\sin X_3-\sin X_5]$$

$$+QRF\sum_{K=1}^{\infty}\frac{1}{8k^2n(n-k)}\Gamma_3\begin{bmatrix}2\sin X_1+2\sin X_2+2\sin X_4+\sin X6\\-2\sin X_3-2\sin X_5\end{bmatrix}$$

$$-QRF\sum_{K=1}^{\infty}\frac{1}{8k^2n(n-k)}\Gamma_4[\sin X_2+\sin X_6-\sin X_3-\sin X_5]$$

$$+QRF\sum_{K=1}^{\infty}\frac{1}{4k^2n(n-k)}\Gamma_5\begin{bmatrix}\cos Y_1+\cos Y_2+\cos Y_3+\cos Y_4\\-\cos Y_5-\cos Y_6-\cos Y_7-\cos Y_8\end{bmatrix}$$

$$-QRF\sum_{K=1}^{\infty}\frac{1}{8k^2n(n+k)}\Gamma_6[2\sin p_1+2\sin p_2+2\sin p_3-\sin p_4-\sin p_5-\sin p]$$

$$-QRF\sum_{K=1}^{\infty}\frac{1}{8k^2n(n+k)}\Gamma_7[\cos p_2+\cos p_3-\cos p_5-\cos p]$$

$$-QRF\sum_{K=1}^{\infty}\frac{1}{8k^2n(n+k)}\Gamma_8[\cos p_2+\cos p_3-\cos p_5-\cos p]$$

$$-QRF\sum_{K=1}^{\infty}\frac{1}{8k^2n(n-k)}\Gamma_{10}\begin{bmatrix}\cos Z_1+\cos Z_2+\cos Z_3+\cos Z_4\\-\cos Z_5-\cos Z_6-\cos Z_7-\cos Z_8\end{bmatrix}$$

$$-QRF\sum_{K=1}^{\infty}\frac{1}{8k^2n(n-k)}\Gamma_{11}\begin{bmatrix}\sin Z_1+\sin Z_2+\sin Z_3+\sin Z_4\\-\sin Z_5-\sin Z_6-\sin Z_7-\sin Z_8\end{bmatrix}$$

$$-QRF\sum_{K=1}^{\infty}\frac{1}{4k^2n(n-k)}\Gamma_{12}\begin{bmatrix}\cos X_2-2\cos X_1+2\cos X_4-\cos X_6\\+\cos X_3-\cos X_5\end{bmatrix}$$

$$-QRF\sum_{K=1}^{\infty}\frac{1}{8k^2n(n-k)}\Gamma_{13}[\sin X_1+\sin X_2+\sin X_6-\sin X_4+\sin X_5]$$

$$+QRF\sum_{K=1}^{\infty}\frac{1}{4k^2n(n-k)}\Gamma_{14}\begin{bmatrix}\cos X_2-2\cos X_6+2\cos X_4-\cos X_5\\+\cos X_1-\cos X_3\end{bmatrix}$$

$$-QRF\sum_{K=1}^{\infty}\frac{1}{4k^2n(n-k)}\Gamma_{15}\left[\sin X_1+\sin X_2+2\sin X_4-\sin X_5+\sin X_3\right]$$

$$+QRF\sum_{K=1}^{\infty}\frac{1}{4k^2n(n-k)}\Gamma_{16}\begin{bmatrix}\sin Y_1-\sin Y_2+\sin Y_3-\sin Y_4\\+\sin Y_7-\sin Y_5+\sin Y_6\end{bmatrix}$$

$$+QRF\sum_{K=1}^{\infty}\frac{1}{4k^2n(n-k)}\Gamma_{17}\begin{bmatrix}2\cos Y_4-\cos Y_3+\cos Y_8-\cos Y_7\\-\cos Y_1+\cos Y_5\end{bmatrix}$$

$$+QRF\sum_{K=1}^{\infty}\frac{1}{4k^2n(n-k)}\Gamma_{18}\begin{bmatrix}\cos p_2-\cos p_3+\cos p_4-\cos p_6\\-\cos p_1+\cos p_5\end{bmatrix}$$

$$+QRF\sum_{K=1}^{\infty}\frac{1}{4k^2n(n-k)}\Gamma_{19}\left[\sin p_3-\sin p_2+\sin p_6-\sin p_5\right]$$

$$+QRF\sum_{K=1}^{\infty}\frac{1}{4k^2n(n-k)}\Gamma_{20}\begin{bmatrix}\cos p_2-2\cos p_3+2\cos p_4-\cos p_6\\-\cos p_1+\cos p_5\end{bmatrix}$$

$$+QRF\sum_{K=1}^{\infty}\frac{1}{4k^2n(n-k)}\Gamma_{21}\left[\sin p_3-\sin p_2+2\sin p_6-\sin p_4-\sin p_5\right] \tag{5}$$

Hence the analytical solution for the displacement of the structure is evaluated to be of the form

$$V(x,t)=\sqrt{\frac{2}{L}}\sin\frac{n\pi x}{L}\times\frac{1}{w_n}\int_0^{\bar{t}}p_n(\tau)\exp\left[-\zeta\omega_n(t-\tau)\sin w_d(t-\tau)\right]d\tau \tag{6}$$

Numerical Calculation and Graphical Results

To illustrate the analysis in this paper numerically and graphically, a program was coded in MATLAB language which was used to implement the scheme in equation (6). The effects of the individual case of the damping ratio ($\zeta < 1$, $\zeta = 1$ and $\zeta > 1$) on the dynamic response of the beam are discussed. Various values of the amplitude of the deflection $V(x,t)$ of the beam for various values of dimensionless time $\bar{t}$ with a fixed value of dimensionless velocity $\overline{U}$ and various value of damping ratio are shown in Table 1 , 2, and 3. The corresponding graphical representations of the numerical solution are also presented in the figures where V_a represents the middle-span deflection values.

Figure 1, 2 and 3 depict the amplitude displacement of the beam for $\zeta < 1$, $\zeta = 1$ and $\zeta > 1$ respectively, where letter "d" represents the damping term ζ.

Table1: The Amplitude displacement of the beam for damping ratio less than one ($\zeta < 1$).

T	d = -0.12	d = 0	d = 0.04
0	-6.84	94400	29.2
4	37900000	-7.79E+11	3.39E+08
8	100000000	**2.07E+12**	9.03E+08
12	-653000000	1.35E+12	-5.9E+07
16	-8.87E+09	**1.83E+12**	7.97E+08
20	-10200000	**1.35E+12**	-9.1E+08
24	-3180000	-20800000	-2.9E+07
28	-4650000	6.16E+10	-4.4E+07

Table2: The Amplitude displacement of the beam for damping ratio equal to one $\zeta = 1$.

t	0	2.5	5	7.5	10	12	15	17.5	20
V_a	0	0.504	0.126	-3.95	5.18	1.35	-2.9	3.12	-0.072

Table3: The Amplitude displacement of the beam for damping ratio greater than one ($\zeta > 1$).

T	d = 1.5	d = 2.0	d = 2.5	d = 3.0	d = 3.5	d = 4.0
0	2.46E+08	1.31E+08	7.73E+07	4.61E+07	2.85E+07	2.11E+09
2	4.83E+09	4.34E+09	3.84E+07	3.35E+09	2.86E+09	2.37E+09
4	1.06E+11	9.84E+10	9.07E+10	8.30E+10	7.53E+10	6.77E+10
6	1.71E+10	1.56E+10	1.41E+10	1.26E+10	1.11E+10	9.65E+09
8	5.81E+10	5.39E+10	4.97E+10	4.55E+10	4.13E+10	3.72E+10
10	5.83E+09	5.32E+09	4.82E+09	4.31E+09	3.81E+09	3.30E+09
12	-2.76E+07	-2.89E+07	-3.03E+07	-3.16E+07	-3.29E+07	-3.43E+07
14	2.56E+07	2.42E+09	7.56E+09	2.13E+09	1.99E+09	1.85E+09
16	7.27E+10	6.73E+10	6.19E+10	5.66E+10	5.11E+10	4.57E+10

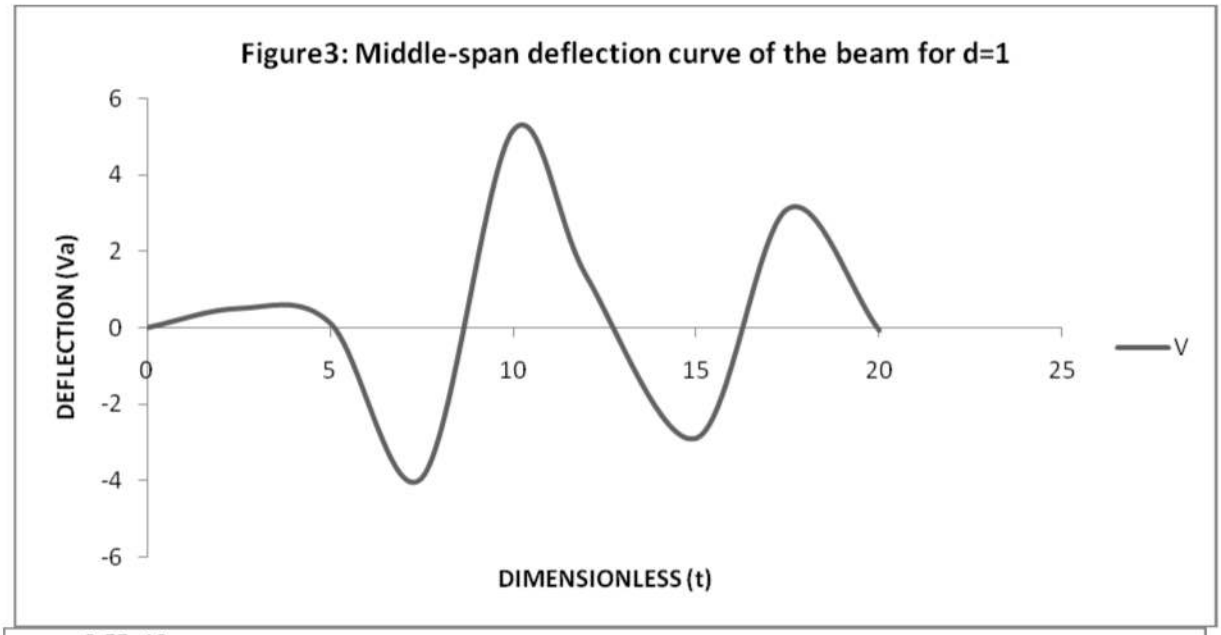

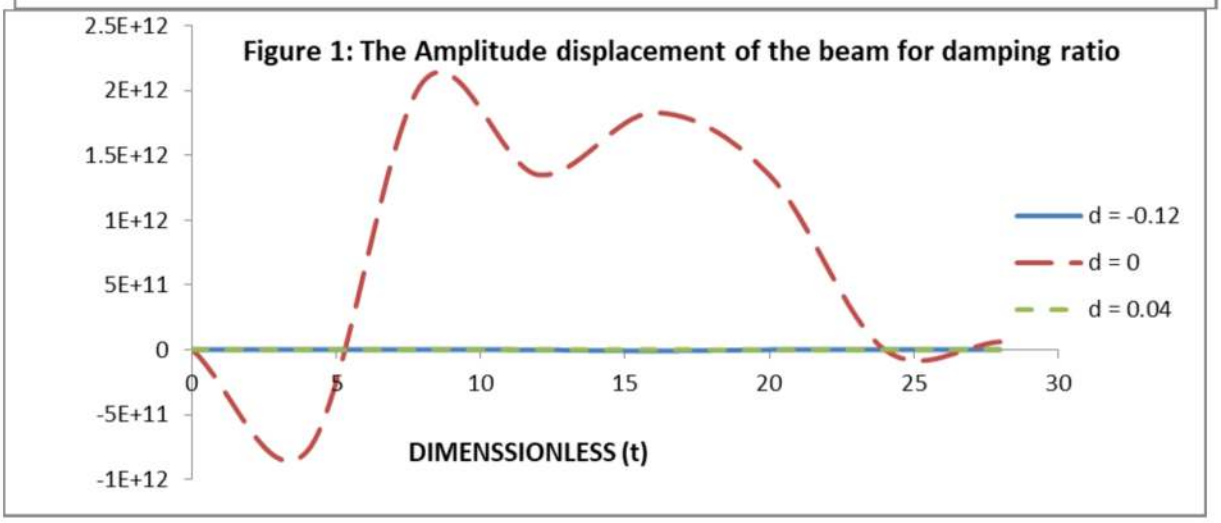

Figure 2: Middle-span deflection curve of the beam for d = 1

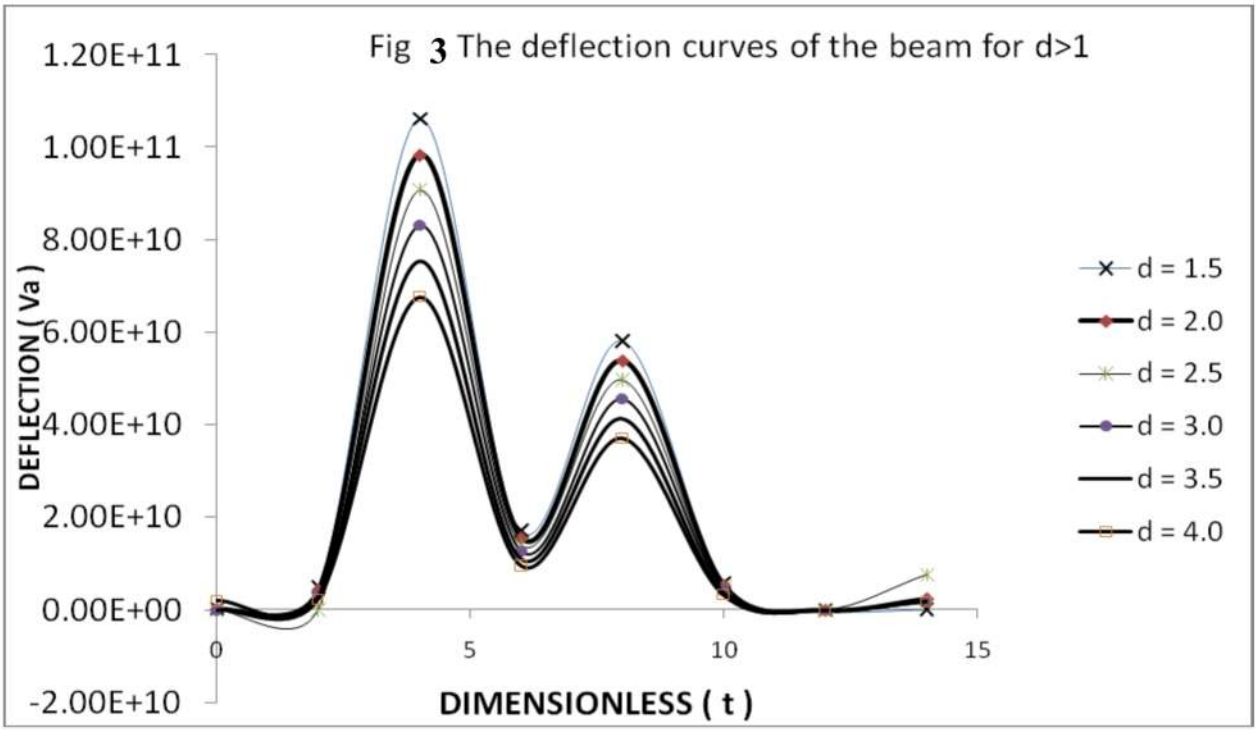

Discussion of Results

The effect of damping on the displacement of the beam was investigated for when damping ratio $\zeta < 1$, $\zeta = 1$ and $\zeta > 1$ at various values of dimensionless time $\bar{t}$. And figures 1, 2, and 3 show the amplitude displacement of the beam for d < 1, d = 1 and d >1 respectively, where d represent the damping term ζ. Moreover, the middle-span deflection of the structure was also presented in figure 2. Thus, when the deflection curve of the vibrating structure was examined, it was noted that the amplitude of the displacement of the beam was maximum for absolute values of deflection when the damping value was zero for damping ratio $\zeta < 1$. This was shown in Table 1 and graphically represented in Figure 1. The response amplitude of deflection of the structure was also investigated for damping ratio $\zeta = 1$. It was found that the deflection curve attains maximum amplitude at dimensionless time $\bar{t} = 10$, which implies that the greatest amplitude of the beam displacement occurred at the middle-span of the structure (Figure 2). In Figure 3, for $\zeta > 1$, various values of damping ratio were considered for a fixed mass of the moving Load at constant velocity $\bar{U} = 5.45$. It was evidently observed that as the damping ratio ζ increases the amplitude displacement of the vibrating beam decreases.

Summary of the Results

The main findings from the investigations carried out on the effects of damping on the response of the beam subjected to moving loads at uniform velocity are summarized as follows:

It is noted that the amplitude of the displacement of the beam is maximum for absolute values of deflection when the damping value was zero for damping ratio $\zeta < 1$. The deflection curve attained maximum amplitude at dimensionless time $\bar{t} = 10$, which implies that the greatest amplitude of the beam displacement occurred at the middle-span of the beam.

Conclusively, it is evidently observed that as the damping ratio ζ increases the amplitude displacement of the vibrating beam decreases.

Conclusion

The importance and practical application of this analysis is seen in moving loads as they transverse along suspended bridges and railways. The Engineers, Applied Mathematicians and Applied Physicists who are concerned in designing structures such as railway and highway bridges may take into consideration the determination of the deflection curves and natural frequencies of the beam. Important attention may be paid to affect these effects to avoid road-rail disaster.

REFERENCES

Gbadeyan J.A and Dada M.S. (2007); The Effect of Linearly Varying Distributed Moving Loads on Beam *Journal of Engineering and Applied Sciences*, 2(6), 1006-1011.

Beer Johnstone (2004); *Statics and Vector Mechanics for Engineers*, 7th Ed; Tat a Mc Graw Hill Publishing Company Ltd, 357-359.

Lev Khazanovich (2003); *Finite Element Analysis of Curling Slab on the Pasternak Foundation*, Paper presented at 16th ASCE Examination conference, University of Washington.

Michalstos, G.T. and Kounadis A.N. (2001) ; The Effects 0f Centripetal and Coriolis Forces on the Dynamics Response of Light Bridges under Moving Loads, *Journal of Vibration and Control* Vol. (7), 315-326.

Erwin Kreyzig (1999); *Advanced Engineering Mathematics* 8th Ed, John Wiley and Sons Inc. 234-235.

Esmailzadeh E. and Gorash M.(1995); Vibration Analysis of Beams Transverse by Uniform Distributed Moving Masses, *Journal of Sound and Vibration*, 184(1), pp 323-238, pp 9-17

Gbadeyan J.A. and Oni S.T (1995); Dynamic Behaviours of Beam and Rectangular Plates under Moving Loads, *Journal of Sound and Vibration*, 185(5), pp 182, 677-695.

Fryba L. (1972) work on the vibration of solids and structures under moving Loads, Noordhoff International Publishing Groningen, pp 342.

Abacus (Mathematics Science Series)
Vol. 49, No 3, September. 2022

FRACTIONAL EPIDEMIC MODEL OF EBOLA VIRUS VIA CAPUTO-ORDER DERIVATIVE

[1]Abdullahi M. Auwal, [2]Abubakar mohammed, [3]Aliyu D. Hina, [4]Bala Umar, [5]Gazali M. A., [6]Aminu. Haruna.

[1,3,4,,6]Mathematics and statistics department, Federal Polytechnics Bauchi
[2,,5]Federal College of Education (Tech), Gombe ederal
auwal2gga@yahoo.com,mabubakarmohammed13@yahoo.com

Abstract

Many new definitions of fractional order derivatives have been proposed and used to develop and analyze mathematical models for a wide variety of real-life problems. The advantages of memory, history, or nonlocal effects of fractional order derivatives motivated this research work. Therefore, in this paper, we extended mathematical models that were based on integer order derivatives to fractional order derivatives; we formulate and analyzed a fractional mathematical modelling of dynamics of Ebola epidemic which includes both vaccination and quarantine via Caputo order derivatives. The existence and uniqueness of the solution of proposed FODE are established through the fixed point theory. The numerical results and simulations of the extended fractional order mathematical model where explored in Caputo sense.

.

Keywords: Caputo fractional order derivative; fractional differential equation; Ebola Virus; fixed point theory.

Introduction

Ebola virus causes hazardous hemorrhagic fever in humans and non-human primates like, chimpanzees, gorillas, fruit bats, monkeys and forest antelope. It is extremely communicable leading to a death rate of up to approximately 87% (Chowell *et al*., 2009). This virus was first identified in 1976 in a place called Nzara and Sudan and later found in a village near a river called Ebola from which the name has been initiated. The Transmission of Ebola virus can spread from human to human via direct contact with the blood and body fluids such as saliva, mucus, vomit, sweat, tears, breast milk, urine and semen of a person who has been affected by the disease. Apart from this transmission the virus can also be spread from animals to human beings. Ebola is characterized by initial -flu like symptoms including fever, fatique, sore throat, muscle pain, headache and vomiting.

As of October 8, 2014, the World Health Organization (WHO) reported 4656 cases of Ebola virus deaths, with most cases occurring in Liberia (Lewnard *et al.,* 2014). The extremely rapid increase of the disease and the high mortality rate make this virus a major problem for public health. Ebola is transmitted through direct contact with blood, bodily secretions and tissues of infected ill or dead humans and nonhuman primates. (Dowell *et al.,* 1999) and (Peters *et al.,* 2002) .

The use of mathematical equations and formula to represent real life problems via mathematical models by Scientists/researchers solved and made remarkable prediction based on the solutions obtained from the problems. Epidemiologists (scientists that study infectious diseases) have played a vital role in investigating the transmission dynamics of some of these diseases and have been able to come up with recommendations for different intervention strategies which have helped to control the spread of some of these diseases.

Many researches of nowadays have extended mathematical models that were based on integer order derivatives to fractional order derivatives in almost all areas as physics, engineering, biological sciences, finance, economics and other related areas. Therefore, fractional calculus is now an area where so many researches are being carried out. Sania *et al.,* (2019) claimed that among the main motives of using the fractional-order operators is their nature of non-locality which offers an infinite degree of freedom that enables selection of suitable values for the fractional-order parameter that leads to more accurate results than their classical counterparts. Diethelm, (2013) was of the view

that fractional derivatives can provide a better agreement between measured and simulated data than the classical derivatives. Eric *et al.,* (2016) added that fractional derivatives have special characteristics of memory effect that depends not only upon its current state but also upon all of its historical states which does not apply to classical derivatives. In support of this notion Musiliu *et al.,* (2019) affirmed that the memory effect is very important during biological processes more specifically, the growth of an epidemic process which is directly associated with the individuals' experiences, which takes place over a period of time. In fact, the real epidemic process is obviously sustained by heredity properties and the memory effects perform a critical role in the subsequent spread of infection. These additional properties increase the accuracy and reliability of fractional order systems than the other ordinary systems.

Many researches prove the above assertions. These include but not limited to Diethelm, (2013); Eric *et al.,* (2016), Nur 'Izzati *et al.,* (2018), Rashid *et al.,* (2019), Amin *et al.,* (2019), Musiliu *et al.,* (2019), Musiliu *et al.,* (2019), Kolade *et al.,* (2019), Sania *et al.,* (2019), Ilknur, (2019), Abdon *et al.,* (2019), Zafar *et al.,* (2020), to mention but few. Therefore the novel of this work is to extend the work of Thomas, Boping and Zunyou, (2017) which is a classical mathematical model of Ebola epidemics to a fractional order mathematical model of Caputo type and carry out its numerical computation and simulations.

Fractional Differential Equations

Fractional Calculus is one of the branches of mathematics that investigate the properties of integrals and derivatives of non – integer orders which involves the notion and methods of solving the differential equations that involves fractional derivatives of the unknown function. There are three important definitions of fractional differential equations; they are the Riemann-Liouville, the Grunwald-Letnikov, and the Caputo definitions. We shall discuss the derivations of these methods one after the other.

Let

$$f'(x) = \lim_{n\to\infty}\left\{\frac{f(x)-f(x-h)}{h}\right\} \tag{2}$$

$$f''(x) = \lim_{n\to\infty}\left\{\frac{f'(x)-f'(x-h)}{h}\right\} \tag{3}$$

$$= \lim_{n\to\infty}\left\{\frac{\left[\frac{f(x)-f(x-h)}{h}\right]-\left[\frac{f(x-h)-f(x-2h)}{h}\right]}{h}\right\} \tag{4}$$

Simplifying (4)

$$f''(x) = \lim_{n\to\infty}\frac{1}{h^2}\{f(x)-2f(x-h)-f(x-2h)\} \tag{5}$$

Using the pattern of (3) and (5) in terms of coefficient, alternating signs and the binomial expressions

$$f'''(x) = \lim_{h\to\infty}\frac{1}{h^3}\{f(x)-3f(x-h)+3f(x-2h)+f(x-3h)\} \tag{6}$$

(6) Can be expressed in a series form as

$$f'''(x) = \lim_{h\to\infty}\frac{1}{h^3}\sum_{j=0}^{\infty}(-1)^j\binom{3}{j}f(x-jh) \tag{7}$$

Where

$(-1)^j$ - stands for the alternating signs

$\binom{3}{j}$ - Combination which stands for binomial coefficient

$f(x-jh)$ - stands for $f(x-jh)$

Hence the n^{th} derivative is given by

$$f^{(n)}(x) = \lim_{h\to 0}\left(\frac{1}{h}\right)^n \sum_{j=0}^{n}(-1)^j \binom{n}{j} f(x-jh) \tag{8}$$

Now for any real number say, $\propto$

$$f^{(\alpha)}(x) = \lim_{h\to 0}\left(\frac{1}{h}\right)^\alpha \sum_{j=0}^{n}(-1)^j \binom{\alpha}{j} f(x-jh) \tag{9}$$

Now $\binom{\propto}{j} = \frac{\propto!}{j!(\propto-j)!}$ by definition of combination

Using gamma function

$$\Gamma(n+1) = n! \tag{10}$$

Therefore,

$$\frac{\alpha!}{j!\,(\alpha-j)!} = \frac{\Gamma(\alpha+1)}{j!\,\Gamma(\alpha-j+1)} \tag{11}$$

Since $j!$ is an integer, so it has no meaning transforming to gamma function.

Putting (11) in to (9)

$$f^{(\propto)}(x) = \lim_{h\to 0}\left(\frac{1}{h}\right)^{\propto} \sum_{j=0}^{n}(-1)^j \frac{\Gamma(\alpha+1)}{j!\,\Gamma(\alpha-j+1)} f(x-jh) \tag{12}$$

$n = \frac{x-a}{h}$, $\quad h \longrightarrow 0$, $\quad n \longrightarrow \infty$ for a constant a, $a < x \Rightarrow \frac{1}{h} = \frac{n}{x-a}$

Therefore,

$$f^{(\alpha)}(x) = \lim_{h\to 0}\left(\frac{n}{x-a}\right)^{\alpha} \sum_{j=0}^{n}(-1)^j \frac{\Gamma(\alpha+1)}{j!\,\Gamma(\alpha-j+1)} f\left(x - j\left(\frac{x-a}{n}\right)\right) \tag{13}$$

GRUNVALD LETNIKOV fractional derivative.

The Grunvald Letnikov fractional derivative is quite complicated because it involves a limit. Therefore, further studies and investigations will be carried out so that a useful definition and useful formula can be achieved.

Now

$$f^{(\alpha)}(x) = \lim_{h\to 0}\left(\frac{1}{h}\right)^{\alpha}\sum_{j=0}^{n}(-1)^{j}\binom{\alpha}{j}f(x-jh) \tag{14}$$

Where $h = \frac{x-a}{n}, \quad a < x$

To change to negative α so that we have integration because integration is a reverse of differentiation.

$\binom{\propto}{j} = \frac{\propto!}{j!(\propto - j)!}$ By definition of combination symbol

$$\frac{\alpha(\alpha-1)...(\alpha-(j-1))(\alpha-j)!}{j!(\alpha-j)!} \tag{15}$$

Switching from $\alpha \to -\alpha$

$$\binom{-\alpha}{j} = \frac{-\alpha(-\alpha-1)...(-\alpha-j+1)!}{j!} \tag{16}$$

Since (-1) is common

$$(-1)\left[\frac{\alpha(\alpha+1)+...+\alpha+j-1)}{j!}\right] \tag{17}$$

Writing (17) from the right end

$$(-1)^{j}\left[\frac{\alpha+j-1+...+(\alpha+1)\alpha}{j!}\right]$$

Multiplying and dividing through by $(\alpha-1)!$

$$(-1)^{j}\left[\frac{\alpha+j-1+...+(\alpha+1)\alpha(\alpha-1)!}{j!(\alpha-1)!}\right] \tag{18}$$

$$= \frac{(-1)^{j}(\alpha+j-1)}{j!(\alpha-1)!} \tag{19}$$

$$\binom{-\alpha}{j} = \frac{(-1)^{j}\Gamma(\alpha+j)}{j!\,\Gamma(\alpha)} \tag{20}$$

Now substituting (20) into (14) we have

$$f^{(-\alpha)}(x) = \lim_{n\to 0} h^{\alpha}\sum_{j=0}^{n}(-1)^{j}\frac{(-1)^{j}\Gamma(\alpha+j)}{j!\,\Gamma(\alpha)}f(x-jh) \tag{21}$$

$$(-1)^{j}(-1)^{j} = 1 \tag{22}$$

$$f^{(-\alpha)}(x) = \lim_{n\to 0} h^{\alpha}\sum_{j=0}^{n}\frac{\Gamma(\alpha+j)}{j!\,\Gamma(\alpha)}f(x-jh) \tag{23}$$

$$I^{(\alpha)}(f) = h^{\alpha} \sum_{j=0}^{n} \frac{\Gamma(\alpha + j)}{j!\,\Gamma(\alpha)} f(x - jh) \tag{24}$$

for $h = \frac{x-a}{n}$, $a < x$

when $\alpha = 1$

$$I^{(1)}(f) = h \sum_{j=0}^{n} \frac{\Gamma(1 + j)}{j!\,\Gamma(1)} f(x - jh) \tag{25}$$

$\Gamma(1 + j)$ by definition of gamma function = $j!$

$\Gamma(1)$ is 0! and 0! is 1

Therefore, $\lim_{n\to\infty} \sum_{j=0}^{n} hf(x - jh) \rightarrow$ which is simpler and famous form of Reiman Integral?

Using $h = \frac{x-a-0}{n}$, $x - t = u$, $-dt = du$, when $t = 0, u = x$

$$\int_{0}^{x-a} f(x-t)dt = -\int_{x}^{a} f(u)du \tag{26}$$

$$I^{(1)}(f) = \int_{a}^{x} f(u)du. \tag{27}$$

when $\alpha = 2$

$$I^{(2)}(f) = \lim_{n\to 0} h^{\alpha} \sum_{j=0}^{n} \frac{\Gamma(2 + j)}{j!\,\Gamma(2)} f(x - jh) \tag{28}$$

$$= \lim_{n\to 0} h^{\alpha} \sum_{j=0}^{n} (1 + j) f(x - jh) \tag{29}$$

$j \rightarrow j - 1$

$$= \lim_{n\to 0} h^{\alpha} \sum_{j-1}^{n+1} j f(x - (j - 1)h) \tag{30}$$

$$= \lim_{n\to 0} h^{\alpha} \sum_{j-1}^{n+1} j f(x - h - jh) \tag{31}$$

Let $x - h = y$

$$= \lim_{n\to 0} h^{\alpha} \sum_{j-1}^{n+1} j f(y - jh) \tag{32}$$

$$= \lim_{n\to 0} h^{\alpha} \sum_{j-1}^{n+1} (jh) f(y - jh)h \tag{33}$$

$$= \int_{0}^{x} f(x-t)dt \text{ using Riemann Integral} \tag{34}$$

Therefore,

Let $x-t=u$, $-dt=du$, $t\to\infty$, $u\to x$, $t\to x$, $a\to a$

$$-\int_{x}^{a}(x-u)f(u)du \tag{35}$$

$$I^{(2)}-\int_{a}^{x}(x-u)f(u)du \tag{36}$$

Therefore, following the pattern

$$I^{(3)}(f)=\frac{1}{2!}\int_{a}^{x}(x-u)^{2}f(u)du \tag{37}$$

‘ ‘ ‘

$$I^{(n)}(f)=\frac{1}{(n-1)!}\int_{a}^{x}(x-u)^{n-1}f(u)du \tag{38}$$

$$I^{(\alpha)}(f)=\frac{1}{\Gamma(\alpha)}\int_{a}^{x}(x-u)^{\alpha-1}f(u)du \tag{39}$$

… (39) is known as **Riemann Liovelle Fractional Integral**

From the Riemann Liovelle fractional integral (39), we then derive the Caputo Fractional Derivative as

$${}_{a}^{c}D_{x}^{\alpha}f(x)={}_{a}I_{x}^{n-\alpha}f^{(n)}(x) \tag{40}$$

$$=\frac{1}{\Gamma(n-\alpha)}\int_{a}^{x}(x-t)^{n-\alpha-1}f^{(n)}(t)dt \qquad n-1\le\alpha\le n \tag{41}$$

When $n=1$

$${}_{a}^{c}D_{x}^{\alpha}f(x)=\frac{1}{\Gamma(1-\alpha)}\int_{a}^{x}(x-t)^{-\alpha}f'(t)dt \tag{42}$$

… (42) is **Caputo Fractional Derivative**

Where $(x-t)^{-\alpha}$ is called kernel of integration.

In this paper, we will use the Caputo definition. The reasons which led to the choice of the Caputo derivative are mainly practical. The Riemann-Liouville approach requires the initial conditions for differential equations in terms of non-integer derivatives which are hardly physically interpreted, whereas the Caputo approach uses integer-order initial conditions. Furthermore, the derivative of a constant function under this fractional operator is not zero.

The extended mathematical model of dynamics of Ebola epidemic which includes both vaccination and quarantine in the sense of Caputo fractional derivative

Mathematical modeling, analysis and Markov Chain Monte Carlo simulation of Ebola epidemics proposed by Tulu *et al.,* (2017), has four compartmental model as follows; Susceptible individuals (S) may become infected (I) after contact with an Ebola infected individuals who are capable of infecting others including nurses, doctors etc at hospitals and with a chance of infecting others before being recovered/removed from the disease (R) or die of Ebola and then join (D).with a constant population.

The population of susceptible individuals is produced by the loss of infection acquired immunity into the Population at the rate γ_1, after contact with infected non quarantined individual at the rate β_1 if acquires infection then the population will be reduced. When vaccination is taking into cognizant the susceptible individuals will further reduced at the rate γ.

The population of infected individuals is generated by the infection of susceptible individuals at the rate β_1 reduced by recovering from Ebola disease at the rate of α_1 and α_2 where $\alpha_1$recovery rate of infected quarantined individual and α_2 is recovery rate of infected non quarantined individuals. This population is further reduced by death due to Ebola at a rate δ_1 and δ_2 where death rate of infected quarantined individual is δ_1 and δ_2 is death rate of infected non quarantined individuals due to Ebola. Let us assumed that α_1 is greater than α_2 and δ_1 is less than δ_2 this can be relevant in ecological studies.

Similarly, the population of individuals who deceased is produced by individuals who die as a result of Ebola and the population of recovered infected individuals is generated by those who recovered from Ebola, and those individual from susceptible because of vaccination at the rate of γ and reduced by individuals that loss immunity the rate of γ_1. Hence, the original integer-order model adopted from Tulu *et al.*. (2017) can be written as:

$$\begin{aligned}
\frac{dS}{dt} &= \gamma_1 R - \frac{\beta_1(1-\beta)S(I)}{N} - \gamma S \\
\frac{dI}{dt} &= \frac{\beta_1(1-\beta)S(I)}{N} - \alpha_1\beta I + \alpha_2(1-\beta)I - \delta_1 I + \delta_2 I \\
\frac{dR}{dt} &= \alpha_1\beta I + \alpha_2(1-\beta)I + \gamma S - \gamma_1 R \\
\frac{dD}{dt} &= \delta_1 I + \delta_2 I
\end{aligned} \tag{44}$$

Where the total population becomes: $N(t) = S(t) + I(t) + R(t) + D(t)$

The extended model is formulated by integrating the Caputo fractional derivative in (44). Following the methods of Rezapour *et al.,* (2020), Baleanu *et al.,* (2020) , Diethelm, (2013), Amin *et al.,* (2019), Sania *et al.,* (2019) and Zafar *et al.,* (2020) where some parameters in the system model are modified to ensure that the right- and left-hand sides of the resultant fractional equations possess the same dimensions. Consequently, our new Caputo fractional model for dynamics of Ebola epidemic model which includes both vaccination and quarantine can therefore be written as follows:

$$\tau^{\alpha-1}\,{}^{C}D_t^{\alpha}S(t) = \gamma_1 R(t) - \frac{\beta_1(1-\beta)S(t)I(t)}{N} - \gamma\, S(t)$$

$$\tau^{\alpha-1}\,{}^{C}D_t^{\alpha}I(t) = \frac{\beta_1(1-\beta)S(t)I(t)}{N} - \alpha_1\beta I(t) + \alpha_2(1-\beta)I(t) - \delta_1 I(t) + \delta_2 I(t) \qquad (45)$$

$$\tau^{\alpha-1}\,{}^{C}D_t^{\alpha}R(t) = \alpha_1\beta I(t) + \alpha_2(1-\beta)I(t) + \gamma S + \gamma_1 R(t)$$

$$\tau^{\alpha-1}\,{}^{C}D_t^{\alpha}V(t) = \delta_1 I(t) + \delta_2 I(t)$$

With initial conditions

$$S(0) = S_0,\quad I(0) = I_0, \qquad R(0) = R_0, \qquad V(0) = V_0 \qquad (46)$$

Existence and uniqueness of solutions of the model

Examine the existence and uniqueness of the solutions of the Caputo fractional model for dynamics of Ebola epidemic in Eq. (45) with initial conditions (46). Using fixed point theory, we can prove existence of solutions for the model as follows

Now Applying the Caputo– fractional integral operator i to both sides of Eq. (45), we have

$$S(t) - S(0) = C_{I_t}^{\alpha}\left[\gamma_1 R - \frac{\beta_1(1-\beta)SI}{N} - \gamma\, S\right],$$

$$I(t) - I(0) = C_{I_t}^{\alpha}\left[\frac{\beta_1(1-\beta)S(I)}{N} - \alpha_1\beta I + \alpha_2(1-\beta)I - \delta_1 I + \delta_2 I\ \right] \qquad (47)$$

$$R(t) - R(0) = C_{I_t}^{\alpha}[\,\alpha_1\beta I + \alpha_2(1-\beta)I + \gamma S - \gamma_1 R],$$

$$V(t) - V(0) = C_{I_t}^{\alpha}[\delta_1 I + \delta_2 I],$$

Applying the definition of fractional integral on the above equations, we get

$$S(t) - S(0) = \frac{\tau^{\alpha-1}}{\Gamma(\alpha)}\int_0^t \left[\gamma_1 R(\varphi) - \frac{\beta_1(1-\beta)S(\varphi)I(\varphi)}{N} - \gamma S(\varphi)\right](t-\varphi)^{1-\alpha}d\varphi$$

$$I(t) - I(0) = \frac{\tau^{\alpha-1}}{\Gamma(\alpha)}\int_0^t \left[\frac{\beta_1(1-\beta)S(\varphi)(I)(\varphi)}{N} - \alpha_1\beta I(\varphi) + \alpha_2(1-\beta)I(\varphi) - \delta_1 I(\varphi) + \delta_2 I(\varphi)\right](t-\varphi)^{1-\alpha}d\varphi$$

$$R(t) - R(0) = \frac{\tau^{\alpha-1}}{\Gamma(\alpha)} \int_0^t [\, \alpha_1 \beta I(\varphi) + \alpha_2(1-\beta) I(\varphi) + \gamma S(\varphi) - \gamma_1 R(\varphi)] \, (t-\varphi)^{1-\alpha} d\varphi$$

(48)

$$V(t) - V(0) = \frac{\tau^{\alpha-1}}{\Gamma(\alpha)} \int_0^t [\delta_1 I(\varphi) + \delta_2 I(\varphi)] \, (t-\varphi)^{1-\alpha} d\varphi$$

The kernel of the above equations can be written as follows

$$\nabla_1\big(t, S(t)\big) = \gamma_1 R(t) - \frac{\beta_1(1-\beta) S(t) I(t)}{N} - \gamma\, S(t)$$

$$\nabla_2\big(t, I(t)\big) = \frac{\beta_1(1-\beta) S(t) I(t)}{N} - \alpha_1 \beta I(t) + \alpha_2(1-\beta) I(t) - \delta_1 I(t) + \delta_2 I(t) \qquad (49)$$

$$\nabla_3\big(t, R(t)\big) = \alpha_1 \beta I(t) + \alpha_2(1-\beta) I(t) + \gamma S(t) + \gamma_1 R(t)$$

$$\nabla_4\big(t, V(t)\big) = \delta_1 I(t) + \delta_2 I(t)$$

Theorem 1. The kernel ∇_1 satisfies the Lipschitz condition and contraction given that the following inequality $0 \leq \frac{\beta_1(1-\beta) I}{N} + \gamma < 1$ hold.

Proof

Choosing $S(t)$ and $\mathrm{S}_1(t)$ we write

$$\begin{aligned}
&\|\nabla_1\big(t, S(t)\big) - \nabla_1\big(t, \mathrm{S}_1(t)\big)\| \\
&\quad = \Big\| [\gamma_1 R(t) - \frac{\beta_1(1-\beta) S(t) I(t)}{N} - \gamma\, S(t)] - [\gamma_1 R(t) - \frac{\beta_1(1-\beta) \mathrm{S}_1(t) I(t)}{N} \\
&\quad - \gamma\, \mathrm{S}_1(t)] \Big\| \\
&\quad \leq \frac{\beta_1(1-\beta) I}{N} \|S(t) - \mathrm{S}_1(t)\| + \gamma \Big\| \leq \frac{\beta_1(1-\beta) I}{N} + \gamma \Big\| \\
&\quad \leq \frac{\beta_1(1-\beta) I}{N} + \gamma \|S(t) - \mathrm{S}_1(t)\| \\
&\quad \leq L_1 \|S(t) - \mathrm{S}_1(t)\|
\end{aligned}$$

Where $L_1 = \frac{\beta_1(1-\beta) I}{N} + \gamma$

Therefore, the kernel ∇_1 satisfies the Lipschitz condition, and the kernel is a contraction. For $0 \leq \frac{\beta_1(1-\beta) I}{N} + \gamma < 1$

Repeating same process we can easily show that the remaining equations satisfy the Lipschitz condition.

$$\|\nabla_2(t, I(t)) - \nabla_2(t, I_1(t))\| \leq L_2\|I(t) - I_1(t)\|$$
$$\|\nabla_3(t, R(t)) - \nabla_3(t, R_1(t))\| \leq L_3\|R(t) - R_1(t)\|$$
$$\|\nabla_4(t, V(t)) - \nabla_4(t, V_1(t))\| \leq L_4\|V(t) - V_1(t)\|$$

Where $a \leq I(t), b \leq S(t)$.

$L_2 = \alpha_1\beta + \alpha_2 - \alpha_2\beta - \delta_1 + \delta_2$, $L_3 = \alpha_1\beta a + (\alpha_2 - \alpha_2\beta)a + \gamma b + \gamma_1$ And $L_4 = \delta_1 a + \delta_2 a$

By using equation (48), we write the recursive formulae as follows

$$S(t) = \frac{\tau^{\alpha-1}}{\Gamma(\alpha)}\int_0^t \nabla_1(t, S(t))\,(t-\varphi)^{1-\alpha}d\varphi$$
$$I(t) = \frac{\tau^{\alpha-1}}{\Gamma(\alpha)}\int_0^t \nabla_2(t, I(t))\,(t-\varphi)^{1-\alpha}d\varphi \qquad (50)$$
$$R(t) = \frac{\tau^{\alpha-1}}{\Gamma(\alpha)}\int_0^t \nabla_3(t, R(t))\,(t-\varphi)^{1-\alpha}d\varphi$$
$$V(t) = \frac{\tau^{\alpha-1}}{\Gamma(\alpha)}\int_0^t \nabla_4(t, V(t))\,(t-\varphi)^{1-\alpha}d\varphi$$

Taking the difference between the recursive terms, by considering the initial condition in equation (46). We have

$$\Delta_{1n}(\mathrm{t}) = \mathrm{S}_{jn}(t) - \mathrm{S}_{jn-1}(t) = \frac{\tau^{\alpha-1}}{\Gamma(\alpha)}\int_0^t (\nabla_1\left(t, \mathrm{S}_{jn-1}(t)\right) - \nabla_1\left(t, \mathrm{S}_{jn-2}(t)\right))\,(t-\varphi)^{1-\alpha}d\varphi$$
$$\Delta_{2n}(\mathrm{t}) = \mathrm{I}_{jn}(t) - \mathrm{I}_{jn-1}(t) = \frac{\tau^{\alpha-1}}{\Gamma(\alpha)}\int_0^t (\nabla_2\left(t, \mathrm{I}_{jn-1}(t)\right) - \nabla_2\left(t, \mathrm{I}_{jn-2}(t)\right))\,(t-\varphi)^{1-\alpha}d\varphi$$
$$\Delta_{3n}(\mathrm{t}) = \mathrm{R}_{jn}(t) - \mathrm{R}_{jn-1}(t) = \frac{\tau^{\alpha-1}}{\Gamma(\alpha)}\int_0^t \left(\nabla_3\left(t, \mathrm{R}_{jn-1}(t)\right) - \nabla_3\left(t, \mathrm{R}_{jn-1}(t)\right)\right)(t-\varphi)^{1-\alpha}d\varphi \quad (51)$$
$$\Delta_{4n}(\mathrm{t}) = \mathrm{V}_{jn}(t) - \mathrm{V}_{jn-1}(t) = \frac{\tau^{\alpha-1}}{\Gamma(\alpha)}\int_0^t (\nabla_4\left(t, \mathrm{V}_{jn-1}(t)\right) - \nabla_4\left(t, \mathrm{V}_{jn-2}(t)\right))\,(t-\varphi)^{1-\alpha}d\varphi$$

We can easily observe that

$\mathrm{S}_{jn}(t) = \sum_{j=0}^{n}\Delta_{1j}(\mathrm{t})$, $\mathrm{I}_{jn}(t) = \sum_{j=0}^{n}\Delta_{2j}(\mathrm{t})$, $\mathrm{R}_{jn}(t) = \sum_{j=0}^{n}\Delta_{3j}(\mathrm{t})$, $\mathrm{V}_{jn}(t) = \sum_{j=0}^{n}\Delta_{4j}(\mathrm{t})$.

Now taking the norm of eqn. (51) and applying the derived Lipschitz conditions on it, we have

$$\|\Delta_{1n}(t)\| \leq \frac{\tau^{\alpha-1}}{\Gamma(\alpha)} \int_0^t \left\| (\nabla_1 \left(t, S_{jn-1}(t)\right) - \nabla_1 \left(t, S_{jn-2}(t)\right))(t-\varphi)^{1-\alpha} \right\| d\varphi$$

$$\|\Delta_{2n}(t)\| \leq \frac{\tau^{\alpha-1}}{\Gamma(\alpha)} \int_0^t \left\| (\nabla_2 \left(t, I_{jn-1}(t)\right) - \nabla_2 \left(t, I_{jn-2}(t)\right))(t-\varphi)^{1-\alpha} \right\| d\varphi$$

$$\|\Delta_{3n}(t)\| \leq \frac{\tau^{\alpha-1}}{\Gamma(\alpha)} \int_0^t \left\| \left(\nabla_3 \left(t, R_{jn-1}(t)\right) - \nabla_3 \left(t, R_{jn-1}(t)\right)\right)(t-\varphi)^{1-\alpha} \right\| d\varphi \quad (52)$$

$$\|\Delta_{4n}(t)\| \leq \frac{\tau^{\alpha-1}}{\Gamma(\alpha)} \int_0^t \left\| (\nabla_4 \left(t, V_{jn-1}(t)\right) - \nabla_4 (t, V_{jn-2}(t)))(t-\varphi)^{1-\alpha} \right\| d\varphi$$

Using the Lipschitz condition in above equations, we have

$$\|\Delta_{1n}(t)\| \leq \frac{\tau^{\alpha-1}}{\Gamma(\alpha)} L_1 \int_0^t \|\Delta_{1(n-1)}(t)\| d\varphi$$

$$\|\Delta_{2n}(t)\| \leq \frac{\tau^{\alpha-1}}{\Gamma(\alpha)} L_2 \int_0^t \|\Delta_{2(n-1)}(t)\| d\varphi$$

$$\|\Delta_{3n}(t)\| \leq \frac{\tau^{\alpha-1}}{\Gamma(\alpha)} L_3 \int_0^t \|\Delta_{3(n-1)}(t)\| d\varphi \quad (53)$$

$$\|\Delta_{4n}(t)\| \leq \frac{\tau^{\alpha-1}}{\Gamma(\alpha)} L_4 \int_0^t \|\Delta_{4(n-1)}(t)\| d\varphi$$

Thus, with eqn. (53) we can easily established the existence of solutions of the fractional order system (45).

Theorem 2. The solution of Ebola virus model involving Caputo fractional-order operator (45) exists for t_0 given that $\frac{\tau^{\alpha-1}}{\Gamma(\alpha)} t_0 L_i < 1, i = 1,2 \ldots 4.$

Proof

Using the recursive equation in (53), we have

$$\|\Delta_{1n}(t)\| \leq \|S_n(0)\| \left[\frac{\tau^{\alpha-1}}{\Gamma(\alpha)} L_1 t\right]^n$$

$$\|\Delta_{2n}(t)\| \leq \|I_n(0)\| \left[\frac{\tau^{\alpha-1}}{\Gamma(\alpha)} L_2 t\right]^n$$

$$\|\Delta_{3n}(t)\| \leq \|R_n(0)\| \left[\frac{\tau^{\alpha-1}}{\Gamma(\alpha)} L_3 t\right]^n \quad (54)$$

$$\|\Delta_{4n}(t)\| \leq \|V_n(0)\| \left[\frac{\tau^{\alpha-1}}{\Gamma(\alpha)} L_4 t\right]^n$$

Solely, the solution of Ebola virus model (45) exists and is continuous.

Now, to manifest the system (48) is the solution of our model (45), we write

$$S(t) - S(0) = S_n(t) - C_{1n}(t)$$

$$I(t) - I(0) = I_n(t) - C_{2n}(t) \quad (55)$$

$$R(t) - R(0) = R_n(t) - C_{3n}(t)$$

$$V(t) - V(0) = V_n(t) - C_{4n}(t)$$

Therefore, we have

$$\|C_{1n}(t)\| = \frac{\tau^{\alpha-1}}{\Gamma(\alpha)} \int_0^t \left\| \left(\nabla_1\left(t, S(t)\right) - \nabla_1\left(t, S_{n-1}(t)\right)\right\| d\varphi \leq \frac{\tau^{\alpha-1}}{\Gamma(\alpha)} L_1 \|S - S_{n-1}\| t$$

Recursively, we write

$$\|C_{1n}(t)\| = \left[\frac{\tau^{\alpha-1}}{\Gamma(\alpha)} L_4 t\right]^{n+1} L_1 h$$

Now at t_0, we obtain

$$\|C_{1n}(t)\| = \left[\frac{\tau^{\alpha-1}}{\Gamma(\alpha)} L_4 t\right]^{n+1} L_1 h$$

As n approaches infinity together with the limit we have $\|C_{1n}(t)\| \to 0$. Similarly, one can easily show that $\|C_{1n}(t)\| \to 0, for\ i = 12, \ldots 4,$. this completes the proof of the existence of the solution. In order to prove the uniqueness of the solution of fractional-order Ebola virus model (45), we assume the system has another solution, say $S^*(t)$, $I^*(t)$, $R^*(t)$ and $V^*(t)$. such that

$$S(t) - S^*(t) = \frac{\tau^{\alpha-1}}{\Gamma(\alpha)} \int_0^t \left(\nabla_1\left(t, S(t)\right) - \nabla_1\left(t, S_{n-1}(t)\right)\right) d\varphi \quad (56)$$

Using the derived Lipschitz condition above and Taking the norms of the equation (56) we have

$$\|S(t) - S^*(t)\| \leq \frac{\tau^{\alpha-1}}{\Gamma(\alpha)} L_1 t \, \|S(t) - S^*(t)\|.$$

This can be written as

$$\|S(t) - S^*(t)\| \left(1 - \frac{\tau^{\alpha-1}}{\Gamma(\alpha)} L_1 t\right) \leq 0. \quad (57)$$

Theorem 3. The fractional-order Ebola virus model (45) has a unique solution given that

$$1-\frac{\tau^{\alpha-1}}{\Gamma(\alpha)}L_1 t\ >0$$

Proof

From Eq. (57),

$$\|S(t)-S^*(t)\|\left(1-\frac{\tau^{\alpha-1}}{\Gamma(\alpha)}L_1 t\right)\leq 0.$$

(58)

And the property of norms, we write $\|S(t)-S^*(t)\|=0$, which is $S(t)=S^*(t)$. Applying the same approach, we can easily show that $I(t)=I^*(t), R(t)=R^*(t)\ and\ V(t)=V^*(t)$. Thus, the fractional-order Ebola virus model (45) has a unique solution.

Numerical Experiment

We now present the numerical results and simulations of the extended fractional order mathematical model in Caputo sense with the help of the derived algorithm and numerical coded written in MATLAB environment using the model equations and the values of the parameters as $N=10.000, \beta_1=230, \beta=0.3, \gamma_1=0.25, \gamma=0.15, \mu_1=0.4, \mu_2=0.25, \delta_1=0.3, \delta_2=0.75$

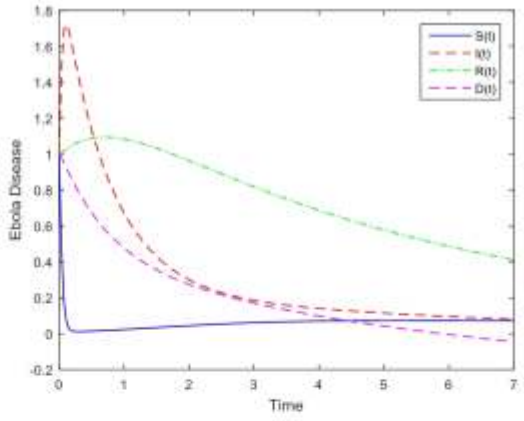

Fig. 1: Numerical Solution by implicit FLMMs at t = [0, 7]

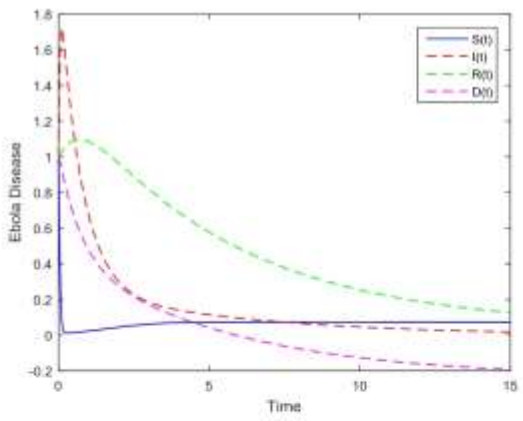

Fig. 2: Numerical Solution by implicit FLMMs at t = [0, 15]

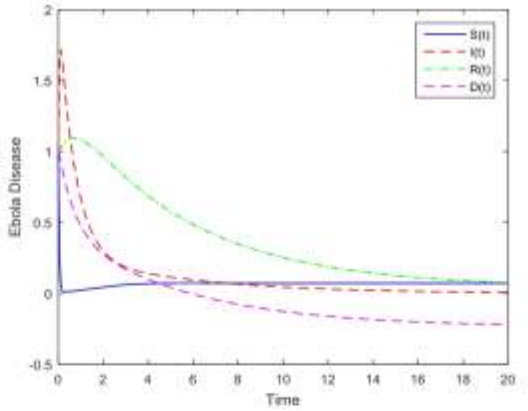

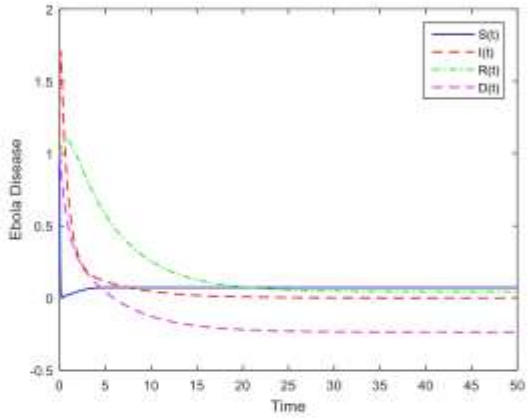

Fig. 3: Numerical Solution by implicit FLMMs at $t = [0, 20]$

Fig. 1: Numerical Solution by implicit FLMMs at $t = [0, 50]$

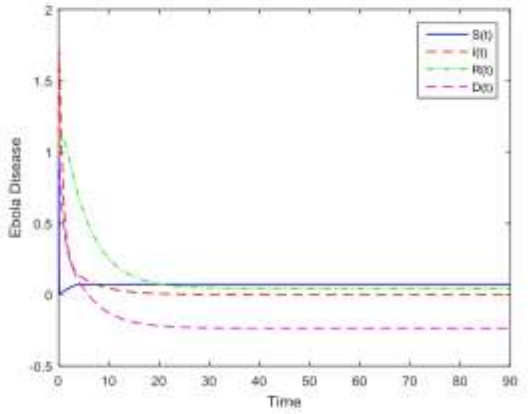

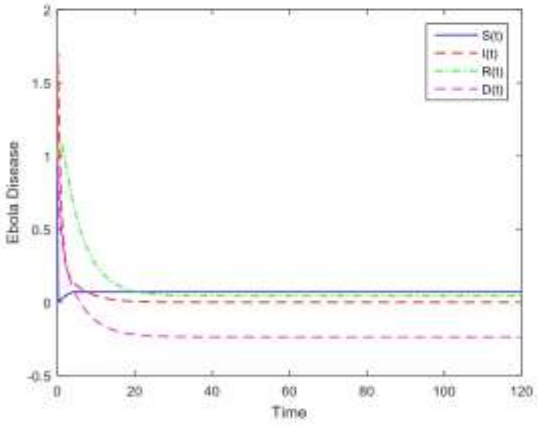

Fig. 5: Numerical Solution by implicit FLMMs at $t = [0, 90]$

Fig. 6: Numerical Solution by implicit FLMMs at $t = [0, 120]$

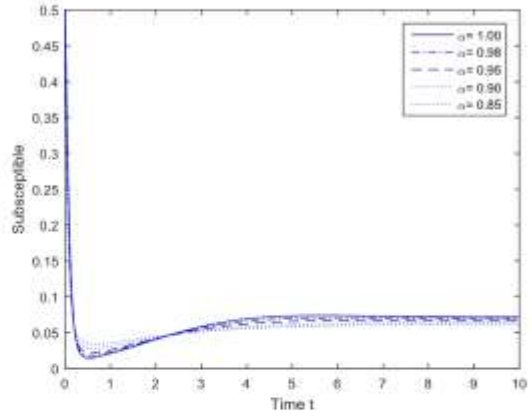

Fig. 7: Numerical Simulation of S(t) at different values of alpha

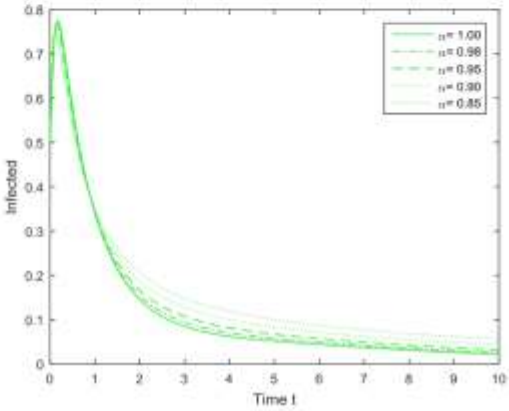

Fig. 8: Numerical Simulation of I(t) at different values of alpha

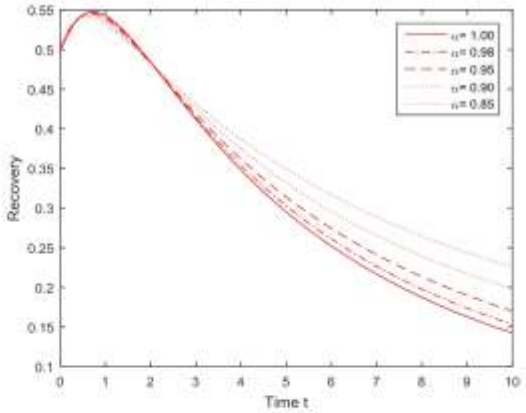

Fig. 9: Numerical Simulation of R(t) at different values of alpha

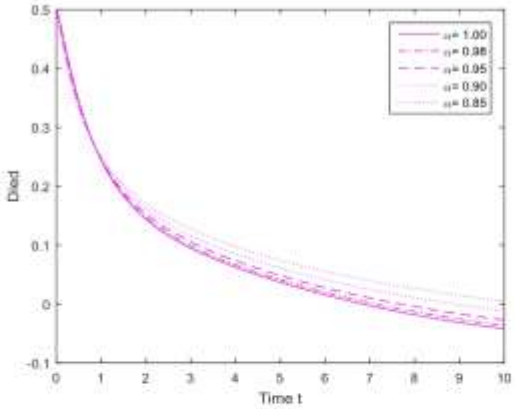

Fig. 10: Numerical Simulation of D(t) at different values of alpha

Discussion

The dynamics of Ebola virus model are examined through the integer-order (ODE) and non-integer-order (FODE) models approach. The integer-order model does not only used to formulate the FODE via the Caputo definition, but also supports some results reported by the FODE model. Putting in different value of alpha (fractional-order α) for the FODE indicates that the results approach the integer one (see Fig. 9 and 10). This finding is similar to the results reported by many authors in different scenarios, Baleanu *et al.,* (2020), Rezapour *et al.,* (2020) and Diethelm, (2013). The systems of FODEs in (45) where solved numerically using the Garrappas code FDE_PI12 accordingly, Garrappa, (2018).

Conclusion

In this research, we have extended the existing work titled Mathematical modeling, analysis and Markov Chain Monte Carlo simulation of Ebola epidemics which is a classical model of integer type to a non – integer type of Numerical Simulation of Fractional Order Mathematical model of Ebola Epidemics in Caputo sense. Based on the results obtained we will conclude that our result is reliable by providing a more realistic mathematical models that will interpret and enhance the understanding of Ebola epidemic and has contributed to research activities in the field of Ebola epidemic, so also the field of fractional derivatives.

References

Thomas Wetere Tulu, Boping Tian aand Zunyou Wu (2017); Mathematical modeling, analysis and Markov Chain Monte Carlo simulation of Ebola epidemics. Results in Physics 7 (2017) 962–968.

Abdon A. and Muhammad A. K. (2019); Validity of Fractal Derivative to Capturing Chaotic Attractors. Chaos, Solitons and Fractals 126 (2019) 50–59.

Amin J., Sadia A., and Dumitru B. (2019); A New Fractional Modeling and Control Strategy for the Outbreak of Dengue Fever. Physica A 535 (2019) 122524.

Diethelm K. (2013) A Fractional Calculus Based Model for the Simulation of an Outbreak of Dengue Fever. Nonlinear Dyn (2013) 71:613 – 619.

Eric O., Francis T. O., Samuel K. A., Isaac K. D., and Nana K. F. (2016); Fractional Order SIR Model with Constant Population. British Journal of Mathematics and Computer Science 14(2): 1 – 12, 2016.

Ilknur K. (2019); Modeling the heat flow equation with fractional-fractal differentiation. Chaos, Solitons and Fractals 128 (2019) 83–91.

Kolade M. O., and Abdon A. (2019); Computational study of multi-species fractional reaction Diffusion system with ABC operator. Chaos, Solitons and Fractals 128 (2019) 280–289.

Musiliu F. F., Sharidan S., Fuaada M. S., and Ilyas K. (2019) Mathematical Modeling of Radiotherapy Cancer Treatment using Caputo Fractional Derivative, Computer Methods, and Programs in Biomedicine.

Musiliu F. F., Sharidan S. Fuaada M. S. and Ilyas K. (2019); Numerical Simulation of Normal and Cancer Cell's Populations with Fractional Derivatives under Radiotherapy, Computer Methods and Program in Biomedicine.

Nur 'Izzati H. and Adem K. (2018); A fractional order SIR epidemic model for dengue transmission. Chaos, Solitons and Fractals 114 (2018) 55–62.

Rashid J., Muhammad A. K., Poom K., and Phatiphat T. (2019); Modeling the Transmission of

Dengue Infection through Fractional Derivatives. Chaos, Solitons and Fractals 127 (2019) 189 – 216.

Sania Q. and Atangana A. (2019); Mathematical analysis of dengue fever outbreak by novel Fractional operators with field data. Physica A 526 (2019) 121127.

Thomas W. T., Boping T., Zunyou W. (2017); Mathematical Modeling, Anlysis and Markov Chain Monte Carlo simulation of Ebola Epidemic.

Zafar I., Nauman A., Dumitru B., Waleed A., Muhammad R., Muhammad A. and Ali S. A. (2020); Positivity and Boundedness Preserving Numerical Algorithm for the Solution of Fractional Nonlinear Model of HIV/AIDS Transmission. Chaos, Solitons and Fractals 134 (2020) 109706.

Chowell G., and Hiroshi N. (2009). Transmission dynamics and control of Ebola virus disease (EVD): a review.

Lewnard J. A., Ndeffo Mbah M. L., J. A. Alfaro-Murillo.(2014) "Dynamics and control of Ebola virus transmission in Montserrado, Liberia: a mathematical modelling analysis," The Lancet Infectious Diseases, vol. 14, no. 12, pp. 1189–1195, 2014.

Dowell S. F., R. Mukunu, Ksiazek T. G., Khan A. S., Rollin P. E., and Peters C. J.(1999) "Transmission of Ebola hemorrhagic fever: a study of risk factors in family members, Kikwit, Democratic Republic of the Congo, 1995. Commission de Lutte contre les Epidemies a Kikwit," Journal of Infectious Diseases, vol. 179, supplement 1, pp. S87–S91,.

Peters C. J. and LeDuc, J. W. (1999) "An introduction to Ebola: the virus and the disease," Journal of Infectious Diseases, vol. 179, supplement 1,.

Rezapour S, Mohammadi H, Samei ME.(2020). SEIR epidemic model for COVID-19 transmission by Caputo derivative of fractional order. Adv Differ Equ;2020(1):1–19.

Baleanu D, Jajarmi A, Mohammadi H, Rezapour S.(2020). A new study on the mathematical modelling of human liver with Caputo–Fabrizio fractional derivative. Chaos Solitons Fractals;134:109705.

Garrappa R. (2018). Numerical solution of fractional differential equations: a survey and a software tutorial. Mathematics;6(2):16.

Abacus (Mathematics Science Series)
Vol. 49, No 3, September. 2022

FORMULATION OF A NINTH ORDER BLOCK IMPLICIT ADAMS MOULTON METHOD FOR THE SOLUTION OF FIRST ORDER ORDINARY DIFFERENTIAL EQUATIONS

JO Oladele and AN Kantiyon

Department of Mathematatics Air Force Institute of Technology, Kaduna
Joshuaoladele70@gmail.com

Abstract

This paper considers the formulation of a ninth order (k=8) block implicit Adams's Moulton methods for the solution of stiff and non-stiff first order Ordinary differential Equations (ODE).We applied the methods of interpolation and collocation procedures to generate the continuous formula, which was evaluated at the grid points. The procedure yields eight discrete schemes which are combined to form the block method. The new method (k=8) is found to be of order 9. The method is consistent and zero-stable, hence convergent. Numerical experiments carried out on the new method shows that implementation in block form converges faster to exact solution with minimal error. Also the results obtained using the block form show that the new method performed better than existing methods.

Keywords: Grid, Implict, Stiff, Block methods, Convergence, Adams-Moulton, consistent

Introduction:

Differential equation play an important role in modeling virtually every physical, technical, or biological process, from celestial motion to bridge design to interactions between neurons.

Often, systems described by differential equations are so complex, or the system that they describe is so large that a purely analytical solution to the equation is not tractable. It is in these complex systems that computer simulation and numerical methods are useful.

Most of the differential equations we need to solve in the real world, have no "nice" algebraic solution. That is, we cannot solve them using the available techniques (e.g. separation of variables, integrable combinations, and the use of integrating factors etc.) or other similar means.

Even if we can solve some differential equations analytically, the solution may be quite difficult and complicated and so, are not very useful. In such case, a numerical approach gives us a good approximate solution.

Consider an initial value problem $y' = f(x, y), y(x_0) = y_0$ in [a, b]
(1.1)

If (1.1) cannot be solved algebraically, it is necessary that we resort to numerical methods to obtain useful approximations to a solution of (1.1).

The main aim of numerical methods is the design and analysis of techniques to give approximate but accurate solutions to hard problems.

It is in the light of the above challenges that we present a suitable numerical method that can easily be used for finding approximate solutions for first order ordinary differential equations.

Many researchers have developed several numerical methods for finding approximate solutions for solving first order ordinary differential equations of the form (1.1). Notable among the researchers are Yahaya and Tijjani (2015), Badmus and Mohammed(2016), Ndanusa (2007), Famurewa, *et al* (2011), Adesanya, *et al* (2012), Awoyemi, *et al* (2014), Fadugba, *et al* (2014) , and Akinfenwa *et al* (2011), to mention a few.

Most life, physical and chemical problems which may not be solved analytically can be modeled into stiff and non-stiff differential equations, hence the need to develop adequate high order algorithm to handle these classes of problem

Also there are differential equations whose exact solution $y(t)$ includes a term that decays exponentially to zero as t increases, but whose derivative are much greater in magnitude than the term itself. Such differential equations are called stiff differential equations. It is important to note that this class of differential equations cannot be handled by ordinary explicit methods. It is in view of the foregoing that we shall develop ninth order (K=8) implicit linear multistep methods (Adams-Moulton) for the solution of stiff and non-stiff first order ordinary differential equations

$$C_q = \frac{1}{q_i}(\propto_1 + 2^q\alpha_2 + 3^q\alpha_3 + \cdots + k^q \propto_k) - \frac{1}{(q-1)!}(\beta_1 + 2^{q-1}\beta_2 + \cdots + k^{q-1}\beta_k), q = 2, 3 \ldots \quad (1.5)$$

Hence, the linear multistep method (1.6) is said to be of order p if in (1.8),

$C_0 = C_1 = C_2 \ \ldots = C_P = 0$ but $C_{p+1} \neq 0$ (1.6)

then C_{p+1} is the error constant.(Badmus and Mohammed, 2016)

Convergence

A numerical method is said to be convergent if the result it generates approaches the exact solution as h approaches zero. That is, when it is applied to initial value problem, it generates a corresponding approximation which tend to the exact solution as n approaches infinity, that is:

$y_n \rightarrow y(x_n)\ as\ n \rightarrow \infty$

Consistence

A numerical method is consistent if it is of order $p \geq 1$, that is, $\sum_{j=0}^{k} \alpha_j = 0$ and $\sum_{j=0}^{k} j\alpha_j = \sum_{j=0}^{k} \beta_j$

Methodology:

Consider the Adams-Moulton method of the form

$$y_{n+k} - y_{n+k-1} = h\sum_{j=0}^{k} \beta_j f_{n+j} \quad (2.1)$$

Given a power series of the form

$$P(x) = \sum_{j=0}^{k} a_j x^j \quad (2.2)$$

Equation (2.2) is used as our basis to produce an approximate solution to (3.36) as

$$y(x) = \sum_{j=0}^{m+t-1} a_j x^j = y_{n+j} \quad (2.3)$$

$$y'(x) = \sum_{j=1}^{m+t-1} j a_j x^{j-1} = f_{n+j} \quad (2.4)$$

Where a_j^s are the parameters to be determined and m and t are the points of collocation and interpolation respectively. This process leads to $(m + t - 1)$ degree of the polynomial required in the method with $(m + t - 1)$ unknown coefficients which are to be determined by the use of maple 17 mathematical software .(Yahaya and Tijjani,2015)

Abacus (Mathematics Science Series)
Vol. 49, No 3, September. 2022

Derivation of Block Method of Implicit L.M.M at K=8

Specifically, the eight step Adams-Moulton method (k=8) is derived as follows.

Using equation (2.3) and (2.4), we set m=8 and t=1. The degree of of the polynomial is

(m+t-1) = 8. Equation (2.3) is interpolated at $x = x_{n+j}\,; j = 6$ and (2.4) is collocated at $x = x_{n+j}\,; j = 0,1,2,3,4,5,6,7,8$

This gives the following non-linear system of equations of the form

$$y(x) = \sum_{j=0}^{8} a_j x_{n+6}^{j} = y_{n+k}\ ,\ k = 7 \qquad (2.5)$$

$$y'(x) = \sum_{j=1}^{8} j a_j x_{n+k}^{j-1} = f_{n+k}\ ,\ k = 0,1,2,3,4,5,6,7,8 \qquad (2.6)$$

Equation (2.5) and (2.6) can be written explicitly as

$$a_0 + a_1 x_{n+7} + a_2 x_{n+7}^2 + a_3 x_{n+7}^3 + a_4 x_{n+7}^4 + a_5 x_{n+7}^5 + a_6 x_{n+7}^6 + a_7 x_{n+7}^7 + a_8 x_{n+7}^8 + a_9 x_{n+7}^9 = y_{n+7}$$

$$a_1 + 2a_2 x_n + 3a_3 x_n^2 + 4a_4 x_n^3 + 5a_5 x_n^4 + 6a_6 x_n^5 + 7a_7 x_n^6 + 8a_8 x_n^7 + 9a_9 x_n^8 = f_n$$

$$a_1 + 2a_2 x_{n+1} + 3a_3 x_{n+1}^2 + 4a_4 x_{n+1}^3 + 5a_5 x_{n+1}^4 + 6a_6 x_{n+1}^5 + 7a_7 x_{n+1}^6 + 8a_8 x_{n+1}^7 + 9a_9 x_{n+1}^8 = f_{n+1}$$

$$a_1 + 2a_2 x_{n+2} + 3a_3 x_{n+2}^2 + 4a_4 x_{n+2}^3 + 5a_5 x_{n+2}^4 + 6a_6 x_{n+2}^5 + 7a_7 x_{n+2}^6 + 8a_8 x_{n+2}^7 + 9a_9 x_{n+2}^8 = f_{n+2}$$

$$a_1 + 2a_2 x_{n+3} + 3a_3 x_{n+3}^2 + 4a_4 x_{n+3}^3 + 5a_5 x_{n+3}^4 + 6a_6 x_{n+3}^5 + 7a_7 x_{n+3}^6 + 8a_8 x_{n+3}^7 + 9a_9 x_{n+3}^8 = f_{n+3}$$

$$a_1 + 2a_2 x_{n+4} + 3a_3 x_{n+4}^2 + 4a_4 x_{n+4}^3 + 5a_5 x_{n+4}^4 + 6a_6 x_{n+4}^5 + 7a_7 x_{n+4}^6 + 8a_8 x_{n+4}^7 + 9a_9 x_{n+4}^8 = f_{n+4}$$

$$a_1 + 2a_2 x_{n+5} + 3a_3 x_{n+5}^2 + 4a_4 x_{n+5}^3 + 5a_5 x_{n+5}^4 + 6a_6 x_{n+5}^5 + 7a_7 x_{n+5}^6 + 8a_8 x_{n+5}^7 + 9a_9 x_{n+5}^8 = f_{n+5}$$

$$a_1 + 2a_2 x_{n+6} + 3a_3 x_{n+6}^2 + 4a_4 x_{n+6}^3 + 5a_5 x_{n+6}^4 + 6a_6 x_{n+6}^5 + 7a_7 x_{n+6}^6 + 8a_8 x_{n+6}^7 + 9a_9 x_{n+6}^8 = f_{n+6}$$

$$a_1 + 2a_2 x_{n+7} + 3a_3 x_{n+7}^2 + 4a_4 x_{n+7}^3 + 5a_5 x_{n+7}^4 + 6a_6 x_{n+7}^5 + 7a_7 x_{n+7}^6 + 8a_8 x_{n+7}^7 + 9a_9 x_{n+7}^8 = f_{n+7}$$

$$a_1 + 2a_2 x_{n+8} + 3a_3 x_{n+8}^2 + 4a_4 x_{n+8}^3 + 5a_5 x_{n+8}^4 + 6a_6 x_{n+8}^5 + 7a_7 x_{n+8}^6 + 8a_8 x_{n+8}^7 + 9a_9 x_{n+8}^8 = f_{n+8} \qquad (2.7)$$

Equation (2.7) is written in matrix equation form as

$$\begin{bmatrix} 1 & x_{n+7} & x_{n+7}^2 & x_{n+7}^3 & x_{n+7}^4 & x_{n+7}^5 & x_{n+7}^6 & x_{n+7}^7 & x_{n+7}^8 & x_{n+7}^9 \\ 0 & 1 & 2x_n & 3x_n^2 & 4x_n^3 & 5x_n^4 & 6x^5{}_n & 7x_n^6 & 8x_n^7 & 9x_n^8 \\ 0 & 1 & 2x_{n+1} & 3x_{n+1}^2 & 4x_{n+1}^3 & 5x_{n+1}^4 & 6x^5{}_{n+1} & 7x_{n+1}^6 & 8x_{n+1}^7 & 9x_{n+1}^8 \\ 0 & 1 & 2x_{n+2} & 3x_{n+2}^2 & 4x_{n+2}^3 & 5x_{n+2}^4 & 6x^5{}_{n+2} & 7x_{n+2}^6 & 8x_{n+2}^7 & 9x_{n+2}^8 \\ 0 & 1 & 2x_{n+3} & 3x_{n+3}^3 & 4x_{n+3}^3 & 5x_{n+3}^4 & 6x^5{}_{n+3} & 7x_{n+3}^6 & 8x_{n+3}^7 & 9x_{n+3}^8 \\ 0 & 1 & 2x_{n+4} & 3x_{n+4}^3 & 4x_{n+4}^3 & 5x_{n+4}^4 & 6x^5{}_{n+4} & 7x_{n+4}^6 & 8x_{n+4}^7 & 9x_{n+4}^8 \\ 0 & 1 & 2x_{n+5} & 3x_{n+5}^3 & 4x_{n+5}^3 & 5x_{n+5}^4 & 6x^5{}_{n+5} & 7x_{n+5}^6 & 8x_{n+5}^7 & 9x_{n+5}^7 \\ 0 & 1 & 2x_{n+6} & 3x_{n+6} & 4x_{n+6}^3 & 5x_{n+6}^4 & 6x^5{}_{n+6} & 7x_{n+6}^6 & 8x_{n+6}^7 & 9x_{n+6}^7 \\ 0 & 1 & 2x_{n+7} & 3x_{n+7} & 4x_{n+7}^3 & 5x_{n+7}^4 & 6x^5{}_{n+7} & 7x_{n+7}^6 & 8x_{n+7}^7 & 9x_{n+7}^7 \\ 0 & 1 & 2x_{n+8} & 3x_{n+8} & 4x_{n+8} & 5x_{n+8}^4 & 6x^5{}_{n+8} & 7x_{n+8}^6 & 8x_{n+8}^7 & 9x_{n+8}^7 \end{bmatrix} \begin{bmatrix} a_0 \\ a_1 \\ a_2 \\ a_3 \\ a_4 \\ a_5 \\ a_6 \\ a_7 \\ a_8 \\ a_9 \end{bmatrix} = \begin{bmatrix} y_{n+6} \\ f_n \\ f_{n+1} \\ f_{n+2} \\ f_{n+3} \\ f_{n+4} \\ f_{n+5} \\ f_{n+6} \\ f_{n+7} \\ f_{n+8} \end{bmatrix} \tag{2.8}$$

The continuous formular for 2.8 is given as

$$y(x) = y_{n+7} + h[\beta_0 f_n + \beta_1 f_{n+1} + \beta_2 f_{n+2} + \beta_3 f_{n+3} + \beta_4 f_{n+4} + \beta_5 f_{n+5} + \beta_6 f_{n+6} + \beta_7 f_{n+7} + \beta_8 f_{n+8}] \tag{2.9}$$

Explicitly equation (2.9) is written as

$$y_{x+8} = y_{n+7} + \left(-\frac{149527}{518400}h + x - \frac{761}{560}\frac{x^2}{h} + \frac{29531}{30240}\frac{x^3}{h^2} - \frac{267}{640}\frac{x^4}{h^3} + \frac{1069}{9600}\frac{x^5}{h^4} - \frac{3}{160}\frac{x^6}{h^5} + \frac{13}{6720}\frac{x^7}{h^6} - \frac{1}{8960}\frac{x^8}{h^7} + \frac{1}{362880}\frac{x^9}{h^8}\right) f_n + \left(-\frac{408317}{259200}h + \frac{4x^2}{h} - \frac{481}{105}\frac{x^3}{h^2} + \frac{349}{144}\frac{x^4}{h^3} - \frac{329}{450}\frac{x^5}{h^4} + \frac{115}{864}\frac{x^6}{h^5} - \frac{73}{5040}\frac{x^7}{h^6} + \frac{1}{1152}\frac{x^8}{h^7} - \frac{1}{45360}\frac{x^9}{h^8}\right) f_{n+1} + \left(-\frac{24353}{259200}h - \frac{7x^2}{h} + \frac{207}{20}\frac{x^3}{h^2} - \frac{18353}{2880}\frac{x^4}{h^3} + \frac{15289}{7200}\frac{x^5}{h^4} - \frac{179}{432}\frac{x^6}{h^5} + \frac{239}{5040}\frac{x^7}{h^6} - \frac{17}{5760}\frac{x^8}{h^7} + \frac{1}{12960}\frac{x^9}{h^8}\right) f_{n+2} + \left(-\frac{542969}{259200}h + \frac{28}{3}\frac{x^2}{h} - \frac{2003}{135}\frac{x^3}{h^2} + \frac{797}{80}\frac{x^4}{h^3} - \frac{268}{75}\frac{x^5}{h^4} + \frac{71}{96}\frac{x^6}{h^5} - \frac{149}{1680}\frac{x^7}{h^6} + \frac{11}{1920}\frac{x^8}{h^7} - \frac{1}{6480}\frac{x^9}{h^8}\right) f_{n+3} + \left(-\frac{343}{3240}h - \frac{35}{4}\frac{x^2}{h} + \frac{691}{48}\frac{x^3}{h^2} - \frac{1457}{144}\frac{x^4}{h^3} + \frac{10993}{2880}\frac{x^5}{h^4} - \frac{179}{216}\frac{x^6}{h^5} + \frac{209}{2016}\frac{x^7}{h^6} - \frac{1}{144}\frac{x^8}{h^7} + \frac{1}{5184}\frac{x^9}{h^8}\right) f_{n+4} + \left(-\frac{368039}{259200}h + \frac{28}{5}\frac{x^2}{h} - \frac{47}{5}\frac{x^3}{h^2} + \frac{4891}{720}\frac{x^4}{h^3} - \frac{1193}{450}\frac{x^5}{h^4} + \frac{2581}{4320}\frac{x^6}{h^5} - \frac{391}{5040}\frac{x^7}{h^6} + \frac{31}{5760}\frac{x^8}{h^7} - \frac{1}{6480}\frac{x^9}{h^8}\right) f_{n+5} + \left(-\frac{261023}{259200}h - \frac{7}{3}\frac{x^2}{h} + \frac{2143}{540}\frac{x^3}{h^2} - \frac{187}{64}\frac{x^4}{h^3} + \frac{2803}{2400}\frac{x^5}{h^4} - \frac{13}{48}\frac{x^6}{h^5} + \frac{61}{1680}\frac{x^7}{h^6} - \frac{1}{384}\frac{x^8}{h^7} + \frac{1}{12960}\frac{x^9}{h^8}\right) f_{n+6} + \left(-\frac{111587}{259200}h\frac{4}{7}\frac{x^2}{h} - \frac{103}{105}\frac{x^3}{h^2} + \frac{527}{720}\frac{x^4}{h^3} - \frac{67}{225}\frac{x^5}{h^4} + \frac{61}{864}\frac{x^6}{h^5} - \frac{7}{720}\frac{x^7}{h^6} + \frac{29}{40320}\frac{x^8}{h^7} -$$

$$\frac{1}{45360}\frac{x^9}{h^8}\Big) f_{n+7} + \Big(\frac{8183}{518400}h - \frac{1}{16}\frac{x^2}{h} + \frac{121}{1120}\frac{x^3}{h^2} - \frac{469}{5760}\frac{x^4}{h^3} + \frac{967}{28800}\frac{x^5}{h^4} - \frac{7}{864}\frac{x^6}{h^5} + \frac{23}{20160}\frac{x^7}{h^6} - \frac{1}{11520}\frac{x^8}{h^7} + \frac{1}{362880}\frac{x^9}{h^8}\Big) f_{n+8} \quad (2.10)$$

Equation (2.10) was obtained by setting $x_n = 0$

Evaluating (2.10) at $(x = x_{n+j}\,; j = 0,12,3,4,5,7,8)$, we get the required eight set of discrete schemes that form our block methods.

The generated block schemes are given below:

$$y[n] = y_{n+7} - \frac{149527}{518400}hf_n - \frac{408317}{259200}hf_{n+1} - \frac{24353}{259200}hf_{n+2} - \frac{542969}{259200}hf_{n+3} - \frac{343}{3240}hf_{n+4} - \frac{368039}{259200}hf_{n+5} - \frac{261023}{259200}hf_{n+6} - \frac{111587}{259200}hf_{n+7} + \frac{8183}{518400}hf_{n+8}$$

$$y[n+1] = y_{n+7} + \frac{9}{1400}hf_n - \frac{241}{700}hf_{n+1} - \frac{477}{350}hf_{n+2} - \frac{387}{700}hf_{n+3} - \frac{209}{140}hf_{n+4} - \frac{387}{700}hf_{n+5} - \frac{477}{350}hf_{n+6} - \frac{241}{700}hf_{n+7} + \frac{9}{1400}hf_{n+8}$$

$$y[n+2] = y_{n+7} - \frac{425}{145152}hf_n + \frac{2525}{72576}hf_{n+1} - \frac{34015}{72576}hf_{n+2} - \frac{75175}{72576}hf_{n+3} - \frac{5125}{4536}hf_{n+4} - \frac{55225}{72576}hf_{n+5} - \frac{93025}{72576}hf_{n+6} - \frac{26365}{72576}hf_{n+7} + \frac{175}{20736}hf_{n+8}$$

$$y[n+3] = y_{n+7} - \frac{13}{14175}hf_n + \frac{104}{14175}hf_{n+1} - \frac{244}{14175}hf_{n+2} - \frac{4402}{14175}hf_{n+3} - \frac{3854}{2835}hf_{n+4} - \frac{9232}{14175}hf_{n+5} - \frac{18724}{14175}hf_{n+6} - \frac{718}{2025}hf_{n+7} + \frac{107}{14175}hf_{n+8}$$

$$y[n+4] = y_{n+7} - \frac{81}{44800}hf_n + \frac{389}{22400}hf_{n+1} - \frac{1719}{22400}hf_{n+2} + \frac{4833}{22400}hf_{n+3} - \frac{209}{280}hf_{n+4} - \frac{17217}{22400}hf_{n+5} - \frac{28809}{22400}hf_{n+6} - \frac{8101}{22400}hf_{n+7} + \frac{369}{44800}hf_{n+8}$$

$$y[n+5] = y_{n+7} - \frac{127}{113400}hf_n + \frac{583}{56700}hf_{n+1} - \frac{1189}{28350}hf_{n+2} + \frac{5581}{56700}hf_{n+3} - \frac{1513}{11340}hf_{n+4} - \frac{13739}{56700}hf_{n+5} - \frac{38149}{28350}hf_{n+6} - \frac{19937}{56700}hf_{n+7} + \frac{119}{16200}hf_{n+8}$$

$$y[n+6] = y_{n+7} - \frac{7297}{3628800} hf_n + \frac{34453}{1814400} hf_{n+1} - \frac{147143}{1814400} hf_{n+2} + \frac{377521}{1814400} hf_{n+3} - \frac{8233}{22680} hf_{n+4} + \frac{876271}{1814400} hf_{n+5} - \frac{1622393}{1814400} hf_{n+6} - \frac{687797}{1814400} hf_{n+7} + \frac{33953}{3628800} hf_{n+8}$$

$$y[n+8] = y_{n+7} - \frac{33953}{3628800} hf_n + \frac{156437}{1814400} hf_{n+1} - \frac{645607}{1814400} hf_{n+2} + \frac{1573169}{1814400} hf_{n+3} - \frac{31457}{22680} hf_{n+4} + \frac{2797679}{1814400} hf_{n+5} - \frac{2302297}{1814400} hf_{n+6} + \frac{2233547}{1814400} hf_{n+7} + \frac{1070017}{3628800} hf_{n+8}$$

(2.11)

Basic Analysis of the proposed block Method

Order and Error Constant of the Method

The order and error constant of the scheme for (2.11)are obtained by Taylors series expansion of the terms involved in the schemes, and the evaluation and simplification are done using maple 17 software. We set the following :

$y_n = y_0, f_n = hY_n = hy$,in order to carry out the procedures

we established from our procedure that equation (2.11) are of order $[9,9,9,9,9,9,9,9]^T$ with small Error constant

$$\left(-\frac{889623523004867}{419904000}, -\frac{47563276288}{55125}, -\frac{26635434755705}{23514624}, -\frac{40714164539383}{40186125}, -\frac{31201509280523}{28224000}, -\frac{5660029883537}{5740875}, -\frac{25838654747025299}{20575296000}, -\frac{814296227424101971}{20575296000}\right)^T$$

From the definition of consistency above, it is clear that the eight step Adams-Moulton method is consistent since the order is greater than 1.

Zero Stability of the Method K=8

Similarly the discrete schemes in equation (2.11) can be represented in matrix form as shown below

Abacus (Mathematics Science Series)
Vol. 49, No 3, September. 2022

$$\begin{bmatrix} 1&0&0&0&0&0&-1&0\\ 0&1&0&0&0&0&-1&0\\ 0&0&1&0&0&0&-1&0\\ 0&0&0&1&0&0&-1&0\\ 0&0&0&0&1&0&-1&0\\ 0&0&0&0&0&1&-1&0\\ 0&0&0&0&0&0&-1&0\\ 0&0&0&0&0&0&-1&1 \end{bmatrix} \begin{bmatrix} y_{n+1}\\ y_{n+2}\\ y_{n+3}\\ y_{n+4}\\ y_{n+5}\\ y_{n+6}\\ y_{n+7}\\ y_{n+8} \end{bmatrix} = \begin{bmatrix} 0&0&0&0&0&0&0&0\\ 0&0&0&0&0&0&0&0\\ 0&0&0&0&0&0&0&0\\ 0&0&0&0&0&0&0&0\\ 0&0&0&0&0&0&0&0\\ 0&0&0&0&0&0&0&0\\ 0&0&0&0&0&0&0&-1\\ 0&0&0&0&0&0&0&0 \end{bmatrix} \begin{bmatrix} y_{n-7}\\ y_{n-6}\\ y_{n-5}\\ y_{n-4}\\ y_{n-3}\\ y_{n-2}\\ y_{n-1}\\ y_n \end{bmatrix} +$$

$$h \begin{bmatrix} -\frac{241}{700} & -\frac{477}{350} & -\frac{387}{700} & -\frac{209}{140} & -\frac{387}{700} & -\frac{477}{350} & -\frac{241}{700} & \frac{9}{1400}\\ \frac{2525}{72576} & -\frac{34015}{72576} & -\frac{75175}{72576} & -\frac{5125}{4536} & -\frac{55225}{72576} & -\frac{93025}{72576} & -\frac{26365}{72576} & \frac{175}{20736}\\ \frac{104}{14175} & -\frac{244}{14175} & -\frac{4402}{14175} & -\frac{3854}{2835} & -\frac{9232}{14175} & -\frac{18724}{14175} & -\frac{718}{2025} & \frac{107}{14175}\\ \frac{389}{22400} & -\frac{1719}{22400} & \frac{4833}{22400} & -\frac{209}{280} & -\frac{17217}{22400} & -\frac{28809}{22400} & -\frac{8101}{22400} & \frac{369}{44800}\\ \frac{583}{56700} & -\frac{1189}{28350} & \frac{5581}{56700} & -\frac{1513}{11340} & -\frac{13739}{56700} & -\frac{38149}{28350} & -\frac{19937}{56700} & \frac{119}{16200}\\ \frac{34453}{1814400} & -\frac{14743}{1814400} & \frac{377521}{1814400} & -\frac{8233}{22680} & \frac{876271}{1814400} & -\frac{1622393}{1814400} & -\frac{687797}{1814400} & \frac{33953}{3628800}\\ -\frac{408317}{259200} & -\frac{24353}{259200} & -\frac{542969}{259200} & -\frac{343}{3240} & -\frac{368039}{259200} & -\frac{261023}{259200} & -\frac{111587}{259200} & \frac{8183}{518400}\\ \frac{156437}{1814400} & -\frac{645607}{1814400} & \frac{1573169}{1814400} & -\frac{31457}{22680} & \frac{2797679}{1814400} & -\frac{2302297}{1814400} & \frac{2233547}{1814400} & \frac{1070017}{3628800} \end{bmatrix} \begin{bmatrix} f_{n+1}\\ f_{n+2}\\ f_{n+3}\\ f_{n+4}\\ f_{n+5}\\ f_{n+6}\\ f_{n+7}\\ f_{n+8} \end{bmatrix}$$

$$+h \begin{bmatrix} 0&0&0&0&0&0&0&\frac{9}{1400}\\ 0&0&0&0&0&0&0&-\frac{425}{145152}\\ 0&0&0&0&0&0&0&-\frac{13}{14175}\\ 0&0&0&0&0&0&0&-\frac{81}{44800}\\ 0&0&0&0&0&0&0&-\frac{127}{113400}\\ 0&0&0&0&0&0&0&-\frac{7298}{3628800}\\ 0&0&0&0&0&0&0&-\frac{149527}{518400}\\ 0&0&0&0&0&0&0&-\frac{33953}{3628800} \end{bmatrix} \begin{bmatrix} f_{n-7}\\ f_{n-6}\\ f_{n-5}\\ f_{n-4}\\ f_{n-3}\\ f_{n-2}\\ f_{n-1}\\ f_n \end{bmatrix} \tag{2.12}$$

Abacus (Mathematics Science Series)
Vol. 49, No 3, September. 2022

Equation (2.11) can be represented as

$$AY_{w+1} = BY_w + h[CF_{w+1} + DF_w] \tag{2.13}$$

Let $A=\begin{bmatrix} 1 & 0 & 0 & 0 & 0 & 0 & -1 & 0 \\ 0 & 1 & 0 & 0 & 0 & 0 & -1 & 0 \\ 0 & 0 & 1 & 0 & 0 & 0 & -1 & 0 \\ 0 & 0 & 0 & 1 & 0 & 0 & -1 & 0 \\ 0 & 0 & 0 & 0 & 1 & 0 & -1 & 0 \\ 0 & 0 & 0 & 0 & 0 & 1 & -1 & 0 \\ 0 & 0 & 0 & 0 & 0 & 0 & -1 & 0 \\ 0 & 0 & 0 & 0 & 0 & 0 & -1 & 1 \end{bmatrix}$, $B=\begin{bmatrix} 0 & 0 & 0 & 0 & 0 & 0 & 0 & 0 \\ 0 & 0 & 0 & 0 & 0 & 0 & 0 & 0 \\ 0 & 0 & 0 & 0 & 0 & 0 & 0 & 0 \\ 0 & 0 & 0 & 0 & 0 & 0 & 0 & 0 \\ 0 & 0 & 0 & 0 & 0 & 0 & 0 & 0 \\ 0 & 0 & 0 & 0 & 0 & 0 & 0 & 0 \\ 0 & 0 & 0 & 0 & 0 & 0 & 0 & -1 \\ 0 & 0 & 0 & 0 & 0 & 0 & 0 & 0 \end{bmatrix}$,

$$C = \begin{bmatrix} -\frac{241}{700} & -\frac{477}{350} & -\frac{387}{700} & -\frac{209}{140} & -\frac{387}{700} & -\frac{477}{350} & -\frac{241}{700} & \frac{9}{1400} \\ \frac{2525}{72576} & -\frac{34015}{72576} & -\frac{75175}{72576} & -\frac{5125}{4536} & -\frac{55225}{72576} & -\frac{93025}{72576} & -\frac{26365}{72576} & \frac{175}{20736} \\ \frac{104}{14175} & -\frac{244}{14175} & -\frac{4402}{14175} & -\frac{3854}{2835} & -\frac{9232}{14175} & -\frac{18724}{14175} & -\frac{718}{2025} & \frac{107}{14175} \\ \frac{389}{22400} & -\frac{1719}{22400} & \frac{4833}{22400} & -\frac{209}{280} & -\frac{17217}{22400} & -\frac{28809}{22400} & -\frac{8101}{22400} & \frac{369}{44800} \\ \frac{583}{56700} & -\frac{1189}{28350} & \frac{5581}{56700} & -\frac{1513}{11340} & -\frac{13739}{56700} & -\frac{38149}{28350} & -\frac{19937}{56700} & \frac{119}{16200} \\ \frac{34453}{1814400} & -\frac{14743}{1814400} & \frac{377521}{1814400} & -\frac{8233}{22680} & \frac{876271}{1814400} & -\frac{1622393}{1814400} & -\frac{687797}{1814400} & \frac{33953}{3628800} \\ -\frac{408317}{259200} & -\frac{24353}{259200} & -\frac{542969}{259200} & -\frac{343}{3240} & -\frac{368039}{259200} & -\frac{261023}{259200} & -\frac{111587}{259200} & \frac{8183}{518400} \\ \frac{156437}{1814400} & -\frac{645607}{1814400} & \frac{1573169}{1814400} & -\frac{31457}{22680} & \frac{2797679}{1814400} & -\frac{2302297}{1814400} & \frac{2233547}{1814400} & \frac{1070017}{3628800} \end{bmatrix}$$

$$D = \begin{bmatrix} 0\ 0\ 0\ 0\ 0\ 0\ 0 & \frac{9}{1400} \\ 0\ 0\ 0\ 0\ 0\ 0\ 0 & -\frac{425}{145152} \\ 0\ 0\ 0\ 0\ 0\ 0\ 0 & -\frac{13}{14175} \\ 0\ 0\ 0\ 0\ 0\ 0\ 0 & -\frac{81}{44800} \\ 0\ 0\ 0\ 0\ 0\ 0\ 0 & -\frac{127}{113400} \\ 0\ 0\ 0\ 0\ 0\ 0\ 0 & -\frac{7298}{3628800} \\ 0\ 0\ 0\ 0\ 0\ 0\ 0 & -\frac{149527}{518400} \\ 0\ 0\ 0\ 0\ 0\ 0\ 0 & -\frac{33953}{3628800} \end{bmatrix}$$

Using definition (1.3.3)as h→ 0,we find out the zero stability using The first characteristics polynomial $\rho(r)$ which is given as

$$\rho(r) = \det(r.A - B) = 0$$

$$= \det \begin{bmatrix} r & 0 & 0 & 0 & 0 & 0 & -r & 0 \\ 0 & r & 0 & 0 & 0 & 0 & -r & 0 \\ 0 & 0 & r & 0 & 0 & 0 & -r & 0 \\ 0 & 0 & 0 & r & 0 & 0 & -r & 0 \\ 0 & 0 & 0 & 0 & r & 0 & -r & 0 \\ 0 & 0 & 0 & 0 & 0 & r & -r & 0 \\ 0 & 0 & 0 & 0 & 0 & 0 & -r & 1 \\ 0 & 0 & 0 & 0 & 0 & 0 & -r & r \end{bmatrix} = 0$$

$(-r^2 + r)r^6 = 0$

Equating to zero, we then obtain the roots

$$r_1 = 1, r_2 = r_3 = r_4 = r_5 = r_6 = r_{7=}\, r_{8=} 0 \quad |r_i| \leq 1, i = \ 1,2,3, \ldots 8$$

From definition of zero stability above, it is clear that the seven step block implicit Adams-mouton method is zero stable since the root conditions are satisfied.

Numerical Experiment

4. Implementation Strategy Using the Block Methods

The eightstep (k=8) Adams Moulton method will be implemented in block form using the following examples as shown below.

Problem 4.1

$$y' = -yy(0) = 1{,}0 \leq x \leq 1,\ \text{h= } 0.1$$

Exact Solution: $y(x) = e^{-x}$

Problem 4.2

$$y' = -y^2, where\ h = 0.1, y(0) = 10 \leq x \leq 1$$

Exact solution $y(x) = \frac{1}{x+1}$

Problem 4.3:

$$y' = -60y + 10x\ y(0) = \frac{1}{6},\ h = 0.1$$

Exact Solution: $y(x) = \frac{1}{6}\ (x + e^{-60x}$

Table4.1: Approximate solution and Absolute Error for problem 4.1 at k=8

X	Exact Solution	Error in Areo *et al*(2009)	Error in Umar *et al* (2014)	Error at LMM k=8
0.1	0.904837418035960	3.60E-10	7.36E-10	5.09E-13
0.2	0.818730753077982	1.80E-10	4.78E-10	3.64E-13
0.3	0.740818220681718	5.80E-10	4.82E-10	3.58E-13
0.4	0.670320046035639	7.40E-10	4.36E-10	2.99E-13
0.5	0.606530659712633	8.10E-10	9.13E-10	3.01E-13
0.6	0.548811636094026	9.90E-10	6.94E-10	2.35E-13
0.7	0.496585303791410	9.90E-10	6.91E-10	3.08E-13
0.8	0.449328964117222	1.00E-9	6.17E-10	2.32E-13
0.9	0.406569659740599	1.10E-9	9.41E-10	1.70E-14
1.0	0.367879441171442	1.20E-9	7.71E-10	2.80E-14

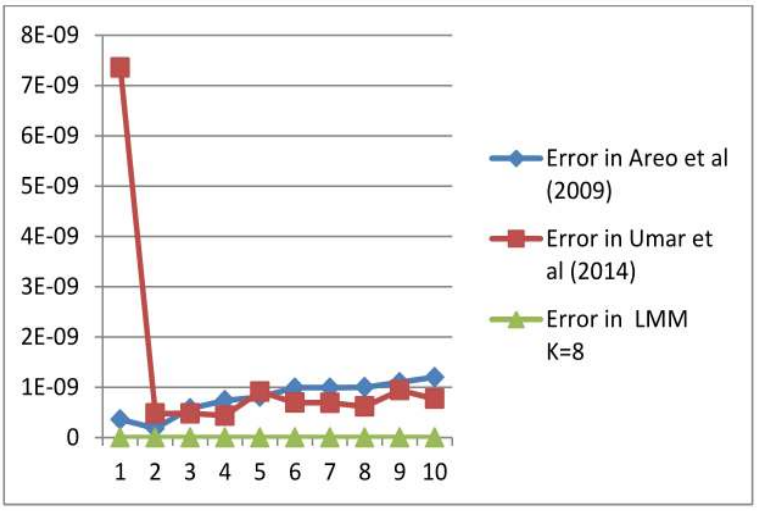

Figure 4.1: Error graph of problem 4.1 for Areo et al(2009), Umaru et al(2014) and Block LMM K=8

Table 4.2 : Comparison of absolute errors arising from Areo *et al* (2008) and new methods at k=8, using problem 4.2

X	Exact Solution	Block L.M.M k=8	Error in Areo et al (2008)	Error at LMM k=8
0.1	0.909090909090909	0.909090807813408	2.4E-04	1.013E-7
0.2	0.833333333333333	0.833333265801687	5.6E-04	6.753E-8
0.3	0.769230769230769	0.769230705535263	7.1E-04	6.370E-8
0.4	0.714285714285714	0.714285663006128	8.4E-04	5.128E-8
0.5	0.666666666666667	0.666666618560268	9.6E-04	4.811E-8
0.6	0.625000000000000	0.624999962888623	1.1E-04	3.711E-8
0.7	0.588235294117647	0.588235248106108	1.1E-03	4.601E-8
0.8	0.555555555555556	0.555555581966252	1.3E-03	2.641E-8
0.9	0.526315789473684	0.526315812592188	1.5E-03	2.312E-8
1.0	0.500000000000000	0.500000020968616	1.6E-02	2.097E-8

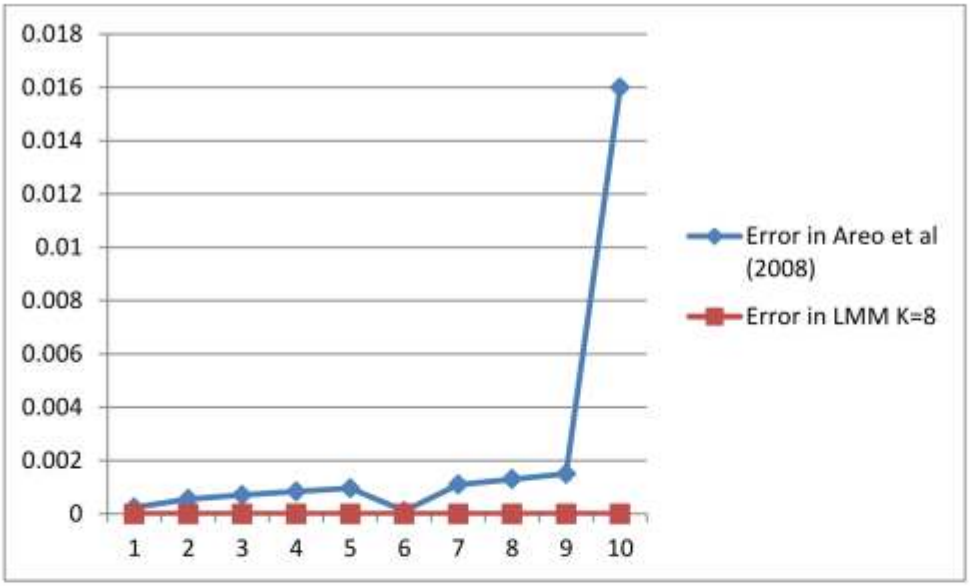

Figure 4.2: Error graph of problem 4.2 for Areo et al(2008) and Block LMM k=8

Table 4.3: Approximate solution and Absolute Error for problem 4.3 at k=8 , h=0.1

X	Exact Solution	Block L.M.M k=8	Error at LMM k=8
0.1	0.017079792029444	0.003734308150983	1.335E-2
0.2	0.033334357368726	0.032956969713152	3.774E-4
0.3	0.050000002538330	0.046184702563597	3.815E-3
0.4	0.066666666672959	0.064622773460737	2.044E-3
0.5	0.083333333333349	0.079738622302336	3.595E-3
0.6	0.100000000000000	0.098669921104349	1.330E-3
0.7	0.116666666666667	0.109500764193569	7.166E-3
0.8	0.133333333333333	0.158722474700955	2.539E-2
0.9	0.150000000000000	0.145534216129496	4.466E-3
1.0	0.166666666666667	0.164288078361483	2.379E-3

SUMMARY, DISCUSSSION OF RESULT AND CONCLUSION

In this research, we derived a ninth order(k=8) block implicit linear multistep methods (Adams-Moulton) through collocation procedure. The eight-step Adams Moulton method was found to be of order 9. The derived method was then implemented in block form and was found to converge faster to exact solution with minimal error. . A comparison of the absolute error of our new method with an existing method, Areo *et al.*(2008), showed that our new method performed relatively better, producing lesser error with respect to the exact solution.

In conclusion, our derived method was found to be zero stable and consistent, hence convergent and can compete favourably with existing methods for solving stiff and non-stiff linear and non-linear first order ordinary differential equations(O.D.E

REFERENCES

Adesanya A.O, Remilekun M . and Alkali M.A. (2012). Three Steps Block- Predictor-Block Corrector Method for the Solution of General Second Order Ordinary Differential Equation. *International Journal of Engineering Research and Application (IJERA).* 2(4): 2297- 2301

Areo E.A, Ademiluyi R.A and Babalola P.O (2008) "Accurate collocation Multistep method for integration of first order ordinary differential equations"*Journal of Mathematical physics, volume 9 : 149-154*

Areo, E.A. and Adeniyi, R.B. (2009). One-Step Embedded Butcher Type Two-Step Block Hybrid Methods for IVPs in ODEs. Advances in Mathematics,1 (120-128): Proceedings of a Memorial Conference in Honour of Late Professor C.O.A. Sowumi, University of Ibadan Nigeria

Awoyemi D. O, Kayode S.J, and Adoghe L.O. (2014). A four-point fully Implict Method for the Numerical Integration of third order Ordinary Differential Equations. *International Journal of Physical Sciences,* 9(1):7-12

Badmus A.M. and Mohammed M.S.(2016). Construction of Some Implicit Linear Multi-Step Methods into Runge-Kutta Types Methods for Initial Value Problems (IVP) of First Order Differential Equations. *Acedemy Journal of Science and Engineering.*10(1):73-87

Fadugba S.E., Ogunyebi S.N. and Okunlola J.T. (2014).On the Comparative Study of Some Numerical Methods for the Solution of Initial Value Problems in Ordinary Differential Equations.*International Journal in Science and Mathematics*. 2(1):61-67.

Famurewa O. K. E, Ademiluyi R.A. and Awoyemi D.O. (2011).A Comparative Study of Class of Implicit derivative methods for Numerical Solution of Non-Stiff and Stiff First Order Ordinary Differential Equations. *African Journal of Mathematics and Computer Science Research*, 4(2): 120-135

Ndanusa A.(2007). Derivation and Application of Linear Multistep Numerical Scheme .*Leonardo Journal of Sciences*, 10, 9-16.

Suli E.(2014).*Numerical Solution of Ordinary Differential Equation*. Oxford: Oxford University Press.

Yahaya Y.A. and A.A. Tijjani (2015). Formulation of Corrector Methods from 3-Step Hybrid Adams type Methods for the Solution of First Order Ordinary Differential Equation. *The IIER International Conference, Dubai, UAE,* 102-107.

Abacus (Mathematics Science Series)
Vol. 49, No 3, September. 2022

ANALYSIS OF CAPUTO-FABRIZIO FRACTIONAL ORDER DERIVATIVE EQUATION MODEL OF THE DYNAMICS OF CHOLERA

[1]Abdullahi M. Auwal, [2]Aliyu D. Hina [3]Luka Joshua, and [4]Hamisu ldi

[1,2,3,4]Mathematics and Statistics Department, Federal Polytechnics Bauchi.
auwal2gga@yahoo.com

Abstract

This paper formulates and analyze non integer derivatives of cholera dynamics model, the fractional-order differential equation (FODE) is devised via the Caputo-fabrizio fractional order derivative. The existence and uniqueness of the solution of proposed FODE model are examined through the fixed point theory and an iterative method. The model disease-free and an endemic equilibrium point is detemined. The Conditions for the existence of the endemic equilibrium point and for the local asymptotic stability of the disease-free equilibrium point were derived. Its shows that the disease-free equilibrium point is gradationally stable as the fractional order is decreased. Finally, the numerical simulations for a range of fractional order at different values of alpha in all state variables were comfirmed.

.

Keywords: Caputo–Fabrizio fractional order derivative; cholera epidemic model; Non-singularity; fixed-point theorem and an iterative method.

Introduction

The disease of dirty hands/environment is usually charactirize as Cholera. It is an infection of the small intestine caused by some strains of the bacteria called vibrio cholerae. Symptoms may not show up, but when one notices high dehydration of the infected person through watery diarrhea that lasts a few days. This may results in sunken eyes, cold skin, decreased skin elasticity, and wrinkling of the hand and feet. Although it is classified as a pandemic since 2010, it is rare in developed countries. Children are mostly affected especially in Africa and Southeast Asia, in some areas where access to treatment is unavailable. Vibrio Cholerae can survive in some aquatic environment for more than three months up to two years living in association with zoo-plankton, phytoplankton and the aquatic organisms such as bacteriophages. The Vibrio cholerae have the ability to colonize the hosts small intestine.

Cholera is an epidemic infectious disease caused by the ingestion of food or water contaminated with the bacterium vibrio cholera. It is characterized by watery diarrhea, extreme loss of fluid and electrolytes and severe dehydration, vomiting, leg cramps and if untreated, it leads to rapid dehydration, acidosis, circulatory collapse and death within 12–24 hr [2, 9].

Cholera can either be transmitted through interaction between humans or through interaction between humans and their environment (i.e., ingestion of contaminated water and food from the environment). Vaccination has been a commonly used method for diseases control and works by reducing the number of susceptible individuals in a population [10]. Cholera involves multiple interactions between the human host, the pathogen, and the environment [10], which contribute to both direct human-to-human and indirect environment to-human transmission. Due to its huge impact on public health, and social and economic development, cholera has been the subject of extensive studies in clinical, experimental and theoretical fields. It remains an important global cause of mortality and causing periodic epidemic disease [11]. Cholera affects 3 –5 million people and causes 100,000 –130,000 deaths in the world annually and it remains a global threat to public health and a key indicator

of lack of social development [12, 14]. Modern sewage and water treatment have virtually eliminated cholera in industrialized countries. The last major outbreak in the United States occurred in 1911 [12]. But cholera is still present in Africa, Southeast Asia and Haiti [14]. Many cholera epidemic models have been proposed to predict and control the spread of the disease (see, e.g., [2,12-14] and the references cited therein).

Mathematical model and simulation is a practical essential tool that helps us to improve our understanding of the real world [16]. It can help to determine the characteristics and magnitude of epidemic disease transmission, to predict its outbreak and to see which parameters are more influential in the dynamics of the disease

In recent decades, many physical problems have been modeled using the fractional calculus. The main reasons given for using fractional derivative models are that many systems show memory, history, or nonlocal effects, which can be difficult to model using integer order derivatives. The basic theory and applications of fractional calculus and fractional differential equations can now be found in many studies (see, e.g., [15–19]). Although most of the early studies were based on the use of the Riemann–Liouville fractional order derivative or the Caputo fractional order derivative, it has been pointed out recently that these derivatives have the problem that their kernels have a singularity that occurs at the end point of an interval of definition. As a result, many new definitions of fractional derivatives have now been proposed in the literature (see, e.g., [20–28]). The fundamental differences among the fractional derivatives are their different kernels which can be selected to meet the requirements of different applications. For example, the main differences between the Caputo fractional derivative [16], the Caputo–Fabrizio derivative [22], and the Atangana– Baleanu fractional derivative [30] are that the Caputo derivative is defined using a power law, the Caputo–Fabrizio derivative is defined using an exponential decay law, and the Atangana–Baleanu derivative is defined using a Mittag–Leffler law. Examples of the applications of the new fractional operators to real world problems have been given in a number of recent papers. For example, Tateishi *et al*. [24] have compared the classical and new fractional time-derivatives in a study of anomalous diffusion. Also, Atangana *et al*. have compared the Caputo–Fabrizio fractional derivative and the Atangana–Baleanu fractional derivative in modeling fractional delay differential equations [29] and in modeling chaotic systems [29]. They found that the power law derivative of the Riemann–Liouville fractional derivative or the Caputo–Fabrizio fractional derivative provides noisy information due to its specific memory properties. However, the Caputo–Fabrizio fractional derivative gives less noise than the power law one while the Atangana–Baleanu fractional derivative provides an excellent description.

In this study, The existence and uniqueness of the solution of the fractional model of a cholera epidemic that includes an environment compartment are established using fixed-point theory and an iterative method, via Caputo–Fabrizio fractional order derivative with an exponential decay kernel to a cholera epidemic model .

Preparatory of fractional order model

Recently, Caputo and Fabrizio [22] developed a new fractional order derivative without any singularity in its kernel which accurately describe the memory effect in a real life problem. The kernel of the new fractional derivative has the form of an exponential function. More recently, Losada and Nieto [23] derived the fractional integral associated with the new fractional Caputo–Fabrizio fractional derivative. Now, let us summarize the definitions and properties for the Caputo–Fabrizio (CF) fractional operators as follows.

Let $H^1(a,b) = \{f | f \in L^2(a,b)\}$, *where* $L^2(a,b)$ *is the space of the square integrable functions on interval* (a,b).

Defination 1.

Let $f \in H^1(a,b)$ *and* $\rho \in (0,1)$ *then the caputo* $-$ *fabrizio fractional derivative* [19] *is*

defined as $CF_{D_t^\rho}(f(t)) = \frac{M(\rho)}{1-\rho}\int_a^t f'(x)\, exp\left[-\rho\frac{t-x}{1-\rho}\right]dx,$ (1)

where $M(\rho)$ *is a normalization function such that* $M(0) = M(1) = 1$. *However, if* $f \notin L^1(a,b)$, *then the derivatives defined as*

$$CF_{D_t^\rho}(f(t)) = \frac{\rho M(\rho)}{1-\rho}\int_a^t f(t) - f(x)\, exp\left[-\rho\frac{t-x}{1-\rho}\right]dx, \quad (2)$$

Remark 1. If we let $\sigma = \frac{1-\rho}{\rho}\epsilon(0,\infty), then\ \rho = \frac{1}{1+\sigma}\ \epsilon(0,1)$from [22], in consequence, eq. 2 can be reduced to

$$CF_{D_t^\rho}(f(t)) = \frac{N(\sigma)}{\sigma}\int_a^t f'(x)\, exp\left[-\frac{t-x}{\sigma}\right]dx, \quad (3)$$

Where N(σ) is the normalization term corresponding to M(ρ) such that N(0) = N(∞) = 1.

Remark 2. ([22]) We have the following property:

$\lim_{\sigma\to 0}\frac{1}{\sigma}exp\left[-\frac{t-x}{\sigma}\right] = \delta(x-t)$, where δ(x – t) is the Dirac delta function. (4)

Nieto and Losada [23] systematically modified the above Caputo–Fabrizio fractional derivative as

$$CF_{D_t^\rho}(f(t)) = \frac{(2-\rho)M(\rho)}{2(1-\rho)}\int_a^t f'(x)\, exp\left[-\rho\frac{t-x}{1-\rho}\right]dx, \quad (5)$$

Nieto and Losada [23] further characterized the fractional integral corresponding to the derivative in Eq. (5) in the following form.

Definition 2. Let $0 < \rho < 1$. The fractional integral of order ρ of a function f is defined by

$$CF_{I_t^\rho}(f(t)) = \frac{2(1-\rho)}{(2-\rho)M(\rho)}f(t) + \frac{2\rho}{(2-\rho)M(\rho)}\int_0^t f(x)dx, \qquad t \geq 0 \quad (6)$$

Remark 2. From Eq. (6), the fractional integral of Caputo–Fabrizio type of a function f of order $0 < \rho < 1$ is a mean between the function f and its integral of order one. Nieto and Losada [23].that is

$$\frac{2(1-\rho)}{(2-\rho)M(\rho)} + \frac{2\rho}{(2-\rho)M(\rho)} = 1 \quad (7)$$

And therefore $M(\rho) = \frac{2}{2-\rho}$, Losada and Nieto consider $M(\rho) = \frac{2}{2-\rho}$ and derived the new Caputo derivative and its corresponding integral as follows.

Definition 3. ([23]) Let $0 < \rho < 1$. The fractional Caputo–Fabrizio derivative of order ρ of a function f is given by

$$CF_{D_t^{\rho}}\left(f(t)\right) = \frac{1}{1-\rho}\int_a^t f'(x)\, exp\left[-\rho\frac{t-x}{1-\rho}\right]dx, \qquad t \geq 0 \tag{8}$$

and its fractional integral is defined as

$$CF_{I_t^{\rho}}\left(f(t)\right) = (1-\rho)f(t) + \rho\int_0^t f(x)dx, \qquad t \geq 0 \tag{9}$$

Caputo–Fabrizio fractional model for dynamics of Cholera

Let us consider the dynamics of Cholera epidemic model with environment compartment which serves as a breeding ground for the bacteria proposed by Kamuhanda *et al*. [1]. In this model, it is assumed that the total population $N(t)$ at time t is divided into four compartments, namely Susceptible humans (S), Infectious humans (I) and Recovered vector (R) and the environment (V). The total population becomes: $N(t) = S(t) + I(t) + R(t) + V(t)$ where $N_0(t) = S_0(t)$.
The population that are at risk of developing an infection from the Cholera disease are $S(t)$; the compartment that consists population that are showing the symptoms of the Cholera disease are $I(t)$; the compartment consists population that have recovered from the disease and got temporal immunity are $R(t)$. Now, let us consider the original integer-order model adopted from [1] as

$$\begin{aligned}
\frac{dS}{dt} &= \Omega - \alpha SI - \mu S + \eta V + \gamma R \\
\frac{dI}{dt} &= \alpha SI - \mu I - \omega I - \xi I - \beta I \\
\frac{dR}{dt} &= \beta I - \mu R - \gamma R \\
\frac{dV}{dt} &= \xi I - \eta V
\end{aligned} \tag{10}$$

The Susceptible humans are recruited into the population at a rate Ω. Susceptible humans acquire the disease through ingestion of contaminated foods and water. Contact with infectious humans at a rate α. Individuals recover from the disease at a rate β. Humans who are infected with Cholera die at a rate ω and the recovered humans may loose immunity and return to the susceptible compartment at a rate γ. The natural death rate of the entire human compartments is μ. Infectious humans contaminate the environment at a rate ξ and the environment infects humans with the bacteria at a rate of η.
We replace the first-order time derivatives of the left-hand side of Eq. (10) by the fractional Caputo–Fabrizio derivative defined in Eq. (5) and obtain our fractional derivative model. Now our new Caputo–Fabrizio fractional model for dynamics of Cholera epidemic model with environment compartment can therefore be written as follows

$$\begin{aligned}
CF_{D_t^{\rho}}S &= \Omega - \alpha SI - \mu S + \eta V + \gamma R \\
CF_{D_t^{\rho}}I &= \alpha SI - \mu I - \omega I - \xi I - \beta I \\
CF_{D_t^{\rho}}R &= \beta I - \mu R - \gamma R \\
CF_{D_t^{\rho}}V &= \xi I - \eta V
\end{aligned} \tag{11}$$

With initial conditions

$$S(0) = S_0, \;\; I(0) = I_0, \;\; R(0) = R_0, \;\; V(0) = V_0 \tag{12}$$

we will assume that the fractional orders ($0 < \rho i < 1, i = 1, 2, \ldots, 4$) for each of the four populations can be different.

Existence and uniqueness of solutions of the model

Examine the existence and uniqueness of the solutions of the Caputo– Fabrizio fractional model for dynamics of Cholera epidemic in Eq. (11) with initial conditions (12). Using fixed point theory [33, 34], we can prove the existence of solutions for the model as follows
Applying the Caputo–Fabrizio fractional integral operator in Eq. (6) to both sides of Eq. (11), we have

$$\begin{aligned} S(t) - S(0) &= CF_{I_t}^{\rho 1}[\Omega - \alpha SI - \mu S + \eta V + \gamma R], \\ I(t) - I(0) &= CF_{I_t}^{\rho 2}[\alpha SI - \mu I - \omega I - \xi I - \beta I] \\ R(t) - R(0) &= CF_{I_t}^{\rho 3}[\beta I - \mu R - \gamma R], \\ V(t) - V(0) &= CF_{I_t}^{\rho 4}[\xi I - \eta V], \end{aligned} \tag{13}$$

Then, the kernels of the model system can be written as follows

$$\begin{aligned} K_1(t,s) &= \Omega - \alpha S(t)I(t) - \mu S(t) + \eta V(t) + \gamma R(t), \\ K_2(t,I) &= \alpha S(t)I(t) - \mu I(t) - \omega I(t) - \xi I(t) - \beta I(t), \\ K_3(t,R) &= \beta I(t) - \mu R(t) - \gamma R(t), \\ K_4(t,V) &= \xi I(t) - \eta V(t), \end{aligned} \tag{14}$$

and the functions

$$\Lambda(\rho) = \frac{2(1-\rho)}{(2-\rho)M(\rho)} \ \ and \ \ \Delta(\rho) = \frac{2\rho}{(2-\rho)M(\rho)} \tag{15}$$

In proving the following theorems, we will assume that S,I,R, and V are nonnegative bounded functions, i.e.,$\|S(t)\| \le \theta_1, \|I(t)\| \le \theta_2, \|R(t)\| \le \theta_3, and \ \|V(t)\| \le \theta_4$ *where* $\theta_1, \theta_2, \theta_3, and\ \theta_4$ are some positive constants. Denote

$$\aleph_1 = \alpha\theta_2 + \mu, \ \aleph_2 = \alpha\theta_1 + \mu + \omega + \xi + \beta\ , \ \aleph_3 = \mu + \gamma \ and \ \aleph_4 = \eta, \tag{16}$$

Applying the definition of the Caputo–Fabrizio fractional integral in Eq. (6) to Eq. (13), we obtain.

$$\begin{aligned} S(t) - S(0) &= \Lambda(\rho_1)K_1(t,S) + \Delta(\rho_1)\int_0^t K_1(y,S)dy, \\ I(t) - I(0) &= \Lambda(\rho_2)K_2(t,I) + \Delta(\rho_2)\int_0^t K_2(y,I)dy \\ R(t) - R(0) &= \Lambda(\rho_3)K_3(t,R) + \Delta(\rho_3)\int_0^t K_3(y,R)dy, \\ V(t) - V(0) &= \Lambda(\rho_4)K_4(t,V) + \Delta(\rho_4)\int_0^t K_4(y,V)dy, \end{aligned} \tag{17}$$

Theorem 1. If the following inequality holds $0 \leq M = \max\{\aleph_1, \aleph_2, \aleph_3, \aleph_4\} < 1$, (18) then the kernels $K_1, K_2, K_3, \text{ and } K_4$ satisfy Lipschitz conditions and are contraction mappings.

Proof. We consider the kernel K_1. Let S and S_1 be any two functions, then we have

$$\|K_1(t,S) - K_1(t,S_I)\| = \|-\alpha I(t)(S(t) - S_1(t)) - \mu(S(t) - S_1(t))\| \quad (19)$$

Using the triangle inequality for norms on the right-hand side of Eq. (19), we obtain

$$\|K_1(t,S) - K_1(t,S_I)\| \leq \|-\alpha I(t)\big(S(t) - S_1(t)\big)\| + \|\mu\big(S(t) - S_1(t)\big)\| \leq (\alpha\|I(t)\| + \mu)\|S(t) - S_1(t)\| \leq (\alpha\theta_2 + \mu)\|S(t) - S_1(t)\| = \aleph_1\|S(t) - S_1(t)\|. \quad (20)$$

Where $\aleph_1$ is defined in Eq. (16). Similar results for the kernels $K_2, K_3, \text{ and } K_4$ can be obtained using $\{I, I_1\}$, $\{R, R_1\} and \{V, V_1\}$, respectively, as follows:

$$\|K_2(t,I) - K_2(t,I_I)\| \leq \aleph_2\|I(t) - I_1(t)\|$$
$$\|K_3(t,R) - K_3(t,R_I)\| \leq \aleph_3\|R(t) - R_1(t)\|$$
$$\|K_4(t,V) - K_4(t,V_I)\| \leq \aleph_4\|V(t) - V(t)\|$$

where $\aleph_1, \aleph_2, \aleph_3 \text{ and } \aleph_4$ are defined in Eq. (16). Therefore, the Lipschitz conditions are satisfied for $K_2, K_3, \text{ and } K_4$. In addition, since $0 \leq M = \max\{\aleph_1, \aleph_2, \aleph_3, \aleph_4\} < 1$, the kernels are contractions. From Eq. (17), the state variables can be displayed in terms of the kernels as follows:

$$\begin{aligned} S(t) &= S(0) + \Lambda(\rho_1)K_1(t,S) + \Delta(\rho_1)\int_0^t K_1(y,S)dy, \\ I(t) &= I(0) + \Lambda(\rho_2)K_2(t,I) + \Delta(\rho_2)\int_0^t K_2(y,I)dy \\ R(t) &= R(0) + \Lambda(\rho_3)K_3(t,R) + \Delta(\rho_3)\int_0^t K_3(y,R)dy, \\ V(t) &= V(0) + \Lambda(\rho_4)K_4(t,V) + \Delta(\rho_4)\int_0^t K_4(y,V)dy, \end{aligned} \quad (21)$$

Using Eq. (21), we now introduce the following recursive formulas:

$$\begin{aligned} S_n(t) &= \Lambda(\rho_1)K_1(t,S_{n-1}) + \Delta(\rho_1)\int_0^t K_1(y,S_{n-1})dy, \\ I_n(t) &= \Lambda(\rho_2)K_2(t,I_{n-1}) + \Delta(\rho_2)\int_0^t K_2(y,I_{n-1})dy \\ R_n(t) &= \Lambda(\rho_3)K_3(t,R_{n-1}) + \Delta(\rho_3)\int_0^t K_3(y,R_{n-1})dy, \\ V_n(t) &= \Lambda(\rho_4)K_4(t,V_{n-1}) + \Delta(\rho_4)\int_0^t K_4(y,V_{n-1})dy, \end{aligned} \quad (22)$$

The initial components of the above recursive formulas are determined by the given initial conditions as follows:

$$\begin{aligned} S_0(t) &= S(0), I_0(t) = I(0) \\ R_0(t) &= R(0), V_0(t) = V(0) \end{aligned} \quad (23)$$

The differences between the consecutive terms for the recursive formulas can be written as

$$\psi_n(t) = S_n(t) - S_{n-1}(t)$$
$$= \Lambda(\rho_1)(K_1(t, S_{n-1}) - K_1(t, S_{n-2})) + \Delta(\rho_1)\int_0^t (K_1(y, S_{n-1} - K_1(t, S_{n-2}))dy,$$
$$\phi_n(t) = I_n(t) - I_{n-1}(t)$$
$$= \Lambda(\rho_2)(K_2(t, I_{n-1}) - K_2(t, I_{n-2}))$$
$$+ \Delta(\rho_2)\int_0^t (K_2(y, I_{n-1} - K_2(t, I_{n-2}))dy \quad (24)$$
$$\varphi_n(t) = R_n(t) - R_{n-1}(t)$$
$$= \Lambda(\rho_3)(K_3(t, R_{n-1}) - K_3(t, R_{n-2})) + \Delta(\rho_3)\int_0^t (K_3(y, R_{n-1} - K_3(t, R_{n-2}))dy,$$
$$\Phi_n(t) = V_n(t) - V_{n-1}(t)$$
$$= \Lambda(\rho_4)(K_4(t, V_{n-1}) - K_4(t, V_{n-2})) + \Delta(\rho_4)\int_0^t (K_4(y, V_{n-1} - K_4(t, V_{n-2}))dy,$$

For $S_n(t) = \sum_{i=1}^n \psi_i(t)$, $I_n(t) = \sum_{i=1}^n \phi_i(t)$
, $R_n(t) = \sum_{i=1}^n \varphi_{n_i}(t)$, $V_n(t) = \sum_{i=1}^n \Phi_i(t)$ (25)

Now let generate the recursive inequalities for the differences $\psi_n(t), \phi_n(t), \varphi_n(t)$and $\Phi_n(t)$ as follows

$$\|\psi_n(t)\| = \|S_n(t) - S_{n-1}(t)\|$$
$$= \Big\|\Lambda(\rho_1)(K_1(t, S_{n-1}) - K_1(t, S_{n-2}))$$
$$+ \Delta(\rho_1)\int_0^t (K_1(y, S_{n-1} - K_1(t, S_{n-2}))dy\Big\| \quad (26)$$

Using t triangle inequality for norms to Eq. (26), we have

$$\|S_n(t) - S_{n-1}(t)\|$$
$$= \|\Lambda(\rho_1) \| K_1(t, S_{n-1}) - K_1(t, S_{n-2})\|$$
$$+ \Delta(\rho_1)\int_0^t \|K_1(y, S_{n-1}) - K_1(t, S_{n-2})\|dy$$

Then, since the kernel K_1 satisfies the Lipschitz condition with Lipschitz constant $\aleph_1$, we have

$$\|S_n(t) - S_{n-1}(t)\| \le \|\Lambda(\rho_1)\aleph_1 \| S_{n-1} - S_{n-2}\| + \Delta(\rho_1)\aleph_1\int_0^t \|S_{n-1} - S_{n-2}\|dy$$

therefore we have

$$\|\psi_n(t)\| \le \Lambda(\rho_1)\aleph_1\|\psi_{n-1}(t)\| + \Delta(\rho_1)\aleph_1\int_0^t \|\psi_{n-1}(y)\|dy \quad (27)$$

Following the same procedures we have

$$\|\phi_n(t)\| \le \Lambda(\rho_2)\aleph_2\|\phi_{n-1}(t)\| + \Delta(\rho_2)\aleph_2\int_0^t \|\phi_{n-1}(y)\|dy$$
$$\|\varphi_n(t)\| \le \Lambda(\rho_3)\aleph_3\|\varphi_{n-1}(t)\| + \Delta(\rho_3)\aleph_3\int_0^t \|\varphi_{n-1}(y)\|dy \quad (28)$$
$$\|\Phi_n(t)\| \le \Lambda(\rho_4)\aleph_4\|\Phi_{n-1}(t)\| + \Delta(\rho_4)\aleph_4\int_0^t \|\Phi_{n-1}(y)\|dy$$

Theorem 2. If there exists a time $t_0 > 0$ such that the following inequalities hold: $\Lambda(\rho_1)\aleph_1 + \Delta(\rho_1)\,\aleph_1 t_0 > 1, \quad for\ i = 1,2,\ldots,4,$ (29)

then a system of solutions exists for the fractional cholera model (11)–(12).

Proof. Since the functions $S(t), I(t), R(t), and\ V(t)$ are assumed to be bounded and each of the kernels satisfies a Lipschitz condition, the following relations can be obtained.
Using Eqs. (27)–(28) recursively:

$$\begin{aligned}
\|\psi_n(t)\| &\le \|S(0)\|[\Lambda(\rho_1)\aleph_1 + \Delta(\rho_1)\aleph_1]^n \\
\|\phi_n(t)\| &\le \|I(0)\|\,[\Lambda(\rho_2)\aleph_2 + \Delta(\rho_2)\aleph_2]^n \\
\|\varphi_n(t)\| &\le \|R(0)\|[\Lambda(\rho_3)\aleph_3 + \Delta(\rho_3)\aleph_3]^n \\
\|\Phi_n(t)\| &\le \|V(0)\|[\Lambda(\rho_4)\aleph_4 + \Delta(\rho_4)\aleph_4]^n
\end{aligned} \tag{30}$$

Equation (30) shows the existence and smoothness of the functions defined in Eq. (25). To complete the proof, we prove that the functions$S_n(t), I_n(t), R_n(t)\ and\ V_n(t)$ converge to a system of solutions of (11)–(12). We introduce $B_n(t), C_n(t), E_n(t), and\ F_n(t)$, as the remainder terms after n iterations, i.e.,

$$\begin{aligned}
S(t) - S(0) &= S_n(t) - B_n(t), \\
I(t) - I(0) &= I_n(t) - C_n(t) \\
R(t) - R(0) &= R_n(t) - E_n(t), \\
V(t) - V(0) &= V_n(t) - F_n(t),
\end{aligned} \tag{31}$$

Then, using the triangle inequality and the Lipschitz condition for K_1, we have
$\|B_n(t)\| = \left\|\Lambda(\rho_1)(K_1(t,S) - K_1\left(t,S_{n-1)}\right)) + \Delta(\rho_1)\int_0^t (K_1(y,S) - K_1(y,S_{n-1}))dy\right\| \le$
$\Lambda(\rho_1)\|(K_1(t,S) - K_1(t,S_{n-1})\| + \Delta(\rho_1)\int_0^t \|K_1(y,S) - K_1(y,S_{n-1})\|dy \le \Lambda(\rho_1)\aleph_1\|S - S_{n-1}\| + \Delta(\rho_1)\aleph_1 B_n(t)\|S - S_{n-1}\|t.$

Repeating same process we have;

$$\|B_n(t)\| \le [(\Lambda(\rho_1) + \Delta(\rho_1)t)\aleph_1]^{n+1}\theta_1 \tag{32}$$
At t_0 we have $$\|B_n(t)\| \le [(\Lambda(\rho_1) + \Delta(\rho_1)t_0)\aleph_1]^{n+1}\theta_1 \tag{33}$$

Taking the limit on Eq. (33) as $n \to \infty$ and then using condition (29), we obtain $\|B_n(t)\| \to 0$. Using the same process as described above, we have the following relations:

$$\|C_n(t)\| \le [(\Lambda(\rho_2) + \Delta(\rho_2)t_0)\aleph_2]^{n+1}\theta_2 \tag{34}$$
$$\|E_n(t)\| \le [(\Lambda(\rho_3) + \Delta(\rho_3)t_0)\aleph_3]^{n+1}\theta_3 \tag{35}$$
$$\|F_n(t)\| \le [(\Lambda(\rho_4) + \Delta(\rho_4)t_0)\aleph_4]^{n+1}\theta_4 \tag{36}$$

Similarly, taking the limit on Eqs. (34)-(36) as $n \to \infty$ and then using condition (29), we have $\|C_n(t)\| \to 0, \|E_n(t)\| \to 0\ and\ \|F_n(t)\| \to 0$. Therefore, the existence of the system of solutions of system (11)–(12) is proved.
We now give conditions for the system of solutions to be unique.

Theorem 3. System (11) along with the initial conditions (12) has a unique system of solutions if the following conditions hold: $1 - \Lambda(\rho_i)\aleph_i + \Delta(\rho_i)\aleph_i t > 0, \quad for\ i = 1,2,\dots,4,$ (37).

Proof. Assume that $\{S_1(t), I_1(t), R_1(t), V_1(t)\}$ is another set of solutions of model (11)– (12) in addition to the solution set $\{S(t), I(t), R(t), V(t), R(t), V(t)\}$ proved to exist in Theorems 1 and 2 then

$$S(t) - S_1(t) = \Lambda(\rho_1)(K_1(t,S) - K_1(t,S_1) + \Delta(\rho_1)\int_0^t (K_1(y,S) - K_1(y,S_1))dy, \quad (38)$$

Taking the norm and triangle inequality on both sides of Eq. (38), we have

$$\|S(t) - S_1(t)\| \le \Lambda(\rho_1)\|K_1(t,S) - K_1(t,S_1)\| + \Delta(\rho_1)\int_0^t \|(K_1(y,S) - K_1(y,S_1)\| \quad (39)$$

Using the Lipschitz condition for the kernel K_1, we find

$$\|S(t) - S_1(t)\| \le \Lambda(\rho_1)\aleph_1\|S(t) - S_1(t)\| + \Delta(\rho_1)\aleph_1 t\|S(t) - S_1(t)\| \quad (40)$$

If Eq. (40) rearranging we obtain

$$\|S(t) - S_1(t)\|1 - \Lambda(\rho_i)\aleph_i + \Delta(\rho_i)\aleph_i t \le 0 \quad (41)$$

Finally, applying condition (37) for i = 1 to Eq. (41), we obtain

$$\|S(t) - S_1(t)\| = 0 \quad (42)$$

Hence $S(t) = S_1(t)$.

Applying a similar procedure to each of the following pairs

$(I(t), I_1(t)), (R(t), R_1(t))\ , and\ \ (V(t), V_1(t))$.

with inequality (37) $for\ i = 1,2,\dots,4$, respectively, we have

$$I(t) = I_1(t),\ R(t) = R_1(t)\ , and\ V(t) = V_1(t). \quad (43)$$

Thus, the uniqueness of the system of solutions of the fractional order system is proved.

Equilibrium points of the model and asymptotic stability

We can determine the equilibrium points of the fractional order system (11) by equating its right-hand side to zero. Solving the resulting algebraic system, we obtain two equilibrium points, namely, a disease-free and an endemic equilibrium point, which are the same as the equilibrium points given in [1].Let $E^0 = (S^0, I^0, R^0, V^0)$ denote the disease-free equilibrium point of the model and $E^* = (S^*, I^*, R^*, V^*)$ denote the endemic equilibrium point of the model. From [1], we have the disease-free equilibrium point given as

$$E^0 = (S^0, 0,0,0) = \left(\frac{\Omega}{\mu}, 0,0,0\right) \quad (44)$$

and the endemic equilibrium point given by

$$S^* = \frac{(\mu+\omega+\xi+\beta)}{\alpha},\ I^* = \frac{(\gamma+\mu)R^*}{\beta},$$

$$R^* = \frac{(\alpha I^*+\mu)S^*-\Omega}{\gamma},\ V^* = \frac{\xi}{\eta}\frac{(\gamma+\mu)R^*}{\beta} \quad (45)$$

Now using the next generation matrix method [33, 34], the basic reproduction number R_0 is

$$R_0 = \frac{\mu\Omega}{\mu} - (\mu + \omega + \xi + \beta) \quad (46)$$

For $R_0 < 1$, the disease free equilibrium point is locally asymptotically stable. And we can observed that the unique endemic equilibrium point E^* exists if $R_0 > 1$.

Consider the following fractional-order linear system described by the Caputo–Fabrizio derivative.

$$^{CF}D_t^{\rho} x(t) = Ax(t) \quad (47)$$

Where $x(t) \in R^n, A \in R^{nXn}\ \ 0 < \rho < 1$.

Definition 4. ([37]) The characteristic equation of system (47) is
$det(s(1-(1-\rho)A)-\rho A)=0$
(48)

Theorem 4. ([37]) If $(s(1-(1-\rho)A)-\rho A)$ is invertible, then system (47) is asymptotically stable if and only if the real parts of the roots to the characteristic equation of system (47) are negative.

The linearization matrix of model (11) evaluated at the disease-free equilibrium point E^0 is

$$J(E^0)=\begin{pmatrix} -\mu & \frac{-\alpha\Omega}{\mu} & 0 & \gamma \\ 0 & \frac{\alpha\Omega}{\mu}-(\mu+\omega+\xi+\beta) & 0 & 0 \\ 0 & \xi & -\eta & 0 \\ 0 & \beta & 0 & -(\gamma+\mu) \end{pmatrix} \quad (49)$$

Let $\rho_1=\rho_2=\rho_3=\rho_4=\rho\epsilon(0,1)$ be the commensurate order of model system (11), therefore, the linearization of model system (11) has the following characteristic equation at E^0:

$$det\left(s\left(1-(1-\rho)J(E^0)\right)-\rho J(E^0)\right)=0 \quad (50)$$

Theorem 5. The disease-free equilibrium point E^0 of model (11) with a commensurate order $\rho\epsilon(0,1)$ is asymptotically stable if and only if real parts of the roots of the characteristic equation (50) are negative.

Proof. Equation (50) is a quartic/bi-quadratic polynomial equation. Then we denote its four roots by $s_1, s_2, s_3\ and\ s_4$. However, the first two roots of Eq. (50). Are as follows:

$$s_1=\frac{\rho(\gamma+\mu)}{(\rho-1)\mu+(\rho-1)\gamma}, s_2=\frac{\rho\mu}{(\rho-1)\mu-1}$$

The two roots of Eq. (50), $s_1\ and\ s_2$ is obviously negative because $0<\rho<1$. Then $s_3\ and\ s_4$ can be found from the following equation

$$det\left(\begin{bmatrix} a & 0 \\ -s(1-\rho)\xi-\rho\beta & b \end{bmatrix}\right)=0 \quad (51)$$

Where $a=s(1-(1-\rho)(\frac{\alpha\Omega}{\mu}-\mu-\omega-\xi-\beta))—\rho\left(\frac{\alpha\Omega}{\mu}-\mu-\omega-\xi-\beta\right)$,

$b=s(1-(1-\rho)(\eta))-\rho(\eta).$ (52)

Given $R_e(s_3)<0\ and\ R_e(s_4)<0$, this implies that the real parts of the two roots of Eq. (51) are negative, by Theorem 1 the equilibrium point E^0 of model system (11) is asymptotically stable.

Numerical computation

The numerical results and simulations of the extended fractional order mathematical model in equation (11) was achieved with the help of the derived algorithm and numerical coded written in MATLAB environment using the model equations and the values of the parameters as Ω =0.000096274, μ = 0.00002537, ω = 0.0004, β =5, ξ =10 , η = 0.075, α =0.011 and γ =0.002. The extended fractional order mathematical model where solved numerically using the Garrappas code FDE_PI12 accordingly; [38].

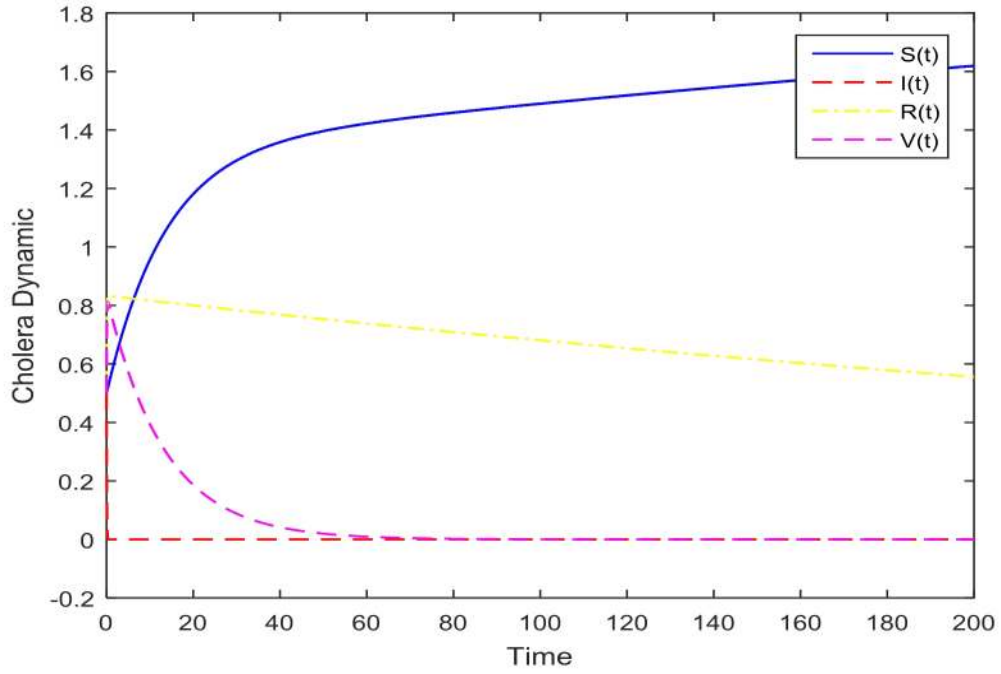

Figure 1 The time series plots for cholera dynamics in model (11)

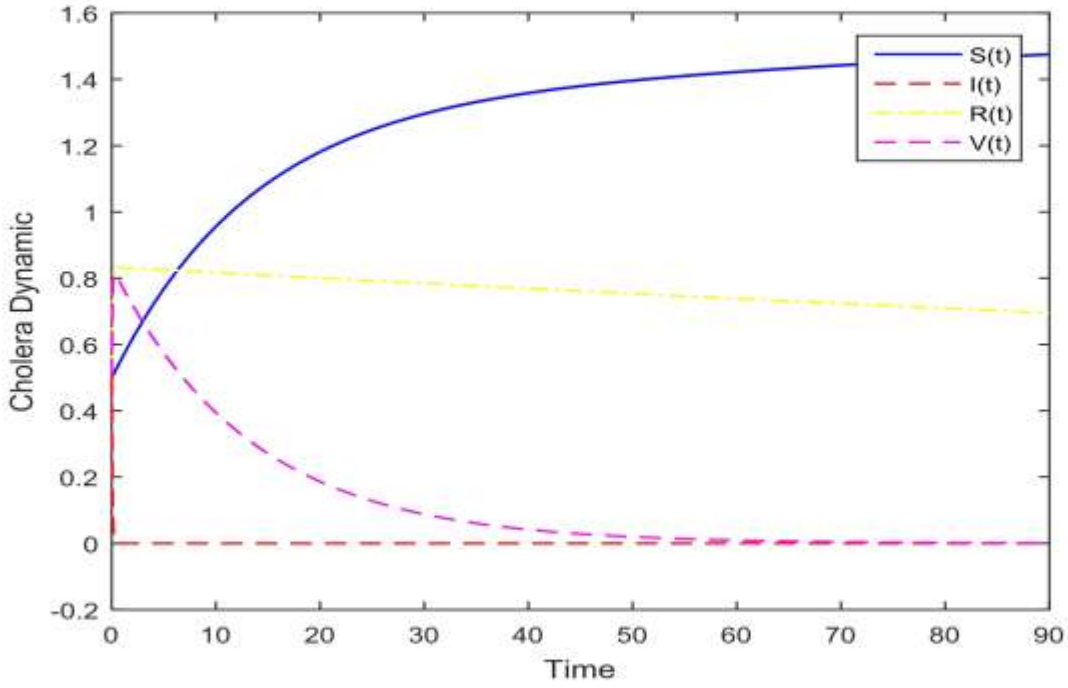

Figure 2 The time series plots for cholera dynamics in model (11)

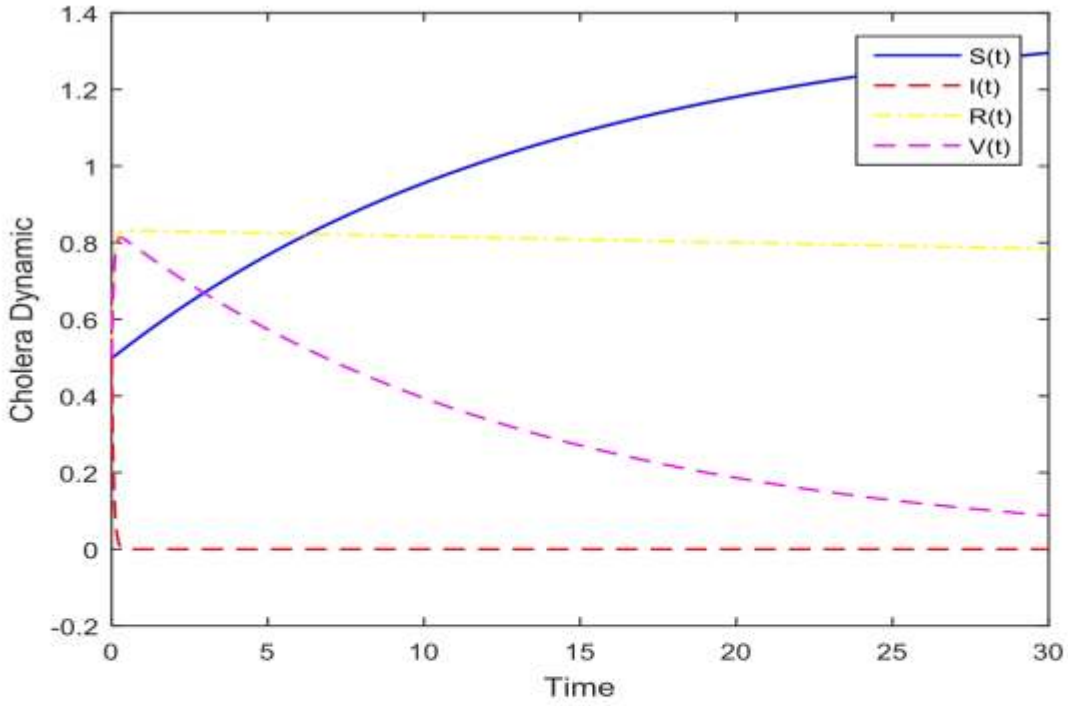

Figure 3. The time series plots for cholera dynamics in model (11)

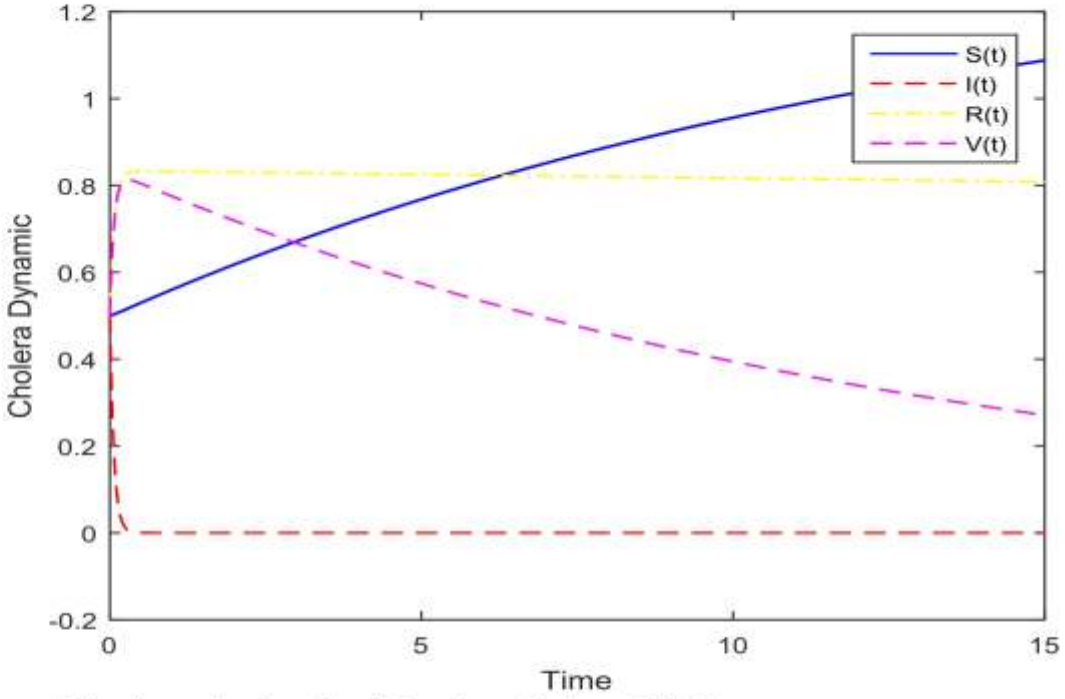

Figure 4. The time series plots for cholera dynamics in model (11)

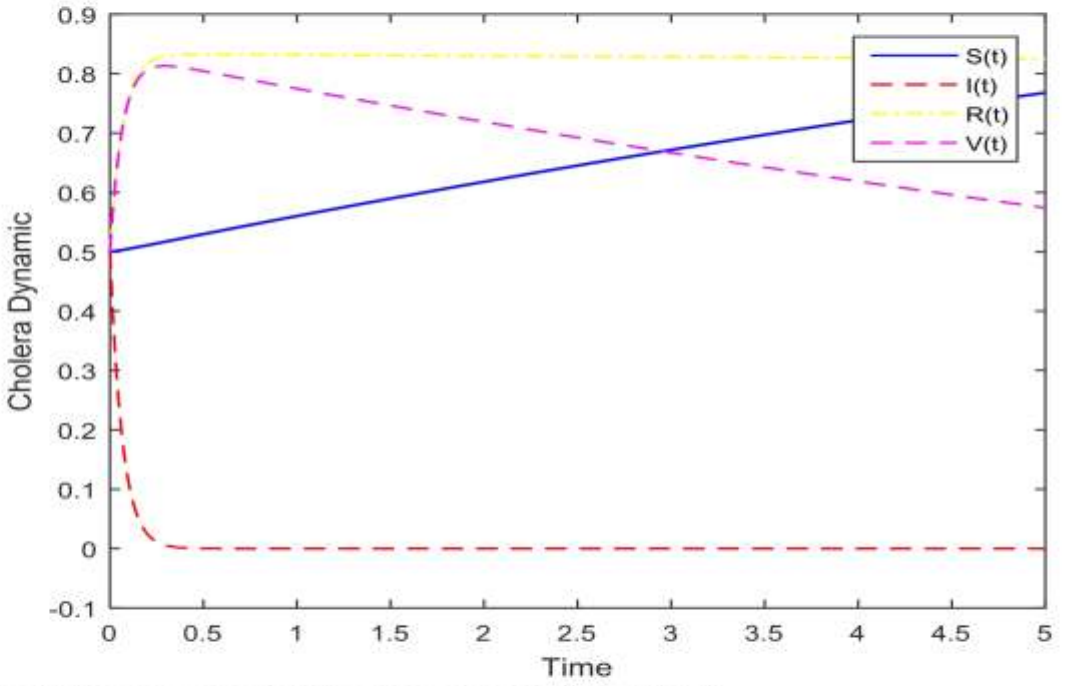

Figure 5. The time series plots for cholera dynamics in model (11)

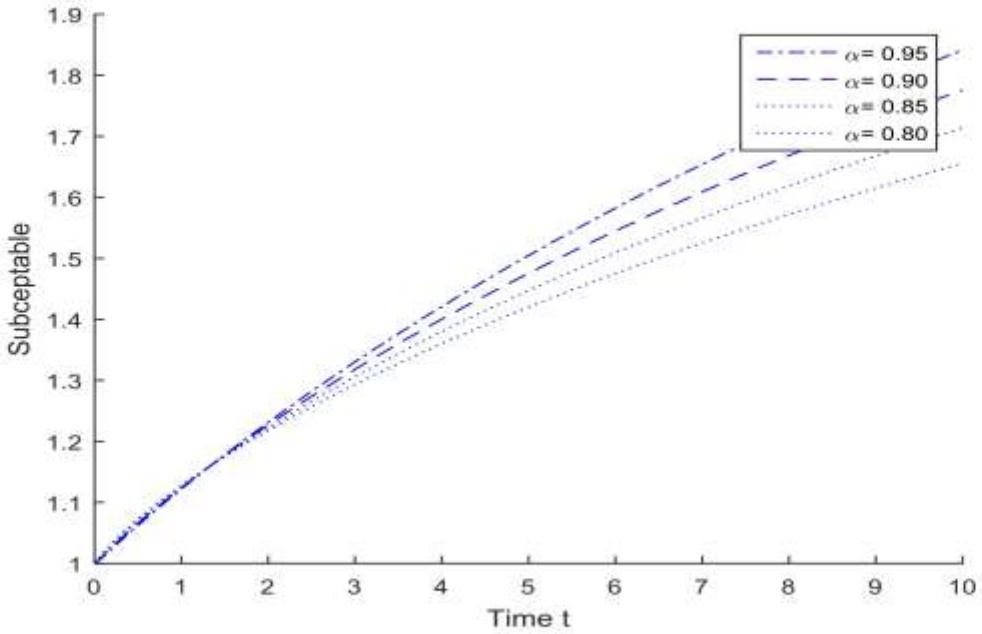

Figure 6. The time series plots for subceptable population in model (11) at different values of alpha

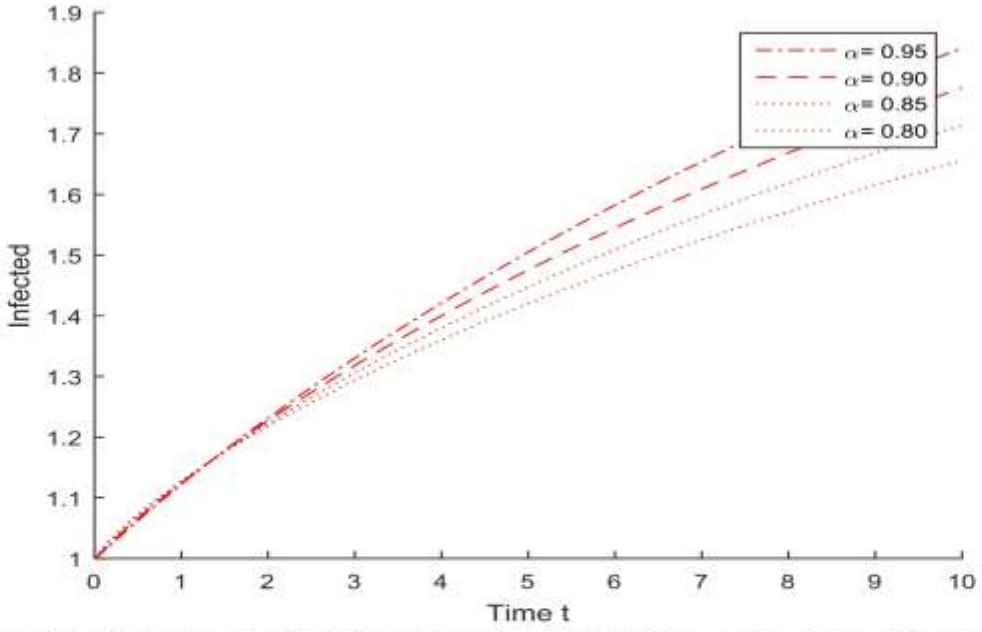

Figure 7. The time series plots for infected population in model (11) at different values of alpha

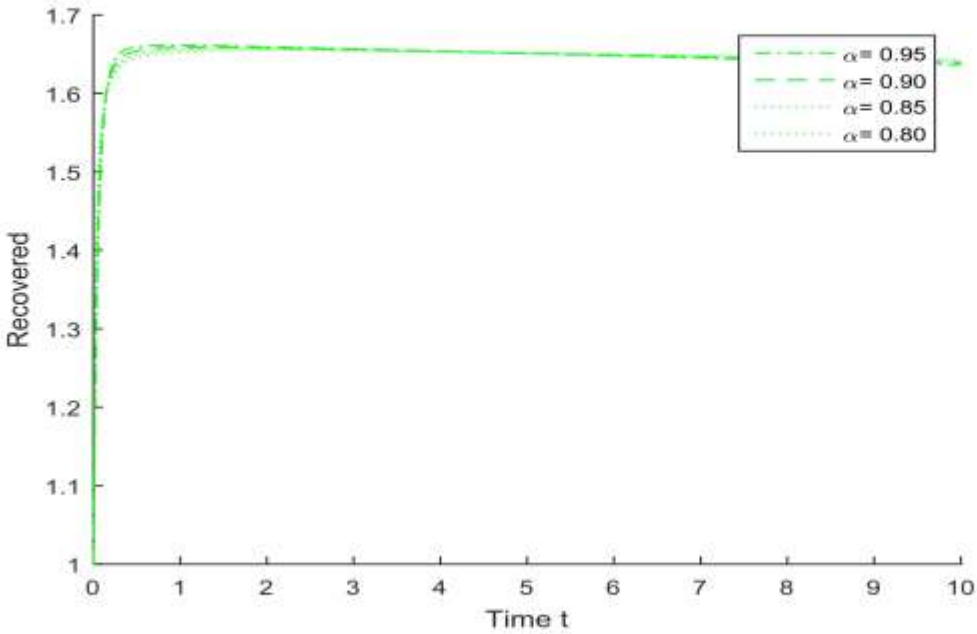

Figure 8. The time series plots for recovery population in model (11) at different values of alpha

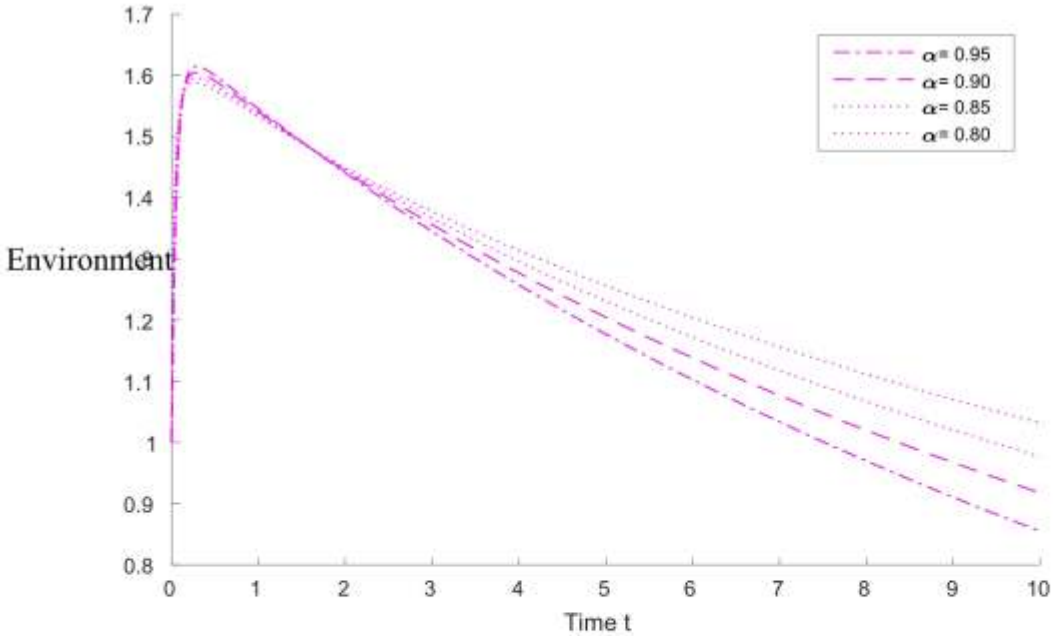

Figure 9. The time series plots for Effects of increasing or decreasing infectious contact with environment in model (11) at different values of alpha

Discussion

In this paper, the dynamics of cholera model are examined via Caputo–Fabrizio fractional order differential equation model approaches:. Varying the values of fractional-order α for the FODE, Due to the lack of any disease control measures, the number of subceptable and infected population dramatically increases (see Figure 6 and 7), since both the susceptible and infected population live together in the environment that serves as a breeding ground for the bacteria and actively interact among themselves. Moreover, we can easily observe from Figure 6 and 7 that when $\alpha \to 1$ the Caputo–Fabrizio non-integer order derivative reveals more absorbing characteristics. Consequently, this causes the cholera dynamic to stay at almost a constant rate for a long period of time (see Figures 1,2,3,4 and 5). However, the Effects of increasing or decreasing infectious contact with environment in model (11) at different values of alpha in figure 9 indicate the vulnerability of all state variables. The Determination of existence and uniqueness solution of the model through the fixed-point theorem and an iterative method, was establisheb an important properties of our proposed FODE model.

Conclusions

In this paper, a Caputo–Fabrizio fractional differential equation model for dynamic of cholera has been developed and analyzed, Using fixed point theory and an iterative method. This fractional model is based on the use of the non-singular exponentially decreasing kernels appearing in the Caputo–Fabrizio fractional derivative; the existence and uniqueness of the system of solutions for the model have been obtained. We have determined the equilibrium points of the model and the conditions for local asymptotic stability of the disease-free equilibrium point. We obtained numerical solutions of the fractional system, and compared the numerical simulations with respect to different values of the fractional order and explored the mechanism of the use of the Caputo–Fabrizio fractional derivative as a model for description of real life problems that include/ and relate memory effect.

References

[1] Kamuhanda, A. E., Shaibu O., and Mary W. (2018). Mathematical Modelling and Analysis of the Dynamics of Cholera. Global Journal of Pure and Applied Mathematics. ISSN 0973-1768 Volume 14, Number 9 (2018), pp. 1259–1275.

[2] Sanches, R. P., Ferreira, C. P., and Kraenkel, R. A. (2011). The role of immunity and seasonality in cholera epidemics. Bulletin of mathematical biology, 73(12), 2916-2931.

[3] Stephen Wiggins. Introduction to applied nonlinear dynamical systems and chaos, Springer Science and Business Media, 2, 2003.

[4] Tian, J. P., and Wang, J. (2011). Global stability for cholera epidemic models. Mathematical biosciences, 232(1), 31-41.

[5] Tien, J. H., and Earn, D. J. (2010). Multiple transmission pathways and disease dynamics in a waterborne pathogen model. Bulletin of mathematical biology, 72(6), 1506-1533.

[6] The Telegraph News, 09th May 2018, Race against time to curb cholera outbreak in Yemen, https://www.telegraph.co.uk/news/0/race-against-time-curbcholera-outbreak-yemen

[7] Tognotti, E. (2013). Lessons from the history of quarantine, from plague to influenza A. Emerging infectious diseases, 19(2), 254.

[8] Tuite, A. R., Tien, J., Eisenberg, M., Earn, D. J., Ma, J., and Fisman, D. N. (2011). Cholera epidemic in Haiti, 2010: using a transmission model to explain spatial spread of disease and identify

optimal control interventions. Annals of internal medicine, 154(9), 593-601.

[9] WHO, Cholera infected country profiles, http://www.who.int/cholera/countries/en/ (accessed 27.01.08).

[10] Hethcote, H. W. (1998). Oscillations in an endemic model for pertussis. Can. Appl. Math. Quart, 6, 61-88.

[11] Mukandavire, Z., Liao, S., Wang, J., Gaff, H., Smith, D. L., and Morris, J. G. (2011). Estimating the reproductive numbers for the 20082009 cholera outbreaks in Zimbabwe. Proceedings of the National Academy of Sciences, 108(21), 8767-8772.

[12] WHO/Cholera Fact 2010.

[13] Reyes-Robles, T., Dillard, R. S., Cairns, L. S., Silva-Valenzuela, C. A., Housman, M., Ali, A., ... , Camilli, A. (2018). Vibrio cholerae outer membrane vesicles inhibit bacteriophage infection. Journal of bacteriology, 200(15), e00792-17.

[14] Z. Shuai, J.H. Tien, P. van den Driessche, Cholera models with hyperinfectivity and temporary immunity, Bull. Math. Biol. 74 (2012) 24232445.

[15] Mainardi, F. (1997): Fractional calculus: some basic problems in continuum and statistical mechanics. In: Carpinteri, A., Mainardi, F. (eds.) Fractals and Fractional Calculus in Continuum Mechanics. Springer,

[16] Diethelm, K. (2010).: The Analysis of Fractional Differential Equations: An Application-Oriented Exposition Using Differential Operators of Caputo Type. Springer.

[17] Kumar, D., Singh, J., Baleanu, D. (2016).: Numerical computation of a fractional model of differential-difference equation. J. Comput. Nonlinear Dyn. 11(6), 061004

[18] Area, I., Batarfi, H., Losada, J., Nieto, J.J., Shammakh, W., Torres, Á. (2015): On a fractional order Ebola epidemic model. Adv. Differ. Equ. 2015(1), 278.

[19] Ma, M., Baleanu, D., Gasimov, Y.S., Yang, X.-J. (2016): New results for multidimensional diffusion equations in fractal dimensional space. Rom. J. Phys. 61, 784–794.

[20] Atangana, A., Alkahtani, B.S.T. (2015): Analysis of the Keller–Segel model with a fractional derivative without singular kernel. Entropy 17(6), 4439–4453.

[21] Alsaedi, A., Nieto, J.J., Venktesh, V. (2015): Fractional electrical circuits. Adv. Mech. Eng. 7(12), 1687814015618127.

[22] Caputo, M., Fabrizio, M. (2015): A new definition of fractional derivative without singular kernel. Prog. Fract. Differ. Appl. 1(2), 1–13.

[23] Losada, J., Nieto, J.J. (2015): Properties of a new fractional derivative without singular kernel. Prog. Fract. Differ. Appl. 1(2), 87–92.

[24] Tateishi, A.A., Ribeiro, H.V., Lenzi, E.K. (2017): The role of fractional time-derivative operators on anomalous diffusion. Front. Phys. 5, 52.

[25] Kumar, D., Singh, J., Al Qurashi, M., Baleanu, D. (2017): Analysis of logistic equation pertaining to a new fractional derivative with non-singular kernel. Adv. Mech. Eng. 9(2), 1687814017690069.

[26] Owolabi, K.M., Atangana, A. (2017): Analysis and application of new fractional Adams–Bashforth scheme with Caputo–Fabrizio derivative. Chaos Solitons Fractals 105, 111–119.

[27] Kumar, D., Tchier, F., Singh, J., Baleanu, D. (2018): An efficient computational technique for fractal vehicular traffic flow. Entropy 20, 259.

[28] Singh, J., Kumar, D., Baleanu, D. (2019): New aspects of fractional Biswas–Milovic model with Mittag–Leffler law. Math. Model. Nat. Phenom. 14(3), 303.

[29] Atangana, A. (2018): Blind in a commutative world: simple illustrations with functions and

chaotic attractors. Chaos Solitons Fractals 114, 347–363.

[30] Atangana, A., Gómez-Aguilar, J.F. (2018): Decolonisation of fractional calculus rules: breaking commutativity and associativity to capture more natural phenomena. Eur. Phys. J. Plus 133(4), 166.

[31] Podlubny, I. (1999): Fractional Differential Equations. Academic, San Diego (1999).

[32] Kilbas, A.A., Srivastava, H.M., Trujillo, J.J. (2006): Theory and Applications of Fractional Differential Equations, vol. 204. North-Holland, Amsterdam.

[33] Kreyszig, E. (1978): Introductory Functional Analysis with Applications. Wiley, New York .

[34] Hunter, J.K., Nachtergaele, B. (2001): Applied Analysis. World Scientific, Singapore.

[35] Van den Driessche, P., Watmough, J. (2002: Reproduction numbers and sub-threshold endemic equilibria for compartmental models of disease transmission. Math. Biosci. 180(1–2), 29–48).

[36] Bani-Yaghoub, M., Gautam, R., Shuai, Z., Van Den Driessche, P., Ivanek, R. (2012): Reproduction numbers for infections with free-living pathogens growing in the environment. J. Biol. Dyn. 6(2), 923–940

[37] Li, H., Cheng, J., Li, H.-B., Zhong, S.-M. (2019): Stability analysis of a fractional-order linear system described by the Caputo–Fabrizio derivative. Mathematics 7(2), 200 .

[38] Garrappa R. (2018). Numerical solution of fractional differential equations: a survey and a software tutorial. Mathematics;6(2):16.

Abacus (Mathematics Science Series)
Vol. 49, No 3, September. 2022

A COMPARATIVE STUDY ON THE ALPHA POWER TRANSFORMED FAMILY OF DISTRIBUTIONS

Jacob C. Ehiwario[1], John N. Igabari[2] and Jophet E. Okoh[3]

[1]Department of Statistics, University of Delta, Agbor, Delta State, Nigeria
[2]Department of Mathematics, Delta State University, Abraka, Delta State, Nigeria.
[3]Department of Statistics, Dennis Osadebay University, Asaba, Delta State, Nigeria.
[*] Corresponding Author Email: jacob.ehiwario@unidel.edu.ng

Abstract

In the theory of statistical analysis, it is indisputable to state that the flexibility of statistical distributions are enhanced through the addition of extra parameter(s). Several methods have been introduced in literature. Nevertheless, not all methods are suitable to enhance the flexibility of existing models.In this paper, we present a comparative study on the alpha power family of distributions. More specifically, the Weibull, log-logistic, Bur II, power4Lindley, Gompertz distributions, and their corresponding alpha power transformed versions are studied. Some of the mathematical properties of the distributions are discussed and three real data sets were used to examine the effect of the extra parameter in the alpha power transformed method on the baseline distributions.

Keywords: Alpha power transformation; Hazard rate function; Quantile; Moments

Introduction

Generalization of classical lifetime distributions have become a significant interest among statisticians due to their usefulness in statistical analysis of real-world phenomena. Over decades, several methodologies have been introduced to add extra parameter(s) to existing models with the sole aim of increasing their performance and flexibility in real-life data fittings. Included among the methodologies are; the exponentiated Weibull family of distributions introduced by Mudholka and Srivastava (1993), the beta-generated family of distributions due to Eugene et al. (2002), the Marshall-Olkin extended family of distributions developed by Marshall and Olkin (2007), the transmuted-G family of distributions introduced by Shaw and Buckley (2009), the Weibull-G family of distributions proposed by Bourguignon et al. (2014), Kumaraswamy-G family of distributions due to Cordeiro and de Castro (2011), the Topp-Leone generated family of distributions proposed by Al-Shomraniet al. (2016), the alpha-power poisson-G family of distributions developed by Jemilohun and Ipinyomi (2022), etc.

Recent research study has shown in many cases the usefulness of these methods in improving the flexibility of existing lifetime distributions. However, it is imperative to note that some of these methods are not suitable for certain lifetime distributions.

In this paper, we are motivated to conduct a comparative study on the alpha-power transformed family of distributions developed by Mahdavi and Kundu (2017). Primarily, we investigate the effect of the "α-parameter" on some classical lifetime distributions. The remaining sections of the paper are structured as follows: Section 2 presents the alpha-power transformed method and a brief review of some generalized lifetime distributions based on the alpha-power transformed frame work. In Section 3, we applied the generalized lifetime distributions to fit three real data sets in other to examine the effect of the "α-parameter" on the generalized lifetime distributions. Section 4 concludes the paper.

The Alpha-Power Transformed Family of Distributions

Mahdavi and Kundu (2017) have introduced a novel method of adding an extra parameter to an existing lifetime distribution. Suppose F(x) is the

cumulative distribution function, (cdf) of a continuous random variable X following a known lifetime distribution, Mahdavi and Kundu (2017) defined the alpha-power transformation of F(x) for x $\in$ R as

$$G_{APT}(x) = \begin{cases} \frac{\alpha^{F(x)}-1}{\alpha-1}, & if \quad \alpha > 0, \ \alpha \neq 1 \\ \\ F(x), & if \quad \alpha = 1 \end{cases} \tag{1}$$

The probability density function (pdf) associated to (1) is obtained as

$$g_{APT}(x) = \begin{cases} \frac{\log \alpha}{\alpha-1} f(x)\, \alpha^{F(x)}, & if \quad \alpha > 0, \ \alpha \neq 1 \\ \\ f(x), & if \quad \alpha = 1 \end{cases} \tag{2}$$

The following subsections is dedicated to a brief review of some generalized lifetime distributions arising from (1) and (2).

The Alpha-Power Weibull Distribution (APWD)

Let F(x) be the cdf of a two-parameter Weibull random variable X. Nassar et al. (2017) introduced the alpha-power Weibull distribution with the cdf and pdf respectively defined as

$$G_{APW}(x) = \begin{cases} \frac{\alpha^{1-e^{-\lambda x^{\beta}}}-1}{\alpha-1}, & if \quad \alpha > 0, \ \alpha \neq 1 \\ \\ 1-e^{-\lambda x^{\beta}}, & if \quad \alpha = 1 \end{cases} \tag{3}$$

and

$$g_{APW}(x) = \begin{cases} \frac{\log(\alpha)}{\alpha-1} \lambda \beta x^{\beta-1} e^{-\lambda x^{\beta}} \alpha^{1-e^{-\lambda x^{\beta}}}, & if \quad \alpha > 0, \ \alpha \neq 1 \\ \\ \lambda \beta x^{\beta-1} e^{-\lambda x^{\beta}}, & if \quad \alpha = 1 \end{cases} \tag{4}$$

The survival and hazard rate functions of the APW distribution are respectively obtained from (1) and (2) as

$$s_{APW}(x) = \begin{cases} \frac{\alpha}{\alpha-1}(1-\alpha^{-e^{-\lambda x^{\beta}}}), & if \quad \alpha > 0, \ \alpha \neq 1 \\ \\ e^{-\lambda x^{\beta}}, & if \quad \alpha = 1 \end{cases} \tag{5}$$

$$h_{APW}(x) = \begin{cases} \frac{\log(\alpha)\lambda\beta x^{\beta-1} e^{-\lambda x^{\beta}}}{\alpha^{e^{-\lambda x^{\beta}}}-1}, & if \quad \alpha > 0, \ \alpha \neq 1 \\ \\ \lambda \beta x^{\beta-1}, & if \quad \alpha = 1 \end{cases} \tag{6}$$

Mathematical properties such as quantile, moments, entropy, order statistics, mean residual life function and stress-strength parameter were also obtained. The maximum likelihood method was employed to estimate the unknown parameters and two real data sets were used to demonstrate the importance of the APW distribution in real-life data fitting.

The Alpha-Power Transformed Log-Logistic Distribution (APTLLD)

Suppose X is a random variable following the log-logistic distribution with cdf and pdf defined as

$$F(x) = 1 - \left(1 + \left(\frac{x}{\lambda}\right)^{\beta}\right)^{-1}, \qquad x > 0 \tag{7}$$

and

$$f(x) = \beta\lambda^{-\beta}x^{\beta-1}\left(1 + \left(\frac{x}{\lambda}\right)^{\beta}\right)^{-2}, \qquad x > 0 \tag{8}$$

Aldahlan (2020) developed the alpha-power transformed log-logistic (APTLL) distribution by inserting (7) and (8) into (1) and (2), yielding

$$G_{APTLL}(x) = \begin{cases} \dfrac{\alpha^{1-\left(1+\left(\frac{x}{\lambda}\right)^{\beta}\right)^{-1}} - 1}{\alpha - 1}, & if \quad \alpha > 0,\ \alpha \neq 1 \\ 1 - \left(1 + \left(\frac{x}{\lambda}\right)^{\beta}\right)^{-1}, & if \quad \alpha = 1 \end{cases} \tag{9}$$

and

$$g_{APTLL}(x) = \begin{cases} \dfrac{\log(\alpha)}{\alpha - 1}\beta\lambda^{-\beta}x^{\beta-1}\left(1 + \left(\frac{x}{\lambda}\right)^{\beta}\right)^{-2}\alpha^{1-\left(1+\left(\frac{x}{\lambda}\right)^{\beta}\right)^{-1}}, & if \quad \alpha > 0,\ \alpha \neq 1 \\ \beta\lambda^{-\beta}x^{\beta-1}\left(1 + \left(\frac{x}{\lambda}\right)^{\beta}\right)^{-2}, & if \quad \alpha = 1 \end{cases} \tag{10}$$

(9) and (10) respectively represent the cdf and pdf of the alpha-power transformed log-logistic (APTLL) distribution. From (9) and (10), the survival function and the hazard rate function of the APTLL distribution are given respectively as

$$s_{APTLL}(x) = \begin{cases} \dfrac{\alpha}{\alpha - 1}\left(1 - \alpha^{-\left(1+\left(\frac{x}{\lambda}\right)^{\beta}\right)^{-1}}\right), & if \quad \alpha > 0,\ \alpha \neq 1 \\ \left(1 + \left(\frac{x}{\lambda}\right)^{\beta}\right)^{-1}, & if \quad \alpha = 1 \end{cases} \tag{11}$$

and

$$h_{APTLL}(x) = \begin{cases} \dfrac{\log(\alpha)\beta\lambda^{-\beta}x^{\beta-1}\left(1+\left(\frac{x}{\lambda}\right)^{\beta}\right)^{-2}}{\left(\alpha^{\left(1+\left(\frac{x}{\lambda}\right)^{\beta}\right)^{-1}-1}\right)}, & if \quad \alpha > 0,\ \alpha \neq 1 \\ \beta\lambda^{-\beta}x^{\beta-1}\left(1+\left(\frac{x}{\lambda}\right)^{\beta}\right)^{-1}, & if \quad \alpha = 1 \end{cases} \tag{12}$$

Other mathematical properties which include, the quantile, moments, probability weighted moments (PWMs), Renyi entropy, order statistics were derived. As a way of illustrating the flexibility of the APTLL distribution, one data set was used in data fittings. Although, the author compared the result of APTLL distribution with other non-nested models, the result of the log-logistic distribution which is apparently the baseline distribution of the proposed APTLL distribution was omitted.

The Alpha-Power Transformed Extended Bur II Distribution (APTEBIID)

Ogunde *et al*. (2020) introduced a new three parameter generalized Bur II distribution based on the alpha-power transformed method. By inserting the cdf and pdf of the Bur II distribution into (1) and (2), the authors obtained the cdf of the alpha-power transformed extended Bur II distribution as

$$G_{APTEBII}(x) = \begin{cases} \dfrac{\alpha^{\left(1+x^{-\lambda}\right)^{-\beta}}-1}{\alpha-1}, & if \quad \alpha > 0,\ \alpha \neq 1 \\ \left(1+x^{-\lambda}\right)^{-\beta}, & if \quad \alpha = 1 \end{cases} \tag{13}$$

and the corresponding pdf associated with (13) is defined as

$$g_{APTEBII}(x) = \begin{cases} \dfrac{\lambda\beta\log(\alpha)}{\alpha-1}x^{-(\lambda+1)}\left(1+x^{-\lambda}\right)^{-(\beta+1)}\alpha^{\left(1+x^{-\lambda}\right)^{-\beta}}, & if \quad \alpha > 0,\ \alpha \neq 1 \\ \lambda\beta x^{-(\lambda+1)}\left(1+x^{-\lambda}\right)^{-(\beta+1)}, & if \quad \alpha = 1 \end{cases} \tag{14}$$

The survival and hazard rate functions of the APTEBII distribution are respectively obtained as

$$s_{APTEBII}(x) = \begin{cases} \dfrac{\alpha}{\alpha-1}\left(1-\alpha^{\left(1+x^{-\lambda}\right)^{-\beta}-1}\right), & if \quad \alpha > 0,\ \alpha \neq 1 \\ 1-\left(1+x^{-\lambda}\right)^{-\beta}, & if \quad \alpha = 1 \end{cases} \tag{15}$$

and

$$h_{APTEBII}(x) = \begin{cases} \frac{log(\alpha)\lambda\beta x^{-(\lambda+1)}\left(1+x^{-\lambda}\right)^{-(\beta+1)}\alpha^{\left(1+x^{-\lambda}\right)^{-\beta}-1}}{1-\alpha^{\left(1+x^{-\lambda}\right)^{-\beta}-1}}, & if \quad \alpha > 0,\ \alpha \neq 1 \\ \frac{\lambda\beta x^{-(\lambda+1)}\left(1+x^{-\lambda}\right)^{-(\beta+1)}}{1-\left(1+x^{-\lambda}\right)^{-\beta}}, & if \quad \alpha = 1 \end{cases} \tag{16}$$

Mathematical expressions for the quantile, moments, moment generating function, Renyi entropy, order statistics were derived. The maximum likelihood estimation method was employed to estimate the parameter of the APTEBII distribution and two real data sets were used to illustrate the applicability of the model.

The Alpha-Power Transformed Power Lindley Distribution (APTPLD)

Ghitany*et al.* (2013) introduced an extension of the one-parameter Lindley distribution proposed by Lindley (1958). They defined the cdf and pdf of the power Lindley (PL) distribution respectively as

$$F(x) = 1 - \left(1 + \frac{\lambda x^{\beta}}{\lambda+1}\right)e^{-\lambda x^{\beta}}, \qquad x, \lambda, \beta > 0 \tag{17}$$

and

$$f(x) = \frac{\beta\lambda^2}{\lambda+1}x^{\beta-1}(1+x^{\beta})e^{-\lambda x^{\beta}}, \qquad x, \lambda, \beta > 0 \tag{18}$$

By inserting (17) and (18) into (1) and (2), Hassan *et al.* (2019) developed the alpha-power transformed power Lindley (APTPL) distribution with cdf defined as

$$G_{APTPL}(x) = \begin{cases} \frac{\alpha^{1-\left(1+\frac{\lambda x^{\beta}}{\lambda+1}\right)e^{-\lambda x^{\beta}}}-1}{\alpha-1}, & if \quad \alpha > 0,\ \alpha \neq 1 \\ 1-\left(1+\frac{\lambda x^{\beta}}{\lambda+1}\right)e^{-\lambda x^{\beta}}, & if \quad \alpha = 1 \end{cases} \tag{19}$$

and the associated density function given by

$$g_{APTPL}(x) = \begin{cases} \frac{\log(\alpha)}{(\alpha-1)(\lambda+1)}\beta\lambda^2 x^{\beta-1}(1+x^{\beta})e^{-\lambda x^{\beta}}\alpha^{1-\left(1+\frac{\lambda x^{\beta}}{\lambda+1}\right)e^{-\lambda x^{\beta}}}, & if \quad \alpha > 0,\ \alpha \neq 1 \\ \frac{\beta\lambda^2}{\lambda+1}x^{\beta-1}(1+x^{\beta})e^{-\lambda x^{\beta}}, & if \quad \alpha = 1 \end{cases} \tag{20}$$

The survival function and the hazard rate function of the APTPL distribution are given, respectively as follows

$$s_{APTPL}(x) = \begin{cases} \frac{\alpha}{\alpha-1}\left(1-\alpha^{-\left(1+\frac{\lambda x^{\beta}}{\lambda+1}\right)e^{-\lambda x^{\beta}}}\right), & if \quad \alpha>0,\ \alpha\neq 1 \\ \left(1+\frac{\lambda x^{\beta}}{\lambda+1}\right)e^{-\lambda x^{\beta}}, & if \quad \alpha=1 \end{cases} \tag{21}$$

and

$$h_{APTPL}(x) = \begin{cases} \frac{log(\alpha)\beta\lambda^2 x^{\beta-1}(1+x^{\beta})e^{-\lambda x^{\beta}}}{(\lambda+1)\left(\alpha^{\left(1+\frac{\lambda x^{\beta}}{\lambda+1}\right)e^{-\lambda x^{\beta}}}-1\right)}, & if \quad \alpha>0,\ \alpha\neq 1 \\ \frac{\beta\lambda^2 x^{\beta-1}\left(1+x^{\beta}\right)}{(\lambda+1+\lambda x^{\beta})}, & if \quad \alpha=1 \end{cases} \tag{22}$$

The authors presented a detailed study on the mathematical properties of the APTPL distribution. These include; the quantile, moments, moment generating function, probability weighted moments, incomplete moments, Bonferroni and Lorenz curves, Renyi entropy, and stochastic ordering. Four different methods of parameter estimation which include; the maximum likelihood, maximum product spacing, least square and weighted least square estimators were employed to estimate the unknown parameters of the APTPL distribution. The potential of the APTPL distribution in real life data fitting was demonstrated using two data sets.

The Alpha-Power Gompertz Distribution (APGD)

Let *X* be a continuous random variable following the Gompertz distribution, then the cdf and pdf of *X* are defined, respectively as

$$F(x) = 1-exp\left(-\frac{\lambda}{\beta}\left(e^{\beta x}-1\right)\right), \qquad x,\beta,\lambda> \tag{23}$$

and

$$f(x) = \lambda exp\left(\beta x-\frac{\lambda}{\beta}\left(e^{\beta x}-1\right)\right), \qquad x,\beta,\lambda> \tag{24}$$

Eghwerido *et al.* (2020) utilized (23) as the baseline distribution in (1) to develop the alpha power Gompertz (APG) distribution. The cdf of the APG distribution is given as

$$G_{APG}(x) = \begin{cases} \frac{\alpha^{1-exp\left(-\frac{\lambda}{\beta}\left(e^{\beta x}-1\right)\right)}-1}{\alpha-1}, & if \quad \alpha>0,\ \alpha\neq 1 \\ 1-exp\left(-\frac{\lambda}{\beta}\left(e^{\beta x}-1\right)\right), & if \quad \alpha=1 \end{cases} \tag{25}$$

and the pdf given by

$$g_{APG}(x) = \begin{cases} \frac{\log(\alpha)}{\alpha-1}\lambda exp\left(\beta x - \frac{\lambda}{\beta}\left(e^{\beta x}-1\right)\right)\alpha^{1-exp\left(-\frac{\lambda}{\beta}\left(e^{\beta x}-1\right)\right)}, & if \quad \alpha > 0,\ \alpha \neq 1 \\ \lambda exp\left(\beta x - \frac{\lambda}{\beta}\left(e^{\beta x}-1\right)\right), & if \quad \alpha = 1 \end{cases} \tag{26}$$

The survival function and hazard rate function of the APG distribution can be obtained respectively as

$$s_{APG}(x) = \begin{cases} \frac{\alpha}{\alpha-1}\left(1-\alpha^{-exp\left(-\frac{\lambda}{\beta}\left(e^{\beta x}-1\right)\right)}\right), & if \quad \alpha > 0,\ \alpha \neq 1 \\ exp\left(-\frac{\lambda}{\beta}\left(e^{\beta x}-1\right)\right), & if \quad \alpha = 1 \end{cases} \tag{27}$$

and

$$h_{APG}(x) = \begin{cases} \frac{log(\alpha)\lambda exp\left(\beta x - \frac{\lambda}{\beta}\left(e^{\beta x}-1\right)\right)}{\alpha^{exp\left(-\frac{\lambda}{\beta}\left(e^{\beta x}-1\right)\right)-1}}, & if \quad \alpha > 0,\ \alpha \neq 1 \\ \frac{\lambda exp\left(\beta x - \frac{\lambda}{\beta}\left(e^{\beta x}-1\right)\right)}{exp\left(-\frac{\lambda}{\beta}\left(e^{\beta x}-1\right)\right)}, & if \quad \alpha = 1 \end{cases} \tag{28}$$

Other mathematical properties studied by the authors include; the quantile, moments, probability weighted moments, moment generating function, entropy, moments of residuals and reverse residual life function, and order statistics. The maximum likelihood estimation method was employed to estimate the unknown parameters of the APG distribution. The flexibility of the APG distribution was analysed by means of two real data sets.

Data Analysis

In this Section, we fit three data sets using the Weibull distribution (WD), log-logistic distribution (LLD), Bur II distribution (BIID), power Lindley distribution (PLD), Gompertz distribution (GD) and their corresponding alpha-power transformed versions.

Data set 1:

The first data set consist of uncensored data reported in Nicholas and Padgett (2006) on the breaking stress of carbon fibers (in Gba). The data are given below: 3.70, 2.74, 2.73, 2.50,
3.60, 3.11, 3.27, 2.87, 1.47, 3.11, 3.56, 4.42, 2.41, 3.19, 3.22, 1.69, 3.28, 3.09, 1.87, 3.15, 4.90, 1.57, 2.67,
2.93, 3.22, 3.39, 2.81, 4.20, 3.33, 2.55, 3.31, 3.31, 2.85, 1.25, 4.38, 1.84, 0.39, 3.68,
2.48, 0.85, 1.61, 2.79, 4.70, 2.03, 1.89, 2.88, 2.82, 2.05, 3.65, 3.75, 2.43, 2.95, 2.97, 3.39, 2.96,
2.35, 2.55, 2.59, 2.03, 1.61, 2.12, 3.15, 1.08, 2.56, 1.80, 2.53.

Data set 2:

The second data set represents the waiting times (in minutes) before service of 100 bank customers. Ghitany*et al.* (2008) used the data set to illustrate the flexibility of the Lindley distribution over the exponential distribution in real life data fitting. The data set is as follows: 0.8, 0.8, 1.3, 1.5, 1.8, 1.9 ,1.9, 2.1, 2.6, 2.7,2.9, 3.1, 3.2, 3.3 ,3.5, 3.6, 4.0, 4.1, 4.2, 4.2,4.3,

4.3, 4.4, 4.4, 4.6, 4.7, 4.7, 4.8, 4.9, 4.9,5.0, 5.3, 5.5, 5.7, 5.7, 6.1, 6.2, 6.2, 6.2, 6.3,6.7, 6.9, 7.1,
7.1, 7.1, 7.1, 7.4, 7.6, 7.7, 8.0,8.2, 8.6, 8.6, 8.6, 8.8, 8.8, 8.9, 8.9, 9.5, 9.6,9.7, 9.8, 10.7, 10.9,
11.0, 11.0, 11.1, 11.2, 11.2, 11.5,11.9, 12.4, 12.5, 12.9, 13.0, 13.1, 13.3, 13.6, 13.7, 13.9,14.1,
15.4, 15.4, 17.3, 17.3, 18.1, 18.2, 18.4, 18.9, 19.0,19.9, 20.6, 21.3, 21.4, 21.9, 23.0, 27.0, 31.6,
33.1, 38.5.

Data set 3:

The third data set is the records of 72 exceedances of flood peaks (in m^3/s) of the Wheaton river near Carcross in the Yukon Territory, Canada for the years 1958-1984. Choulakian and Stephens (2001) used the data set to illustrate the performance of the generalized Pareto distribution. The data set obtained as follows: 1.7, 2.2, 14.4, 1.1, 0.4, 20.6, 5.3, 0.7, 1.9, 13.0,
12.0, 9.3, 1.4, 18.7, 8.5, 25.5, 11.6, 14.1, 22.1, 1.1, 2.5, 14.4, 1.7, 37.6, 0.6, 2.2, 39.0, 0.3, 15.0,
11.0, 7.3, 22.9, 1.7, 0.1, 1.1, 0.6, 9.0, 1.7, 7.0, 20.1, 0.4, 2.8, 14.1, 9.9, 10.4, 10.7, 30.0, 3.6, 5.6, 30.8, 13.3,
4.2, 25.5, 3.4, 11.9, 21.5, 27.6, 36.4, 2.7, 64.0, 1.5, 2.5, 27.4, 1.0, 27.1, 20.2, 16.8,
5.3, 9.7, 27.5, 2.5, 27.0.

Statistical results for the three data sets are displayed in Tables 1 - 3. The ranking of the distribution is based on the distribution having the least *K- S* value and the highest *p- value*.

Table 1: Statistical results for data set 1

Distributions	*Estimates*	*−LogL*	*AIC*	*K −S*	*p −value*	*Rank*
WD	β = 3.4409 λ = 0.0212 α = 2785.7791	86.0676	176.1352	0.08823	0.7625	4th
APWD	β = 2.3183 λ = 0.8459	108.0827	222.1654	0.1888	0.0180	9th
LLD	β = 4.8964 λ = 2.7108 α = 2.4036	91.6452	187.2905	0.0937	0.6071	5th
APTLLD	β = 4.8466 λ = 2.4824	91.6168	189.2336	0.0943	0.5997	6th
EBIID	β = 5.8453 λ = 2.2416 α = 346.1171	110.0637	224.1273	0.1940	0.0138	10th
APTEBIID	β = 2.1797 λ = 2.9462	100.3059	206.6118	0.1523	0.0936	8th
PLD	β = 2.5100 λ = 0.1240 α = 11.4166	85.8055	175.6111	0.0789	0.8047	3rd
APTPLD	β = 2.0258 λ = 0.3081	85.0986	176.1974	0.0662	0.9341	1st
GD	β = 1.0708 λ = 0.0372 α = 0.0184	88.0883	180.1767	0.1119	0.3798	7th
APGD	β = 1.3876 λ = 0.0052	85.5447	177.0895	0.0761	0.8391	2nd

Table 2: Statistical results for data set 2

Distributions	*Estimates*	*−LogL*	*AIC*	*K −S*	*p −value*	*Rank*

WD	β = 1.4587 λ = 0.0304 α = 98.3616	318.7307	641.4614	0.0577	0.8926	5th
APWD	β = 1.4876 λ = 3.0765	326.3056	658.6111	0.0842	0.4777	7th
LLD	β = 2.2667 λ = 7.8153 α = 0.9981	319.4098	642.8196	0.0508	0.9581	2nd
APTLLD	β = 2.2676 λ = 7.8184	319.4098	644.8196	0.0509	0.9577	3rd
EBIID	β = 8.8671 λ = 1.2899 α = 60.4239	330.4268	664.8536	0.1027	0.2421	9th
APTEBIID	β = 4.3722 λ = 1.2899	324.3901	654.7802	0.0755	0.6174	6th
PLD	β = 1.0831 λ = 0.1530 α = 0.1535	318.3186	641.2372	0.0519	0.9501	4th
APTPLD	β = 1.1678 λ = 0.0861	317.5037	641.0075	0.0448	0.988	1st
GD	β = 0.0408 λ = 0.0714 α = 0.0092	323.9756	651.9512	0.1059	0.212	10th
APGD	β = 0.0810 λ = 0.0131	322.5371	651.0742	0.0885	0.4135	8th

Table 3: Statistical results for data set 3

Distributions	*Estimates*	*−LogL*	*AIC*	*K −S*	*p −value*	*Rank*
WD	β = 0.9010 λ = 0.1095 α = 64.5115	251.4986	506.9973	0.1052	0.403	2nd

APWD	β = 0.8081 λ = 0.7129	262.6387	531.2774	0.1451	0.0965	9th
LLD		257.8391	519.6782	0.0.1138	0.3092	4th
	β = 1.2127 λ = 6.7586 α = 1.0007					
APTLLD	β = 1.2125 λ = 6.7542	257.8391	521.6782	0.1139	0.3083	5th
EBIID		262.1533	528.3067	0.1542	0.0652	10th
	β = 3.1728 λ = 0.8361 α = 13.0168					
APTEBIID	β = 1.7227 λ = 0.9763	259.988	525.9761	0.1384	0.127	7th
PLD		252.2218	508.4436	0.1050	0.4051	1st
	β = 0.7001 λ = 0.3385 α = 1.3272					
APTPLD	β = 0.6862 λ = 0.3682	252.1909	510.3817	0.1069	0.3829	3rd
GD		252.128	508.2559	0.1422	0.1086	8th
	β = -2.624 $\times 10^{-6} \lambda$ = 0.0082 α = 0.3473					
APGD	β = 0.0096 λ = 0.0554	251.6557	509.3114	0.1286	0.185	6th

Tables 1-3 present the parameter estimates, log-likelihood ($-LogL$), Akaike information criterion (AIC), Komolgorov-Smirnov ($K-S$) test statistic and its corresponding $p-value$, and the ranking of the distributions for the three data sets. Empirical findings reveal that the additional parameter from the alpha-power transformed method has a negative effect on the Weibull and log-logistic distributions and a positive effect on the Bur II, power Lindley and Gompertz distributions.

This is evidently clear, as the Weibull and log-logistic distributions ranked higher than their alpha-power transformed version. Conversely, the alpha-power transformed version of the Bur II, power Lindley and Gompertz distributions ranked higher than the baseline distributions. These results are consistently true for the three data sets, except for the power Lindley distribution in the third data set which was ranked higher than the alpha-power transformed power Lindley distribution.

Conclusion

A comparative study on the alpha-power transformed family of distributions has been considered in this paper. Five classical lifetime distributions which include; the Weibull, log-logistic, Bur II, power Lindley and Gompertz distributions and their corresponding alpha-power transformed versions were treated as case studies Mathematical properties of the distributions such as the cdf, pdf, survival and hazard rate functions were discussed. In other to examine the effect of the "α-parameter" on the lifetime distributions, we obtained the fit of the distributions for the three data sets. Empirical findings based on the data sets revealed that the "α-parameter" had a negative effect on the Weibull and log-logistic distributions and a positive effect on the Bur II, power Lindley and Gompertz distributions.

References

Aldahlan, M. A. (2020). Alpha power transformed log-logistic distribution with application to breaking stress data. Advances in Mathematical Physics, Article ID 2193787, https://doi.org/10.1155/2020/2193787.

Al-Shomrani, A., Arif, O., Shawky, A., Hanif, S., and Shahbaz, M. Q. (2016). ToppLeone family of distributions: Some properties and application. Pakistan Journal Statistics and Operation Research, 12(3), 443-451.

Bourguignon M., Silva, R. B., and Cordeiro, G. M. (2014). The Weibull-G family of probability distributions. Journal of Data Science, 12, 53-68.

Choulakian, V. and Stephens, M. A. (2001). Goodness-of-fit for the generalized Pareto distribution. Technometrics, 43(4), 478-484.

Cordeiro, G. M. and de Castro, M. (2011). A new family of distributions. Journal of Statistical Computation and Simulation, 81, 883-898.

Eghwerido, J. T., Nzei, L. C., and Agu, F. I. (2020). Alpha power Gompertz distribution: properties and applications. Sankhya A - The Indian Journal of Statistics, 83(1), 449-475.

Eugene, N., Lee, C. and Famoye, F. (2002). The beta-normal distribution and its applications. Communications in Statistics-Theory and Methods, 31, 497-512.

Ghitany, M. E., Al-Mutairi, D. K., Balakrishnan, N. and Al-Enezi, L. J. (2013): Power Lindley distribution and associated inference. Computational Statistics and Data Analysis, 64, 20-33.

Ghitany, M., Atieh, B. and Nadarajah, S. (2008). Lindley distribution and its applications. Mathematics and Computers in Simulation, 78, 493-506.

Hassan, A. S., Elgarhy, M., Mohamd, R. E. and Alrajhi, S. (2019). On the alpha power transformed power Lindley distribution. Journal of Probability and Statistics, Article ID8024769.

Jemilohun, V. G. and Ipinyomi, R. A. (2022). Alpha power Poisson-G distribution with an application to Bur XII distribution lifetime data. International Journal of Statistics and Probability, 11(2), 8-28. DOI:10.5539/ijsp.v11n2p8

Lindley, D. V. (1958). Fiducial distributions and Bayes' theorem. Journal of the Royal Statistical Society, Series B, Methodological, 20, 102-107.

Mahdavi, A. and Kundu, D. (2017). A new method for generating distributions with an application to exponential distribution. Communications in Statistics - Theory and Methods, 46(15), 6543-6557

Marshall A. W. and Olkin, I. (2007). A new method for adding a parameter to a family of distributions with applications to the exponential and Weibull families. Biometrika, 84, 641-552.

Mudholka, G. S., and Srivastava, D. K. (1993). Exponentiated Weibull family for analyzing bathtub failure rate data. IEEE Transactions on Reliability, 42, 299-302.

Nassar, M., Alzaatreh, A., Mead, M., and Abo-Kasem, O. (2017). Alpha power Weibull distribution: properties and applications. Communications in Statistics - Theory and Methods, 46, 10236-10252.

Nicholas, M. D. and Padgett, W. J. (2006). A bootstrap control chart for Weibull percentiles. Quality and Reliability Engineering International, 22, 141-151.

Ogunde, A. A., Ajayi, B. and Omosigho, D. O. (2020). Alpha power transformed extended Bur II distribution: Properties and applications. Asian Research Journal of Mathematics, 16(8), 50-63, DOI:

10.9734/ARJOM/2020/v16i830208

Shaw, W. T. and Buckley, I. R. C. (2009). The alchemy of probability distributions: beyond Gram-Charlier expansions, and a skew-kurtotic-normal distribution from a rank transmutation map. UCL discovery repository, http://discovery.ucl.ac.uk/id/eprint/643923.

Abacus (Mathematics Science Series)
Vol. 49, No 3, September. 2022

MATHEMATICAL MODELING OF FRACTIONAL ORDER CORONARY HEART DISEASE

*Corresponding Author:amirusule@yahoo.com

Abstract

Coronary heart disease progresses when the coronary arteries that supply oxygen to the heart muscle develop constricted or congested as a result of the accumulation of plaque, a waxy constituent, inside the lining of larger coronary arteries build up, within the arterial wall. A fractional order mathematical model of the dynamics of disease is developed in this paper. The epidemic thresholds and equilibria for the model are determined and stabilities analyzed. Results from the analysis of the reproduction number propose that treatment will somehow contribute to a decrease in disease cases and reduction in death rate of the infectivity. This result recommends that, the control of the disease should lie more on treatment and public health education. Numerical simulations show the dynamics of the transmission of disease.

Keywords: Fractional Order, Coronary Heart Disease, Mathematical Modelin

Introduction

Coronary heart disease (CHD) *equally recognized as Coronary Artery Disease, Coronary Micro vascular Disease, Coronary Syndrome X, Ischemic Heart Disease, Non obstructive Coronary Artery disease, and Obstructive Coronary Artery Disease.* It is regularly triggered by the collection of plaque, a waxy substance, inside the lining of larger coronary arteries. This accumulation can partly or wholly block blood flow in the large arteries of the heart. Certain forms of this disorder might be instigated by disease or damage affecting how the arteries work in the heart [1.]

It is the main cause of death universally. At the beginning of the 20th century, it remained an uncommon cause of death. Deaths resulting from CHD was at it peaked in the mid-1960s [2]and then declined nevertheless, it remains an outstanding universal public health concern. With over seven million losses annually redited to CHD. It is the foremost reason of death universal, a main source of debility, and a substantial economic liability [1&3]. Over half a century, numerous main risk factors have been acknowledged, such as smoking, diabetes, and high levels of blood pressure and low density lipoprotein cholesterol (LDL-C) [3&4]

The high morbidity and death associated with the infectivity can be avoided, if it's promptly acknowledged and treated. Signs of the disease may be different from person to person even if they have the same type of coronary heart disease. However, because many people have no symptoms, they do not know they have coronary heart disease until

they have chest pain, a heart attack, or sudden cardiac arrest [4].

Natural phenomena can be more accurately explained using the fractional order models than the differential equations of the integer-order as asserted by some scientists, over the last few decades. The fractional calculus has taken on the significance and acceptance of modeling realistic cases, particularly those with memory effects [5]. Additionally, its application is employed in numerous fields of social sciences, engineering and biology [5].

Many literature [5-11] investigated the control of the disease using fish consumption to reduce the infectivity. In the present work, the innovations with respect to the existing literature are exposed and recovered classes.
The key objective of this work is to use the new fractional order to develop a model for Coronary Heart Disease and using Laplace Adomian Decomposition Method for numerical solution. The development of the paper is organized into six sections. The model describing the diseases transmission formulated and its analysis; the general procedure of the model using the Caputo fractional derivative system is discussed. Differential Transform Method was discussed and analyzed to compare the results. Numerical results illustrating the analytical results and the conclusion.

$$\begin{aligned}
\frac{dS(t)}{dt} &= \Lambda - (\tau E(t) - \mu)S(t) + \delta R \\
\frac{dE(t)}{dt} &= \tau S(t)E(t) - (\beta + \mu)E(t) \\
\frac{dI(t)}{dt} &= \beta E(t) - (\mu + \mu_0 + \alpha + \gamma)I \\
\frac{dR(t)}{dt} &= \gamma I - (\mu + \delta)R(t)
\end{aligned} \tag{1}$$

The Model Formulation

The total human population at time t, denoted by $N(t)$, is sub divided into the sub-populations of susceptible individuals $S(t)$, those exposed to the disease $E(t)$. Individuals infected with the disease $I(t)$ and finally those that recovered from the infectivity $R(t)$. So that

$$N(t) = S(t) + E(t) + I(t) + R(t)$$

The susceptible population $S(t)$ is increased as a result of birth and immigration at a rate Λ and recovery at a rate δ. Susceptible individuals are exposed through risk factors which includes: (a sedentary lifestyle, lack of physical activity, poor diet, being overweight or obese: drinking alcohol, high blood pressure, tobacco use [5] at a rate τ. The exposed class progress to the stage $I(t)$ of the infectivity at a rate β. And the classes decreases due to natural death at a rate μ. The recovered class increase as result of recovery after medication from the infected class and decrease as a result of loss of immunity back to the susceptible class. And death due to infectivity at the infected class at a rate μ_0. The above mentioned assumptions and description above give rise to the following

The associated model variables and parameters are described in Table 1 and 2 below

Preliminaries

Definition 1. The Caputo fractional order derivative of a function y on the interval [0, T] is defined by

$$ {}^{c}D^{\alpha}_{0+}y(t)=\frac{1}{\Gamma(n-\alpha)}\int_0^t (t-s)^{n-\alpha-1} y^{(n)}(s)ds \qquad (2)$$

where $n=[\alpha]+1$ *and* $[a]$ *represnt the* Integer part of α

The Riemann-Liouville derivative has certain disadvantages such that the fractional derivative of a constant is not zero. Therefore, we will make use of Caputo's definition owing to its convenience for initial conditions of the fractional differential equations [5].

Definition 2. Laplace transform of Caputo derivative as

$$L\left\{{}^{c}D^{\alpha}y(t)\right\}=s^{\alpha}y(s)-\sum_{k=0}^{n-1}s^{\alpha-k-1}y^{(k)}(0),\ n-1<\alpha<n,\ n\in N.$$

The new system of the differential equation is represented by the fractional system of differential equations is given as follows.

$$\begin{aligned} D^{\alpha_1}S(t)&=\Lambda-(\tau E(t)-\mu)S(t)+\delta R\\ D^{\alpha_2}E(t)&=\tau S(t)E(t)-(\beta+\mu)E(t)\\ D^{\alpha_3}I(t)&=\beta E(t)-(\mu+\mu_0+\alpha+\gamma)I\\ D^{\alpha_4}R(t)&=\gamma I-(\mu+\delta)R(t) \end{aligned} \qquad (3)$$

Wherever, $\alpha\in(0,1]$ whilst all other parameters are positive parameters and the given initial conditions are

$$\begin{cases} S(0)=N_1\\ E(0)=N_2\\ I(0)=N_3\\ R(0)=N_4, \end{cases} \qquad (4)$$

Stability Analysis and Equilibria

Disease-free equilibrium (DFE)

The model (3) has a DFE, obtained by setting the right-hand sides of the equations in (3) to zero, given by

$$\begin{cases} D^{\alpha_1} S(t) = 0 \\ D^{\alpha_2} E(t) = 0 \\ D^{\alpha_3} I(t) = 0 \\ D^{\alpha_4} R(t) = 0 \end{cases} \quad (5)$$

$$E_0 = (S^*, E^*, I^*, R^*) = \left(\frac{\Lambda}{\mu}, 0, 0, 0\right) \quad (6)$$

Theorem 1. The DFE of E_0 is asymptotically stable (LAS) if $R_0 < 1$, and unstable if $R_0 > 1$.

Reproductive number: The threshold result of this equilibrium is:

$$F = \begin{vmatrix} \tau \frac{\Lambda}{\mu} & 0 \\ 0 & 0 \end{vmatrix}$$

$$V := \begin{vmatrix} (\beta + \mu) & 0 \\ -\beta & (\mu + \mu_0 + \alpha + \gamma) \end{vmatrix}$$

The threshold epidemiological of those involved in disease, denoted by $R_0 = \rho(FV^{-1})$, where ρ denotes the spectral radius, is given by

$$\Re_0 = \frac{\tau\Lambda}{\mu(\beta + \mu)} \quad (7)$$

Theorem 2. The *DFE* of model equation (2.1), given (2.9), are locally asymptotically stable (LAS) if $R_0 < 1$, *and* unstable if $R_0 > 1$.

The threshold quantity R_0 is the basic reproduction number of the disease.

Analysis of the Basic Reproduction Number $\Re_0$.

Sensitivity Analysis of Model Parameters

To recognize how best to lower fatality and misery due to the disease, it is vital to recognize the implication of the diverse reasons accountable for the disease spread. Disease spread primarily depends on the basic reproduction number R_0 [12] Sensitivity of each parameter is examined with respect to the basic reproduction number R_0. In this way, the parameters that are more sensitive to the disease transmission are identified. Furthermore, reducing or increasing such parameters will as well reduce or increase the transmission of the disease. This detail is imperative to experimental design, data assimilation and complex nonlinear model reduction [13]. Table 1 gives description of parameters for CHDmodel.

Table 1 Description of parameters for CHD model

Parameter	Description	Est. Value	Ref
Λ	Recruitment rate of CHD patients	50000	7
μ	Natural death rate	0.0057	5
τ	Risk factors	0.6	5
β	Rate of infection	0.005	7
δ	Loss of immunity	0.005	7
γ	Recovery rate	0.05	5
μ_0	Death due to infection	0.002	5

Sensitivity index of the basic reproduction number, R_0 with respect to each parameter is computed as given in Table 2 for the model (3)

Definition 3. [12] The normalized forward sensitivity index of a variable with regard to a parameter is the ratio of the relative change in the variable to the relative change in the parameter. The sensitivity index perhaps on the other hand is represented with the partial derivatives given by

$$\Upsilon_{\beta_m}^{R_0} = \frac{\partial R_0}{\partial \beta_m} \times \frac{\beta_m}{R_0}.$$

Sensitivity indices of R_0

The sensitivity of R_0 each of the 19 different parameters described in Table 2 is determined using the basic reproduction number of model(3) as stated below

$$\Re_0 = \frac{\tau\Lambda}{\mu(\beta+\mu)}$$

Table 2 Sensitivity Indices of R_0

Table 2 Description of parameters for CHD model

Parameter	Est. Value	Sensitivity Index
β	0.005	$-4.58x10^{9}$
μ	0.0057	-1.532
τ	0.6	1.00
Λ	50000	1.00

Sensitivity index of the basic reproduction number, R_0 with respect to each parameter is computed

The parameters on Table 2 are arranged in an ascending order starting from the most sensitive to the least

Endemic equilibrium point (EEP)

Next, conditions for the existence of endemic equilibria for the model (3) are explored. Let $E_1 = (S^{**}, E^{**}, I^{**}, R^{**})$

be the arbitrary endemic equilibrium of model (2), in which at least one of the infected components of the model is non-zero. Setting the right-hand sides of the equations in (3) to zero gives the following expressions.

$$\begin{aligned}
S^{**} &= \frac{\beta_1+\mu}{\tau} \\
E^{**} &= \frac{(\alpha+\delta+\gamma+\mu_0)(\delta+\mu)\beta_1(\mu^2+\mu\beta_1+\tau\Lambda)}{\tau(\mu^3+(\alpha+\delta+\gamma+\mu_0+\beta_1)\mu^2+((\alpha+\delta+\gamma+\mu_0)\beta_1+\delta(\gamma+\mu_0+\alpha))\mu+\delta\beta_1(\alpha+\mu_0))} \\
I^{**} &= \frac{(\delta+\mu)\beta_1(\mu^2+\mu\beta_1+\tau\Lambda)}{\tau(\mu^3+(\alpha+\delta+\gamma+\mu_0+\beta_1)\mu^2+((\alpha+\delta+\gamma+\mu_0)\beta_1+\delta(\gamma+\mu_0+\alpha))\mu+\delta\beta_1(\alpha+\mu_0))} \\
R^{**} &= \frac{\gamma\beta_1(\mu^2+\mu\beta_1+\tau\Lambda)}{\tau(\mu^3+(\alpha+\delta+\gamma+\mu_0+\beta_1)\mu^2+((\alpha+\delta+\gamma+\mu_0)\beta_1+\delta(\gamma+\mu_0+\alpha))\mu+\delta\beta_1(\alpha+\mu_0))}
\end{aligned} \tag{8}$$

Furthermore, using Theorem 2 of [7] the following result is established.

Non-negative solution

$let\ R^4 = \{x \in R^4, x \geq 0\}$

and

$x(t) = (S(t), E(t), I(t), R(t))^T$

Lemma: Let $h(x) \in C[a,b]$ and $D^{\alpha} h(x) \in [a,b]$ for $0 < \alpha \leq 1$. Then

$$h(x) = h(a) + \frac{1}{(\alpha+1)!} D^{\alpha} h(\eta)(x-a)^{\alpha}, \text{with } 0 \leq \eta \leq x \text{ for } x \in (a,b]$$

Theorem 3. There is a unique solution for the initial value problem given by (3), and the solution remains in $R^4, x \geq 0$.

Proof: Aim is to show that the domain $R^4, x \geq 0$. is positively invariant. Since

$$\begin{aligned} D^{\alpha_1} S(t)\big|_{S(t)=0} &= \Lambda \geq 0, \\ D^{\alpha_2} E(t)\big|_{E(t)=0} &= \beta S(t) I(t) + \gamma I(t) \geq 0, \\ D^{\alpha_3} I(t)\big|_{I(t)=0} &= \delta E(t) \geq 0, \\ D^{\alpha_4} R(t)\big|_{R(t)=0} &= kE(t) \geq 0. \end{aligned} \tag{9}$$

The non-negative solution satisfied the vector field point into R^4

Numerical simulations

The simulations were carried out using the following values for initial conditions. The final time was t=100 days. Computations were run in Maple

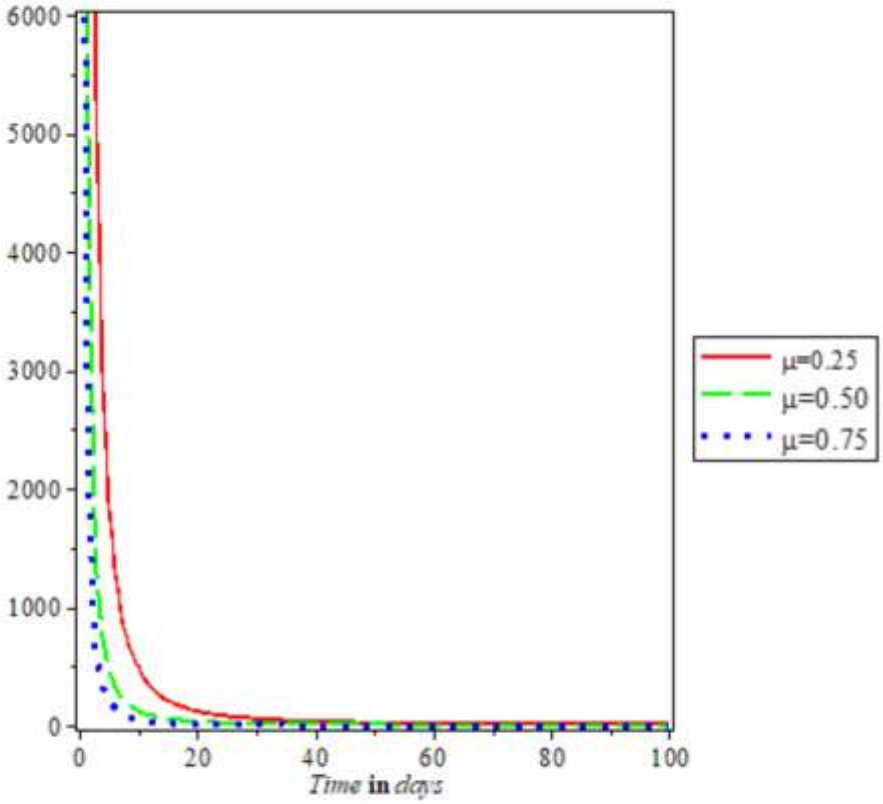

Figure 1 shows the effect of natural death in the disease transmission.

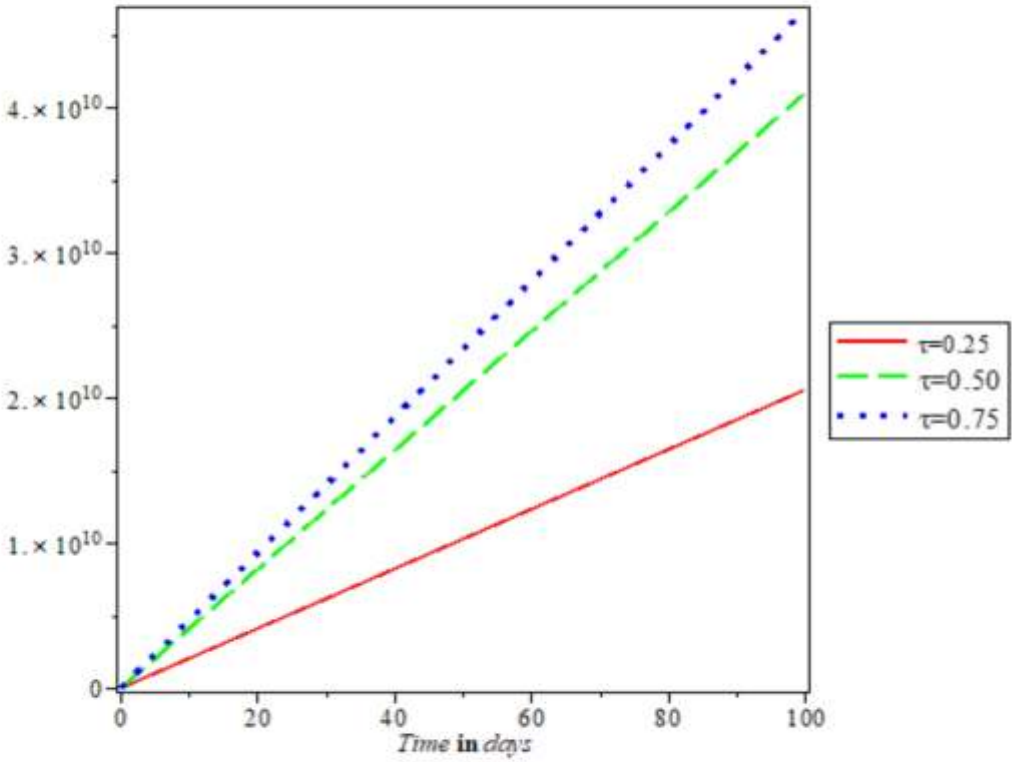

Figure 2 shows the effect of risk factors in the disease transmission.

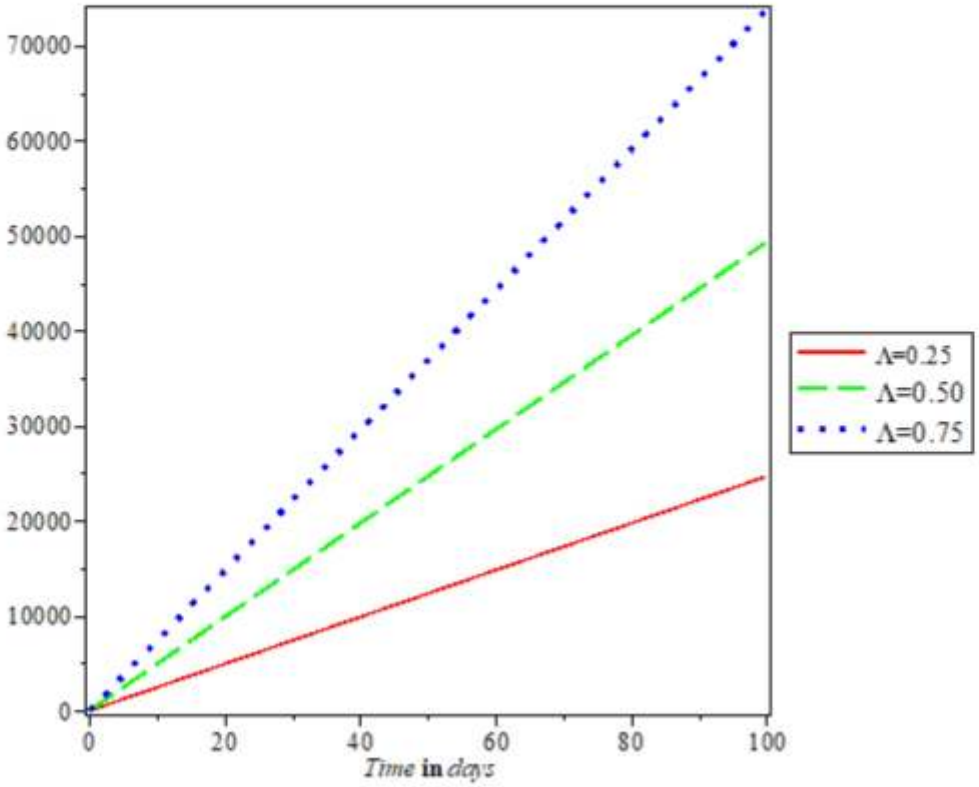

Figure 3 shows the effect of recruitment rate in the disease transmission

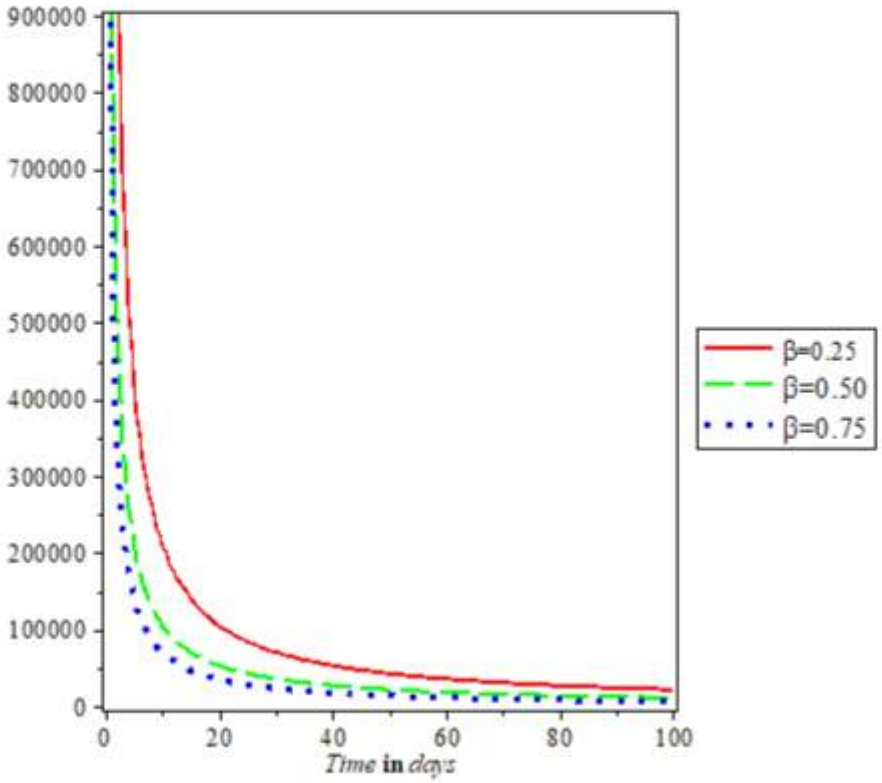

Figure 4 shows the effect of transmission rate in the disease transmission

Conclusion

In this paper, a fractional order mathematical model of the dynamics of disease was developed. The epidemic thresholds and equilibria for the model are determined and stabilities analyzed. Results from the analysis of the basic reproduction number propose that the sedentary lifestyle, lack of physical activity, poor diet, being overweight or obese, drinking alcohol, high blood pressure, tobacco use denoted by will contribute to increase in the disease. This result recommends that, the control of the disease should lie more on public health education. Numerical simulations show the dynamics of the transmission of disease using the basic reproduction number.

References

Shao, C., Wang, J., Tian, J., & Tang, Y. D. (2020). Coronary artery disease: from mechanism to clinical practice. *Coronary Artery Disease: Therapeutics and Drug Discovery*, 1-36.

Shahjehan, R. D., &Bhutta, B. S. (2020). Coronary artery disease. *StatPearls [Internet]*.). Retried on internet on 18th July 2022

Mayosi, B. M. (2007). Contemporary trends in the epidemiology and management of cardiomyopathy and pericarditis in sub-Saharan Africa. *Heart*, *93*(10), 1176-1183.

Huxley, R., Barzi, F., & Woodward, M. (2006). Excess risk of fatal coronary heart disease associated with diabetes in men and women: meta-analysis of 37 prospective cohort studies. *Bmj*, *332*(7533), 73-78.

Ameen, I., Hidan, M., Mostefaoui, Z., & Ali, H. M. (2020). Fractional optimal control with fish consumption to prevent the risk of coronary heart disease. *Complexity*, *2020*.

König, A., Bouzan, C., Cohen, J. T., Connor, W. E., Kris-Etherton, P. M., Gray, G. M., ...&Teutsch, S. M. (2005). A quantitative analysis of fish consumption and coronary heart disease mortality. *American jour*

Mohamed Lamlili, E. N., Boutayeb, A., Moussi, A., Boutayeb, W., &Derouich, M. (2015). Fish consumption impact on coronary heart disease mortality in Morocco: a mathematical model. *Applied Mathematical Sciences*, *9*(60), 2965-2975.

Lamlili, E. N., Boutayeb, A., Derouich, M., Boutayeb, W., &Moussi, A. (2016). Fish Consumption Impact on Coronary Heart Disease Mortality in Morocco: A Mathematical Model with Optimal Control. *Engineering Letters*, *24*(3).

Oomen, C. M., Feskens, E. J., Räsänen, L., Fidanza, F., Nissinen, A. M., Menotti, A., ...&Kromhout, D. (2000). Fish consumption and coronary heart disease mortality in Finland, Italy, and The Netherlands. *American Journal of Epidemiology*, *151*(10), 999-1006.*nal of preventive medicine*, *29*(4), 335-346.

Zhang, B., Xiong, K., Cai, J., & Ma, A. (2020). Fish consumption and coronary heart disease: A meta-analysis. *Nutrients*, *12*(8), 2278.

Mohamed Lamlili, E. N., Boutayeb, A., Moussi, A., Boutayeb, W., & Derouich, M. (2015). Fish consumption impact on coronary heart disease mortality in Morocco: a mathematical model. *Applied Mathematical Sciences*, *9*(60), 2965-2975.

Chitnis, N., Hyman, J. M., & Cushing, J. M. (2008). Determining important parameters in the spread of malaria through the sensitivity analysis of a mathematical model. *Bulletin of mathematical biology*, *70*(5), 1272-1296.

Powell, D. R.., Fair, J., Le Claire, R. J., Moore, L. M., & Thompson, D. (2005) Sensitivity analysis of an infectious disease model, in Proceedings of the International System Dynamics Conference, Boston, Mass, USA,

Abacus (Mathematics Science Series)
Vol. 49, No 3, September. 2022

BLOCK STORMER-COWELL METHOD FOR SOLVING BRATU EQUATIONS

Abstract

This work focuses on the numerical solution of Bratu equations, which is extremely helpful in studying nonlinear systems. Block Stormer-Cowell-method (BSM) is proposed for the direct solution of Bratu initial and boundary value problems using boundary value techniques. The method is implemented in a block-by-block unification version which has unique advantages and is applied without restriction. The method is formulated by adopting a collocation and interpolation technique with carefully selected points within the integration interval. The stability property of the method revealed A (a)-stability. The rate of convergence (ROC), efficiency and solution curves are presented separately to show the proposed method's consistency, efficiency and accuracy advantages. The results show that the method gives accurate solutions and is suitable for Brat equations' direct solution.

Keywords: Bratu Equation; Stormer-Cowell-method; Block unification; A *(a)*-stability.

Introduction

In this article, BSM is proposed for the numerical solution of Bratu initial and Bratu boundary value problems. According to ([1], [2], [3]), this all important equation can be written as

$$u'' + \lambda e^{u} = 0 \quad 0 < x < 1 \tag{1}$$

Subject to

$$u(0) = u(1) = 0.$$

which is considered to be boundary value problem in one dimensional coplanar coordinate. For some obvious reasons, researchers have devoted more efforts and time to the study of this type of equation. These reasons might not be unconnected with the fact that the equation appears in varieties of applications which include physical, chemical and engineering [2]. In specific term, one area of application of this equation in physical sciences can be found in thermal reaction [4]. It can also be found in chemical application such as nano-technology and fluid combustion. According to [2], engineers apply the principle of this equation in Nano-fibers and electro-spinning. Further applications of Bratu-type equation are discussed in (([5], [6]) and that of Bratu's equation in [1], [2], [3], [4],).

In literature [3] and [6] presented algorithms based on cubic spline for the solution of (1), [7] studied the approximate solution of (1) using the application of successive differentiation method, [8] examined (1) by applying variational iterative approach, while [2], [1], [4] in their separate work proposed algorithms that employed major ideal of Adomian decomposition. The work of Habtamu *et al.* [5] titled "Numerical solution of second-order initial value problems of Bratu-type equation

using higher-order Rungu-Kutta method" adopted fifth-order one-step Runge-Kutta method proposed by [9] with little modification. The desire to contribute to BSM is burned out of the need for more numerical methods for the Bratu-type and Bratu equation solution without any restriction.

The BSM considered in this article is carefully constructed to be able to tackle any equation (1) because of its nonlinearity nature. BSM is a multistep finite difference method whose development depends on constructing a continuous collocation scheme through which the main and additional methods needed to implement the BSM in multistep block unification are obtained [10]. The numerical solutions obtained in this study are presented in both 2D and 3D. We present the derivation of the proposed method in the next section of this paper with its implementation in block mode. After that, the analysis of the proposed method to establish the numerical stability, numerical example to demonstrate the efficiency advantages of the proposed method and subsequently, the conclusion drawn on the performance of the proposed method when applied to solve the numerical examples.

Mathematical Formulation of the Method

The sole aim of this work is to derive the multistep collocation method of the form

$$\sum_{r=3}^{k}\alpha_r(x)u_{n+r}=h^2\sum_{r=0}^{k}\beta_r(x)f_{n+r}\ (2)$$

where $\alpha_r(x)$ and $\beta_r(x)$ are coefficients that defined the method. This shall be achieved through the interpolation and collocation of a polynomial

$$u(x)=\sum_{i=0}^{d-1}\phi_i x^i \quad (3)$$

(which are continuously differentiable) on equi-distant mesh points $\{x_j\}$. We set $r+s$ to be equal to d so as to be able to determine $\{\phi_j\}$ uniquely. We interpolate $u(x)$ and collocate $u''(x)$ at the points $\{x_{n+j}\}$ to obtain the following equations

$$u(x_{n+j})=u_{n+j},\quad (j=k-2,k-1) \qquad (4)$$

$$u''(x_{n+j})=f_{n+j}\quad (j=0(1)k) \qquad (5)$$

Note that u_{n+j} and f_{n+j} are interpolation and collocation data $u(x)$ and $u''(x)$ on $\{x_{n+j}\}$ respectively. In the light of [ ], equations (4) and (5) can be expressed in matrix-vector form as:

$$\bar{V}\phi\ (6)$$

where $d-$square matrix $\bar{V}$, the $p-$vectors ϕ and u are defined as follows

$$\bar{V}=\begin{bmatrix} p_{11} & p_{12} \\ p_{21} & p_{22} \end{bmatrix},\ \phi=(\phi_1,\phi_2,...,\phi_{d-1}) \text{ and } u=(u_{n+k-2},u_{n+k-1},f_n,f_{n+1},...,f_{n+k}) \quad (7)$$

Here, $\bar{V}$ are partition into $p_{11},p_{12},p_{21},p_{22}$ square matrices whose entries are generated from equation (4) and (5). We obtain a closed form of (6) by considering the inverse of the Vandermonde matrix $\bar{V}$ that is

$$\phi = Mu \quad (8)$$

where $V^{-1}=M$

We note that after the simplification of (8) and (3) equivalent continuous forms written as

$$u(x)=\alpha_{k-2}(x)u_{n+k-2}+\alpha_{k-1}(x)u_{n+k-1}+h^2\sum_{r=0}^{k}\beta_r(x)f_{n+r} \quad r=0(1)k \quad (9)$$

$$u'(x)=\frac{d}{dx}u(x) \quad (10)$$

where k is the step number, $\alpha_{k-2},\alpha_{k-1}$ and $\beta_r(x)$ are continuous coefficients are obtained. The continuous forms (9) and (10) are then used to generate the discrete and additional first derivative methods for the numerical solution of (1).

Specification of the method

The proposed method is specified by following the procedure discussed in section two above, choosing $k=5$ and the matrix $\bar{v}$ in (6) as defined in (7) contained the following matrix partitions

$$p_{11}=\begin{pmatrix} 1 & x_{n+3} & x_{n+3}^2 & x_{n+3}^3 \\ 1 & x_{n+4} & x_{n+4}^2 & x_{n+4}^3 \\ 0 & 0 & 2 & x_n \\ 0 & 0 & 2 & x_{n+1} \end{pmatrix},\quad p_{12}=\begin{pmatrix} x_{n+3}^4 & x_{n+3}^5 & x_{n+3}^6 & x_{n+3}^7 \\ x_{n+4}^4 & x_{n+4}^2 & x_{n+4}^6 & x_{n+4}^4 \\ 12x_n^2 & 20x_n^3 & 30x_n^4 & 42x_n^5 \\ 12x_{n+1}^2 & 20x_{n+1}^3 & 30x_{n+1}^4 & 42x_{n+1}^5 \end{pmatrix}$$

$$p_{21}=\begin{pmatrix} 0 & 0 & 0 & x_{n+2} \\ 0 & 0 & 0 & x_{n+3} \\ 0 & 0 & 2 & x_{n+4} \\ 0 & 0 & 2 & x_{n+5} \end{pmatrix},\qquad p_{22}=\begin{pmatrix} 12x_{n+2}^2 & 20x_{n+2}^3 & 30x_{n+2}^4 & 42x_{n+2}^5 \\ 12x_{n+3}^2 & 20x_{n+3}^3 & 30x_{n+3}^4 & 42x_{n+3}^5 \\ 12x_{n+4}^2 & 20x_{n+4}^3 & 30x_{n+4}^4 & 42x_{n+4}^5 \\ 12x_{n+5}^2 & 20x_{n+5}^3 & 30x_{n+5}^4 & 42x_{n+5}^5 \end{pmatrix}$$

Inverting the matrix $\bar{V}$ once, using computer algebra, for example, Maple or Matlab software package, give rise to the following continuous scheme

$$u_{n+5}=\alpha_3u_{n+3}+\alpha_4u_{n+4}+h^2(\beta_0f_n+\beta_1f_{n+1}+\beta_2f_{n+2}+\beta_3f_{n+3}+\beta_4f_{n+4}+\beta_5f_{n+5}) \quad (11)$$

Where

$$\left.\begin{aligned}
\alpha_3 &= 4-N \\
\alpha_4 &= N-3 \\
\beta_0 &= \frac{h^2\left(-2N^7+42N^6-357N^5+1575N^4-3836N^3+5040N^2-3176N+672\right)}{10080} \\
\beta_1 &= \frac{h^2\left(10N^7-196N^6+1491N^5-5390N^4+8400N^3-14059N+10668\right)}{10080} \\
\beta_2 &= \frac{h^2\left(-10N^7+182N^6-1239N^5+3745N^4-4200N^3-3140N+9744\right)}{5040} \\
\beta_3 &= \frac{h^2\left(10N^7-168N^6+1029N^5-2730N^4+2800N^3-5813N+13524\right)}{5040} \\
\beta_4 &= \frac{h^2\left(-10N^7+154N^6-861N^5+2135N^4-2100N^3-32N+2688\right)}{10080} \\
\beta_5 &= \frac{h^2\left(2N^7-28N^6+147N^5-350N^4+336N^3-107N-84\right)}{10080}
\end{aligned}\right\} \quad (12)$$

The first derivative of (11) yields

$$u'_{n+5}=\frac{1}{h}\left(\alpha'_3u_{n+3}+\alpha'_4u_{n+4}+h^2\left(\beta'_0f_n+\beta'_1f_{n+1}+\beta'_2f_{n+2}+\beta'_3f_{n+3}+\beta'_4f_{n+4}+\beta'_5f_{n+5}\right)\right)$$

(13)

where

$$\left.\begin{aligned}
\alpha'_3 &= 1 \\
\alpha'_4 &= 1 \\
\beta'_0 &= \frac{h\left(-14N^6+252N^5-1785N^4+6300N^3-11508N^2+10080N-3176\right)}{10080} \\
\beta'_1 &= \frac{h\left(70N^6-1176N^5+7455N^4-21560N^3+25200N^2-14059\right)}{10080} \\
\beta'_2 &= \frac{h\left(-70N^6+1092N^5-6195N^4+14980N^3-12600N^2-3140\right)}{5040} \\
\beta'_3 &= \frac{h\left(70N^6-1008N^5+5145N^4-10920N^3+8400N^2-5813\right)}{5040} \\
\beta'_4 &= \frac{h\left(-70N^6+924N^5-4305N^4+8540N^3-6300N^2-32\right)}{10080} \\
\beta'_5 &= \frac{h\left(14N^6-168N^5+735N^4-1400N^3+1008N^2-107\right)}{10080}
\end{aligned}\right\} \quad (14)$$

Equations (11) and (13) are evaluated at $N=\{0,1,2,5\}$ and $N=\{0,1,2,3,4,5\}$ respectively. Solving the resulting equations simultaneously and writing explicitly yields the following BSM

$$\left.\begin{aligned}
u_{n+1} &= u_n + u'_n + \frac{h^2}{10080}\left(2462f_n + 4315f_{n+1} - 3044f_{n+2} + 1882f_{n+3} - 682f_{n+4} + 107f_{n+5}\right)\\
u_{n+2} &= u_n + 2u'_n + \frac{h^2}{630}\left(355f_n + 1088f_{n+1} - 370f_{n+2} + 272f_{n+3} - 101f_{n+4} + 16f_{n+5}\right)\\
u_{n+3} &= u_n + 3u'_n + \frac{3h^2}{1120}\left(328f_n + 1167f_{n+1} - 24f_{n+2} + 290f_{n+3} - 96f_{n+4} + 15f_{n+5}\right)\\
u_{n+4} &= u_n + 4u'_n + \frac{8h^2}{315}\left(47f_n + 2\left(89f_{n+1} + 11f_{n+2} + 38f_{n+3} - 5f_{n+4} + f_{n+5}\right)\right)\\
u_{n+5} &= u_n + 5u'_n + \frac{25h^2}{2016}\left(122f_n + 475f_{n+1} + 100f_{n+2} + 250f_{n+3} + 50f_{n+4} + 11f_{n+5}\right)\\
u'_{n+1} &= u'_n + \frac{h}{1440}\left(475f_n + 1427f_{n+1} - 798f_{n+2} + 482f_{n+3} - 173f_{n+4} + 27f_{n+5}\right)\\
u'_{n+2} &= u'_n + \frac{h}{90}\left(28f_n + 129f_{n+1} + 14f_{n+2} + 14f_{n+3} - 6f_{n+4} + f_{n+5}\right)\\
u'_{n+3} &= u'_n + \frac{3h}{160}\left(17f_n + 73f_{n+1} + 38f_{n+2} + 38f_{n+3} - 7f_{n+4} + f_{n+5}\right)\\
u'_{n+4} &= u'_n + \frac{2h}{45}\left(7f_n + 32f_{n+1} + 12f_{n+2} + 32f_{n+3} + 7f_{n+4}\right)\\
u'_{n+5} &= u'_n + \frac{5h}{288}\left(19f_n + 75f_{n+1} + 50f_{n+2} + 50f_{n+3} + 75f_{n+4} + 19f_{n+5}\right)
\end{aligned}\right\} \qquad (15)$$

Analysis of the BSM

The proposed BSM is given by the block matrix equation

$$A^{(0)}U_\mu = A^{(1)}U_{\mu-1} + h^2\left(B^{(1)}F_{\mu-1} + B^{(0)}F_\mu\right) \qquad (16)$$

Where $\mu = 1,\ldots,N-1$, $A^{(i)}, B^{(i)}$ are 10×10 square matrix whose entries are the coefficients of (15).

$A^{(0)}$ is an identity matrix. The vectors $U_\mu, U_{\mu-1}, F_{\mu-1}$ and F_μ are defined as follows

$$U_\mu = \left(u_{n+1}, u_{n+2}, \ldots, u_{n+5}, hu'_{n+1}, hu'_{n+2}, \ldots, hu'_{n+5}\right)$$

$$F_\mu = \left(f_{n+1}, f_{n+2}, \ldots, f_{n+5}, hf'_{n+1}, hf'_{n+2}, \ldots, hf'_{n+5}\right)$$

$$U_{\mu-1} = \left(u_{n-1}, u_{n-2}, u_{n-3}, u_{n-4}, u_{n-4}, u_n, hu'_{n-1}, hu'_{n-2}, hu'_{n-3}, hu'_{n-4}, hu'_n\right)$$

$$F_{\mu-1} = \left(f_{n-1}, f_{n-2}, f_{n-3}, f_{n-4}, f_n, hf'_{n-1}, hf'_{n-2}, hf'_{n-3}, hf'_{n-4}, hf'_n\right)$$

where $y_{n-i}, y'_{n-i}, f_{n-i}, f'_{n-i}, i = 1(1)4$ are used to extend the zero entries of the vector notation see [10], [12] and [13]

Local Truncation error and order

With the BSM (16), we associate the linear difference operator L defined by

$$L\left[\bar{U}(x):h\right] = A^{(0)}\bar{U}_{\mu+1} + \left[A^{(1)}\bar{U}_{\mu} + h^2 B^{(1)}\bar{F}_{\mu} + h^2 B^{(0)}\bar{F}_{\mu+1}\right] \quad (17)$$

Where $\bar{U}_{\mu+1} = U_{\mu}, \bar{U}_{\mu} = U_{\mu-1}, \bar{F}_{\mu} = F_{\mu-1}$, and $\bar{F}_{\mu+1} = F_{\mu}$. Also $u_{n\pm j} = u(x_n \pm j), f_{n\pm j} = f\left(x_{n\pm j}, u_{n\pm j}\right)$ and $y^a_{n+j} = y^a(x_n + jh)$, $a = 0(1)N$. Expanding the test function $y(x+jh)$ and its derivatives $y'(x+jh), y''(x+jh)$ as Taylor series about x, and collecting term in (17) gives the following local truncation error:

$$L\left[\bar{U}(x):h\right] = c_0\bar{U}(x) + c_1 h\bar{U}'(x) + \ldots + c_a h^a \bar{U}^a(x) + \ldots \quad (18)$$

where $c_a, a = 0,1,\ldots$ are constant coefficients.

Definition: The block method (17) has algebraic order at least $p \geq 1$ provided there exists a constant $c_{p+2} \neq 0$ such that the local truncation error E_{μ} satisfies $\|E_{\mu}\| = c_{p+2}h^{p+2} + 0\left(h^{p+3}\right)$, where $\|.\|$ the maximum norm [10] is.

Remarks:

a The local truncation error constants c_{p+2} of BSM (16) as defined by (18) are respectively

$$c_8 = -\left(\frac{199}{24192} \quad \frac{19}{945} \quad \frac{141}{4480} \quad \frac{8}{189} \quad \frac{1375}{244192} \quad \frac{863}{60480} \quad \frac{37}{3780} \quad \frac{29}{2240} \quad \frac{8}{945} \quad \frac{275}{12096}\right)^T$$

where $c_0 = c_1 = ,\ldots, c_7 = 0$

b We observed that the order of BSM (18) as obtained from the computation of the local truncation error constants are uniformly $(6,6,6,6,6,6,6,6,6,6)^T$ [11], [12], [13].

Stability of the method

The linear stability of BSM is gotten by applying (18) to test equation $y'' = \lambda^2 y$ where λ is a real constant. Let v be equal to $h\lambda$, the application of (18) to the test equation gives

$$U_{\mu} = \Theta\left(z^2\right)U_{\mu-1}$$

$$\Theta\left(z^2\right) = \left(A^0 + z^2 B^0\right)^{-1}\left(A^1 - z^2 B^1\right) \quad (19)$$

Here $\Theta(z^2)$ is called the amplification matrix and its determines the stability of the method. The stability polynomial for the BSM is gotten as

$$p(\eta, z) = \frac{\eta\left(1200\eta z^5 + 2962\eta z^4 - 20z^5 + 3110\eta z^3 - 2587z^4 - 18900\eta z^2 + 3400z^3 + 75600\eta z - 12600z^2 - 151200\eta + 151200\right)}{2\left(600z^5 + 1481z^4 1555z^3 - 9450z^2 + 37800z - 75600\right)}$$

The Region of Absolute Stability (RAS) of the method is plotted using the root locus technique. The RAS is as shown the figure 1 below

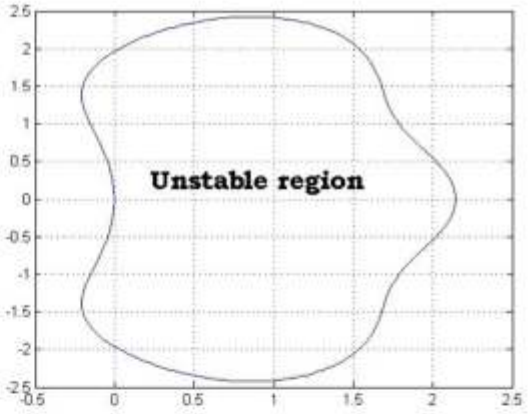

Figure 1: Region of absolute stability of the BSM

Implementation of BSM

Boundary Value Technique is adopted for implementing method (18) via a written code in Wolfram Software called Mathematical version 11.3. The block by block procedures are as itemized below

1 Choose N such that $h=(x_N - x_0)$, on the partition Q_N

2 By adopting (15), $n=0, v=5$, generate the variables $(y_1, y_2, y_3, y_4, y_5)^T$ and $(y_1', y_2', y_3', y_4', y_5')^T$ the interval $[x_0, x_5]$ and store

3 For $n=1, v=2$ generate the variables $(y_6, y_7, y_8, y_9, y_{10})^T$ and $(y_6', y_7', y_8', y_9', y_{10}')^T$ on the sub-interval $[x_6, x_{10}]$ and store

4 Continuing the procedure for $n=2,\ldots,N-1$ and $v=3,\ldots,N$ until all the variables on the sub-intervals $[x_0, x_5], [x_6, x_{10}], \ldots, [x_{N-1}, x_N]$ are obtained.

5 Combine as a single block matrix equation all the block generated in steps 2 and 3 on Q_N

6 Solve simultaneously the single block matrix equation to obtain all the solution of (1) on the entire interval $[x_0, x_N]$

Numerical Experiment

In this section, our efforts shall be directed towards employing BSM as discussed above to obtain the numerical solution of some of Bratu's equations. In order to justify the efficiency and applicability of the presented method, Maximum errors are defined by

$$\text{Max Error} = \text{Max}\left\|U_{n+1} - U(x_{n+1})\right\| \tag{20}$$

where U_{n+1} and $U(x_{n+1})$ are the numerical and exact values of U at points i in the collocation interval of points

$$\left\{x_1 = a, \ldots, x_i = a + (i-1)h, \ldots, x_N = b\right\}, \text{ for } h = \frac{|b-a|}{N-1} \tag{21}$$

The rate of convergence (ROC) is calculated using the formula

$$\text{ROC} = \log_2\left(\frac{Err2h}{Errh}\right),$$

Errh is the maximum error obtained using the step size h. In general, it is shown that the computed ROC is higher but consistent with the theoretical order 6 of the BSM.

Application of BSM to solve Bratu Equations

We first considered classical nonlinear Bratu boundary value problem in one-dimensional planar coordinates given as

$$\left.\begin{aligned} -u''(x) &= \lambda e^{u}, \quad 0 < x < 1 \\ u(0) &= u(1) = 0 \end{aligned}\right\} \tag{22}$$

The Exact solution to (22) is given in [8], [5], [6], [2], [3], [7], as

$$u(x) = -2In\left[\frac{\cosh\left(\frac{x\theta}{2} - \frac{\theta}{4}\right)}{\cosh\left(\frac{\theta}{4}\right)}\right] \tag{23}$$

where θ satisfies $\theta = \sqrt{2\lambda}\cosh\left(\frac{\theta}{4}\right)$.

There are three possible solutions considering the value of λ viz:

1 If $\lambda > \lambda_c$, then the Bratu problem has zero solution.

2 If $\lambda = \lambda_c$, then the Bratu problem has one solution.

3 If $\lambda < \lambda_c$, then the Bratu problem has two solutions.

where the critical value λ satisfies the equation.

$$4 = \sqrt{2\lambda_c}\sinh\frac{\theta_c}{4}, \quad \lambda_c = 3.513830719$$

We first considered the solution of (22) for which λ is equal to 1. The solution curves are as presented in figures 2 and 3 respectively.

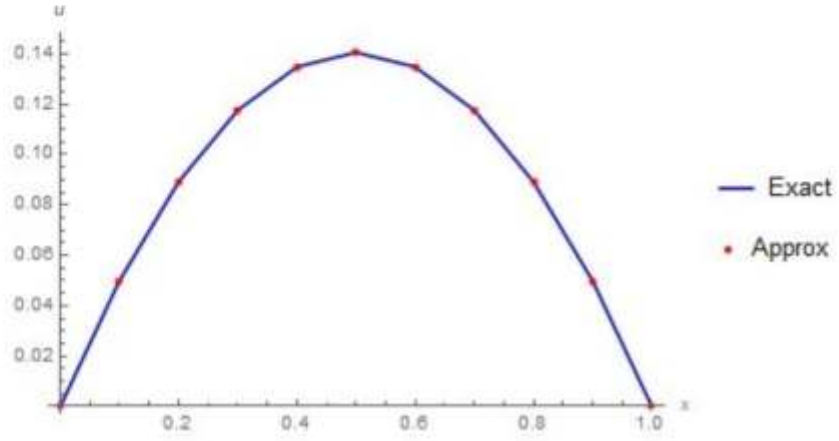

(a) 2D solution curve of Bratu eqution with λ= 1 as compared with the exact solution.

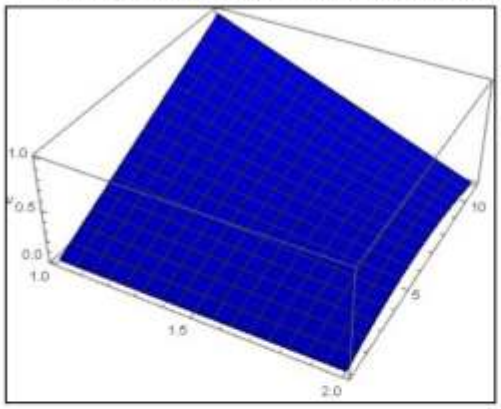

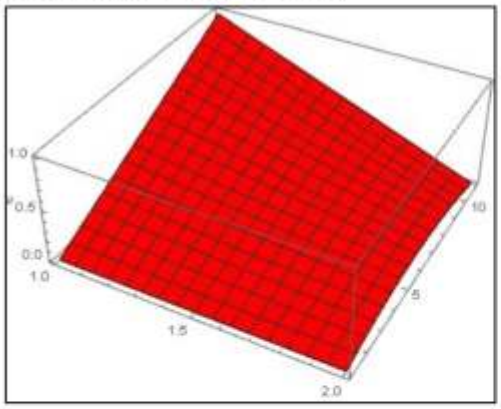

(b) 3D view of exact in figure (a) (c) 3D view of approximate value in figure (a)

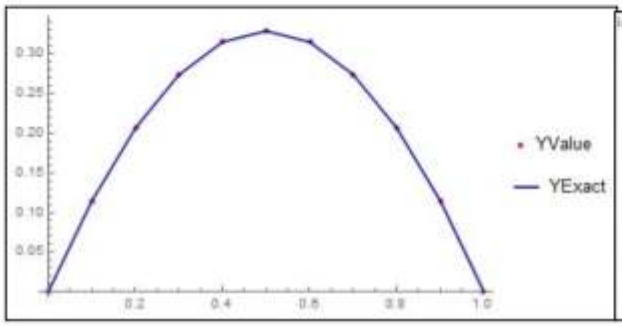

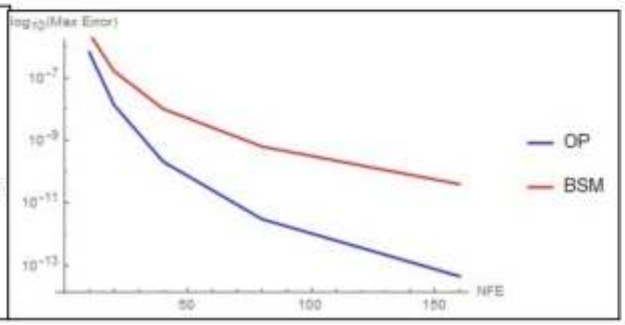

(a) 2D solution curve of Bratu eqution with λ= 2 as compared with the exact solution.

(b) Efficiency curve of BSM with λ= 2 as compared with that of OP.

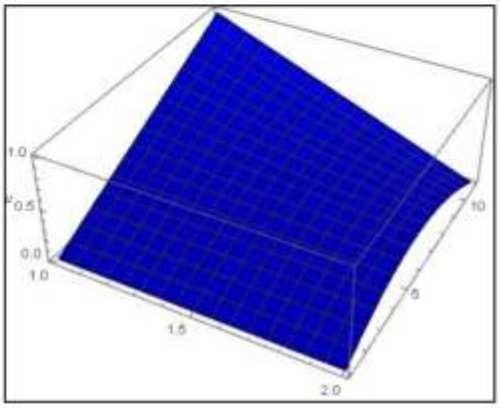

(c) 3D view of exact in figure (a)

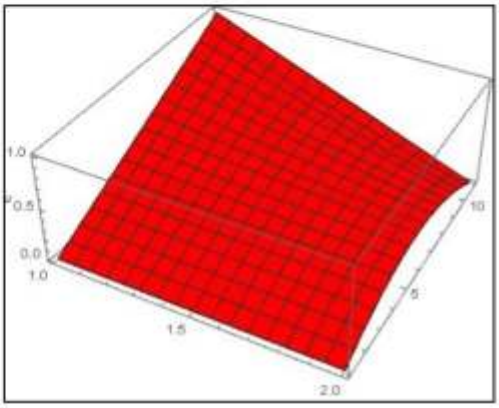

(d) 3D view of approximate value in figure (a)

Application of BSM to solve Bratu-Type Equations

Here, Bratu-type initial value problem of the form

$$\left.\begin{aligned} u''(x) &= 2e^{u}, \quad 0 < x < 1 \\ u(0) &= u'(0) = 0. \end{aligned}\right\} \tag{24}$$

is considered to further demonstrate the efficiency of the proposed method.

Table 1: The Maximum error and ROC of BSM with $\lambda = 1, 2$ and that of OP with $\lambda = 2$ in [6]

N	Max Error($\lambda = 1$)	ROC	Max Error($\lambda = 2$)	ROC	Maxi Error in [6]	ROC of OP in [6]
10	2.21822×10^{-8}		6.5722×10^{-7}		2.64(-6)	
20	4.13283×10^{-10}	5.74613	1.36604×10^{-8}	5.5883	1.64(-7)	4
40	6.68043×10^{-12}	5.95105	2.06726×10^{-10}	6.04614	1.01(-8)	4
80	1.06137×10^{-13}	5.97594	2.99544×10^{-12}	6.10881	6.31(-10)	4
160	1.69309×10^{-15}	5.97013	4.45755×10^{-14}	6.07037	3.94(-11)	4

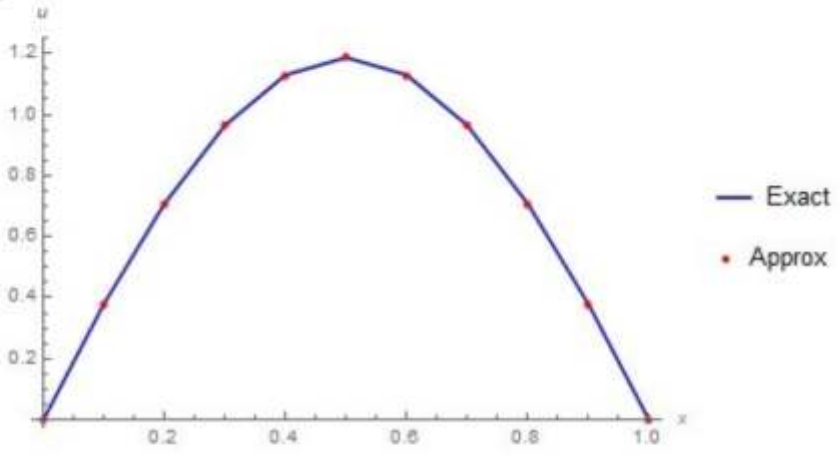

(a) 2D solution curve of Bratu eqution with $\lambda = 3.513830719$ as compared with the exact

solution.

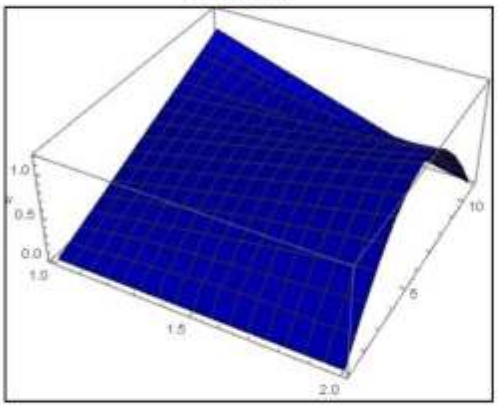

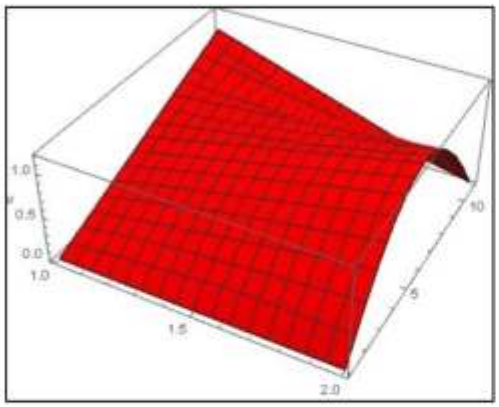

(b) 3D view of exact in figure (a) (c) 3D view of approximate value in figure (a)

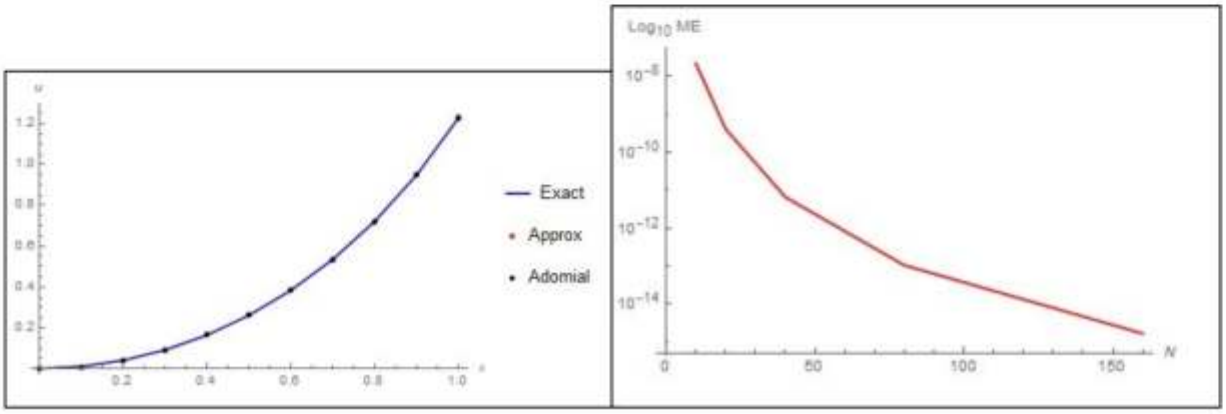

(a) Numerical, Exact and Adomial solution of the Bratu-type IVP (b) Efficiency curve for Bratu equation with $\lambda = 1$

Figure 2

Conclusion

This study has investigated the numerical solution of Bratu and Bratu-type problems by constructing a block

Stomer-Cowell method. The stability study of the proposed method shows $A(\alpha)$ -stable with $\alpha = 71^{o}$. Numerical results of the problems under study are presented in 2D and 3D, respectively. Efficient curves for λ equal to 1 and 2 are presented to show the computational advantage of the proposed method. The convergence rate was obtained for Bratu-equation for various values of λ, and the results show that the method is consistent with the theoretical order. Our future work will present the BSM hybrid type for the numerical solution of second-order Bratu equations.

References

Wazwaz A. M., *Adomian decomposition method for a reliable treatment of the Bratu-type equations* Applied Mathematics and Computation, vol. 166, no. 3, pp. 652-663, Jul. 2016.

Al-Mazmumy M., Al-Mutairi A., and Al-Zahrani K., *An Efficient Decomposition Method for Solving Bratu's Boundary Value Problem* American Journal of Computational Mathematics, vol. 07, no. 01, pp. 84-93, 2017.

Al-Towaiq M. and Ala'yed O., *An Efficient Algorithm based on the Cubic Spline for the Solution of Bratu-Type Equation,* Journal of Interdisciplinary Mathematics, vol. 17, no. 5-6, pp. 471-484, Nov. 2014.

Samuel O. A, Babatope E. S. and Arekete S. A. *A new result on Adomian decomposition Method for solving Bratu' problem.* Mathematical Theory and Modeling, vol.3, no.2, pp. 116-120, 2013

Habtamu G. D., Habtamu B. Y. and Solomon B. K., *Numerical solution of second order initial value problems of Bratu-type equation using higher order Rungu-Kutta method.* International Journal of Scientific and Research Publications, vol. 7, is. 10, pp. 187-197, 2017

Marwan A., Suhell K. and Ali S., *Spline-based numerical treatments of Bratu-type equation.* Palestine Journal of Mathematics, vol.1, pp. 63-70, 2012

Wazwaz A. M., *The successive differentiation method for solving Bratu equation and Bratu-type equation*

Department of Mathematics, Saint Xavier University, Chicago, IL 60655, USA. pp. 774-783, Jul. 2005.

Batiha B, *Numerical solution of Bratu-type equations by the variational iterative method.* Hacettepe Journal of Mathematics and Statistics, vol.39, no. 1, pp.23-29, 2010.

Christodoulou N. S., *An algorithm using Runge-Kutta methods of orders 4 and 5 for system of Odes.* International Journal of Numerical Methods and Application, vol.2, no. 1, pp.47-57, 2009

Jator S. N. and Oladejo H. B., *Block Nystrom Method for Singular Differential Equations of the Lane-˜ Emden Type and Problems with Highly Oscillatory Solutions* International Journal of Applied and Computational Mathematics, vol.3, s1, pp. 1385-1402, 2017

Jator S. N. and Coleman N., *A nonlinear second derivative method with a variable step-size based on continued fractions for singular initial value problems.* Applied & Interdisciplinary Mathematics vol.4, 2017, https://doi.org/10.1080/23311835.2017.1335498

Lambert J. D., *Computational Methods for Ordinary Differential Systems. The Initial Value Problems.* Wiley, Chichester, 1973.

Lambert J. D., *Numerical Methods for Ordinary Differential Systems. The Initial Value Problems.* Wiley, Chichester, 1991.